UNIVERZITA PALACKÉHO V OLOMOUCI

Lékařská fakulta

Ústav Patologické fyziologie

#

STUDIUM EXPRESE A FUNKCE RNA-BINDING PROTEINU RBPMS2 V GASTROINTESTINÁLNÍM STROMÁLNÍM TUMORU (GIST)

Doktorská dizertační práce

Mgr. Ilona HAPKOVÁ

#

Školitel: Prof. MUDr. Jaroslav VESELÝ, CSc.

Spoluškolitel: Dr. Pascal DE SANTA BARBARA

Olomouc 2014

PALACKY UNIVERSITY OLOMOUC

Faculty of Medicine and Dentistry

Department of Pathological Physiology

#

STUDY OF EXPRESSION AND FUNCTION OF THE RNA-BINDING PROTEINS RBPMS2 DURING GASTROINTESTINAL STROMAL TUMOR (GIST)

Thesis of Postgraduate Studies

Ilona HAPKOVA

#

Director of Thesis: Prof. Jaroslav VESELÝ

Co-Director of Thesis: Dr. Pascal DE SANTA BARBARA

Olomouc 2014

BIBLIOGRAFICKA IDENTIFIKACE

Jméno a příjmení autora: Mgr. Ilona Hapková

Název disertační práce: Studium exprese a funkce RNA-binding proteinu RBPMS2 v GastroIntestinálním Stromálním Tumoru (GIST)

Pracoviště: Ústav Patologické fyziologie

INSERM 1046, Francie

Školitel: Prof. MUDr. Jaroslav VESELÝ, CSc.

Spoluškolitel: Dr. Pascal DE SANTA BARBARA

Rok obhajoby disertační práce: 2014

Abstrakt:

Moje PhD práce se zabývá expresí a funkcí RBPMS2 v lidských GISTech. V GISTech jsme analyzovali RBPMS2 a zjistili jsme jeho abnormálně vysokou expresi v nádorových buňkách GISTů. Dále jsme se zabývali funkcí RBPMS2 v buněčné kultuře viscerální hladké svaloviny dospělého člověka. Ukázalo se, že RBPMS2 je klíčový faktor regulace při vývoji viscerální hladké svaloviny, a patofyziologický stav má negativním vliv na diferenciaci a kontraktilitu, a pozitivní vliv na proliferaci buněk viscerální hladké svaloviny. Tyto výsledky naznačují, že RBPMS2 může být potenciálním cílem protinádorové terapie.

Klíčová slova: Gastrointestinální stromální tumory, RNA-Binding Protein s Multiple Splicing 2, buňky viscerální hladké svaloviny, Cajalovy intestinální buňky

BIBLIOGRAPHICAL IDENTIFICATION

Author´s first name and surname: Ilona Hapkova

Title of the doctoral thesis: Study of expression and function of the RNA-Binding Proteins RBPMS2 during GastroIntestinal Stromal Tumor (GIST)

Department: Department of Pathological Physiology
INSERM 1046, France

Director: Prof. Jaroslav VESELY

Co-Director: Dr. Pascal DE SANTA BARBARA

The year of presentation: 2014

Abstract:

My PhD works investigate the expression and function of RBPMS2 in human GISTs. We analyzed the expression of RBPMS2 in human GISTs and we found that RBPMS2 was abnormally highly expressed in the tumoral cells of GISTs. We also analyzed the function of RBPMS2 into human adult SMC cell culture and demonstrated that ectopic expression of RBPMS2 in mature and differentiated SMC cultures increases their proliferation rate and alters their differentiation. These findings suggest that RBPMS2 could be a potential target for cancer therapy.

Keywords: GastroIntestinal Stromal Tumor, RNA-Binding Protein, RBPMS2, Smooth Muscle Cells, Interstitial Cell of Cajal.

I agree the thesis to be lent within the library service.

IDENTIFICATION BIBLIOGRAPHIQUE

Prénom et nom de l'auteur: Ilona Hapkova

Titre de la thèse de doctorat: Etude de l´expression et de la fonction de la protéine de liaison à l´ARN RBPMS2 dans le Tumeur Stromale GastroIntestinale (GIST)

Department: Département de Physiologie et Physiopathologie
INSERM 1046, France

Directeur: Prof. Jaroslav VESELY

Co-Directeur: Dr. Pascal DE SANTA BARBARA

L'année de présentation: 2014

Resumé:

Les Travaux que j'ai réalisés au cours de ma thèse avaient pour objectifs d'étudier l'expression et la fonction de RBPMS2 dans les tumeurs GISTs humains. Nous avons analysé l'expression de RBPMS2 dans les GIST humains et nous avons démontré que RBPMS2 était fortement exprimé dans les GISTs de manière indépendante de l'activité KIT. Nous avons également analysé la fonction de RBPMS2 en culture et avons montré que l'expression ectopique de RBPMS2 dans les SMCs humaines adultes et différenciées culture conduisaient à l'augmentation de leur taux de prolifération et altèreraient leur différenciation. Ces résultats suggèrent que RBPMS2 et les voies de signalisation qu'il contrôle pourraient être des cibles thérapeutiques potentielles dans la thérapie des tumeurs GISTs.

Les mots clés: Tumeurs stromales gastrointestinales, GIST, Protéine de liaison à l'ARN, RBPMS2, Cellules Musculaires Lisses, Cellules Interstitielles de Cajal.

Prohlašuji, že jsem dizertační práci vypracovala sama pod vedením školitelů Prof. MUDR. Jaroslava Veselého, CSc. a Dr. Pascala de Santa Barbary a s použitím literatury, kterou cituji v závěru práce.

V Olomouci dne ……

Mgr. Ilona Hapková

I declare that this dissertation thesis was carried out by myself under the supervision of Prof. Jaroslav Vesely and Dr. Pascal de Santa Barbara. I used the literature, which I quote in the conclusion.

In Olomouc ……

Ilona Hapkova

Děkuji školitelům Prof. MUDR. Jaroslavu Veselému, CSc. a Dr. Pascalu de Santa Barbarovi za cenné rady, pečlivé konzultace a trpělivý přístup po celou dobu práce. Ráda bych také poděkovala Dr. Florence Bernex a RNDr. Miroslavu Rypkovi, CSc za pomoc v experimentální části práce. Dále za to, že disertační práce mohla být řešena v rámci výzkumného záměru IGA LF_2011_015 (SPP prvek: 911100221/31).

I thank my directors of thesis Prof. Jaroslav Vesely and Dr. Pascal de Santa Barbara for valuable advice, consultation and careful patient approach during my thesis. I should also thank Dr. Florence Bernex and Dr. Miroslav Rypka for assistance in the experimental part. Also consider that the thesis could be resolved within the research project IGA LF_2011_015 (SPP element: 911100221/31).

THESIS CONTENTS

TABLE OF CONTENTS

List of Tables

List of Figures

LIST OF ABBREVIATIONS

BMP	Bone Morphogenic Protein
CT	Computing Tomography
DNA	DeoxyriboNucleic Acid
EC	ExtraCellular
EGIST	Extra-GastroIntestinal Stromal Tumor
GANT	Gastrointestinal Autonomic Nerve Tumor
GI tract	GastroIntestinal tract
GIST	GastroIntestinal Stromal Tumor
HERMES	Heart RNA Recognition Motif Expressed Sequence
Hh	Hegehog
HIF1α	Hypoxia-Inducible Factor 1α
hnRNP	heterogeneous nuclear RiboNucleoProtein
ICC	Interstitial Cells of Cajal
IGF	Insulin-like Growth Factor
IGFR	Insulin-like Growth Factor Receptor
Ig-like	Immunoglobulin-like
IHC	Immunohistochemistry
ISEMF	Intestinal SubEpithelial MyoFibriblast
JM	JuxtaMembrane
LMS	LeioMyoSarcoma
miR	Micro RNA Precursor
MRI	Magnetic Resonance Imaging
mRNA	Messenger RiboNucleic Acid
NF1	NeuroFibromatosis type 1
NK	Natural Killer
P	AutoPhosphorylation
PDGFRA	Platelet-Derived Growth Factor Receptor Alpha
PKCtheta	Protein Kinase C theta
pre-mRNA	precursors mRNA
RBP	RNA-Binding Protein
RBPMS2	RNA-Binding Protein with Multiple Splicing 2
RNA	RiboNucleic Acid
RND	RNA-Binding Domain
RNP	RiboNucleoProtein
RRM	RNA Recognition Motif
rRNA	Ribosomal RiboNucleic Acid
RTK	Receptor Tyrosine Kinase
SCF	Stem Cell Factor
SDH	Succinete DeHydrogenase
SMC	Smooth Muscle Cells
snRNP	small nuclear RiboNucleoProtein
STAT	Signal Transducer and Activator of Transcription
TKI	Tyrosine kinase inhibitor
VEGF	Vascular Endothelial Growth Factor
WT	Wild-type
αSMA	Alpha Smooth Muscle Actin

FOREWORD

The gastrointestinal tract consists of a hollow muscular tube starting from the oral cavity, where food enters the mouth, continuing through the pharynx, esophagus, stomach and intestines to the rectum and anus, where food is expelled. There are various accessory organs that assist the tract to help physiological functions include digestion and absorption of nutrients, colonic fermentation, gut-associated immune activities, secretion of endocrine peptides, control of mucosal cell kinetics, secretion of mucins and stool production inter alia. Food is propelled along the length of the gastrointestinal tract by peristaltic movements of the muscular walls.

Cancers of the gastrointestinal tract remain a major challenge for oncologists and other cancer specialists in the worldwide. We are especially interested of the most frequent mesenchymal tumor, Gastrointestinal stromal tumor, that may occur anywhere in the Gastrointestinal tract, from esophagus to anus, encompass a heterogeneous and as yet incompletely understood. What is the origin of Gastrointestinal stromal tumor? It is included in the tumor processes next gen? What is the function of this gene during the development smooth muscle cells? And we have a lot of other questions for which we have no yet answers.

Our laboratories are interested in processes that will permit the development and proper functioning of the gastrointestinal tract. In particular, we try to understand what is in the developing molecular determinants that permit the development and remodeling of smooth muscle cells.

The work that is presented here reported expression and function of RNA-binding protein with multiple splicing 2 in human gastrointestinal stromal tumors. Ours studies have allowed us to characterize the function and mechanism of RNA-binding protein with multiple splicing 2 into human adult smooth muscle cell cultures.

INTRODUCTION

1 Gastrointestinal Tract

The gastrointestinal (GI) tract is a remarkably complex three-dimensional, specialized, and vital organ system derived from a simple tubular structure. The vertebrate GI tract includes the luminal digestive system of the esophagus, stomach, intestines, and colon (Fig. 1). The GI tract derivates are thyroid, lungs, liver, and pancreas.

The GI tract (gut) is composed of the three germ layers. Endoderm forms the epithelial lining, mesoderm forms the smooth muscle layers (which involves smooth muscle cells, myofibroblast, immune cells, and so on), and ectoderm which includes the enteric nervous system. These tissues show regionally specific differentiation along the anterior-posterior axis designating the foregut (pharynx, esophagus, and stomach), midgut (small intestines), and hindgut (colon).

Different molecular pathways and transcription factors used in these processes have been described and studied. Such critical pathways as the Hedgehog (Hh), Bone morphogenetic protein (BMP), and Notch signalling pathways, the Hot and Sox transcription factors, the Eph receptor/ephrin ligand (Eph-ephrin) signaling system, the Wnt/β-catenin and T cell factor signaling pathways. Many of these systems are best known as critical control factors in general body plan developmental processes. They also play as role in organ pattern formation and have key roles in GI development. These developmentally critical pathways continue to be important in cell differentiation, homeostasis, and apoptosis.

In 1893, Spanish Nobel Laureate physician and neuropathologist Santiago Ramon y Cajal, was the first to describe cells that are located between the nerve endings and smooth muscle cells in the GI tract. Their location prompted him to call them “interstitial”. They are now known as the Interstitial Cells of Cajal (ICCs) (Cajal 1911; Mostafa et al. 2010).

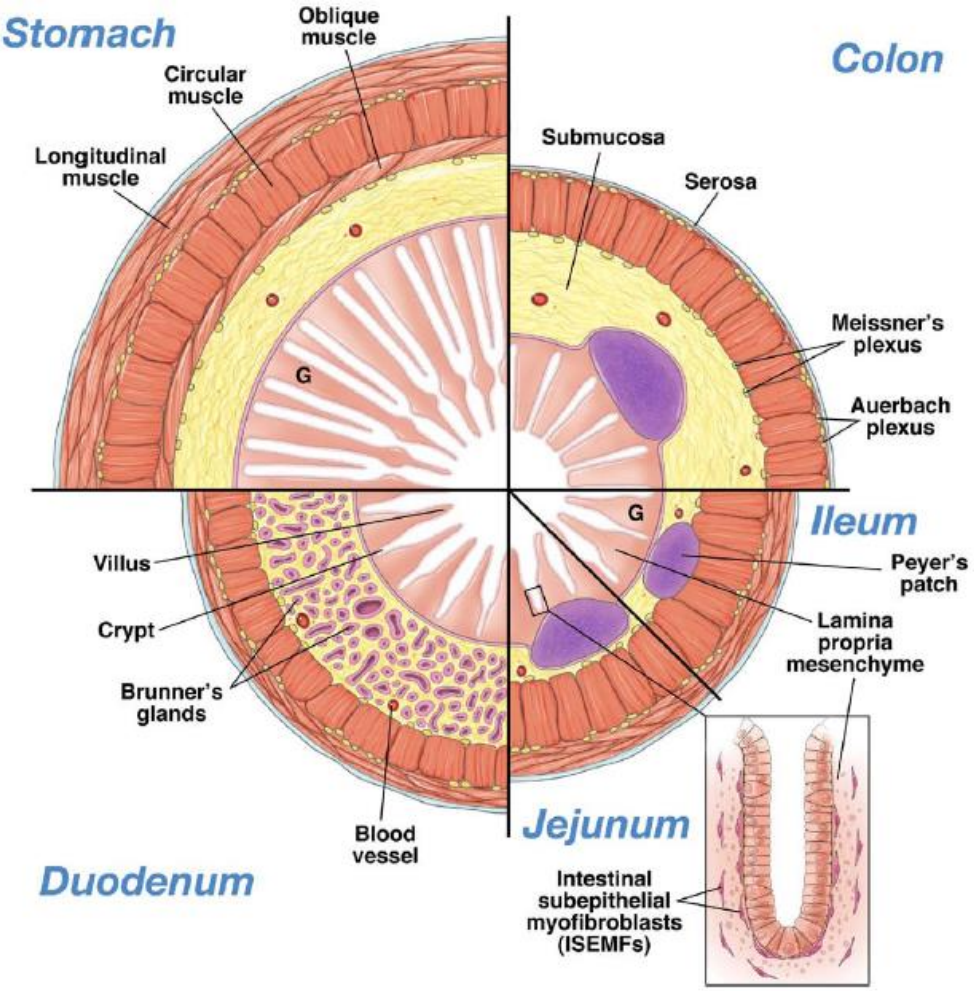

Figure 1. Schematic section through the adult GI tract. Each quadrant represents a different segment of the GI tract, from the stomach to the colon; mesenchymal structures are shown in detail. The following structures are conserved along the craniocaudal axis: the lamina propria mesenchyme, the muscularis mucosa, mesenchymal blood vessels, the intestinal subepithelial myofibriblassts (ISEMFs), the Meissner's plexus, the longitudinal inner and circular outer layers of the muscularis propria, the Auerbach plexus, and the serosa. These structures are represented in all quadrants. The stomach (left upper quadrant) is characterized by an additional oblique inner layer of the muscularis propria. Its epithelium is characterized by deep, bifid glands (G) that fulfill the secretory and endocrine functions of the stomach. In the duodenum (left lower quadrant), the submucosa is recognizable by its abundance of Brunner's glands, which are epithelial in origin. Consistent with the rest of the small intestine, the duodenal epithelium is characterized by the presence of crypts and villi. The other 2 components of the small intestine are the jejunum and ileum (right lower quadrant). The ileum is characterized by the presence of

Peyer's patches, which are large lymphoid aggregates in the submucosa. In the jejunum and the colon, the lymphoid aggregates are located in the mucosal tunic rather than in the submucosa. ISEMFs are adjacent to the epithelium lining crypts and villi. Finally, in the colon (right upper quadrant), the epithelium is characterized by straight glands (G) but does not include villi or crypts. The characteristic feature of the colon mesenchyme is the thinner, circular outer layer of the muscularis propria. Adapted from McLin et al. 2009.

In the end of the last century where researchers began to assume ICC as a regulator of GI motility in animal, including humans, throughout the esophagus to the inner sphincter region of anus. They show different distribution patterns and morphological features depending on their anatomical locations, and according to which they are classified into several subtypes (Fig. 2) (Hagger et al. 1998; Komuro 2006). Many studies indicated that ICC is the genuine pacemaker cells which generate spontaneous electrical activities, known as slow waves for orderly processing of food, absorption of nutrients and elimination. Slow waves from ICC spread passively via gap junctions to neighboring GI smooth muscle cells and then produce spontaneous contraction like peristalsis (Torihashi et al. 1997).

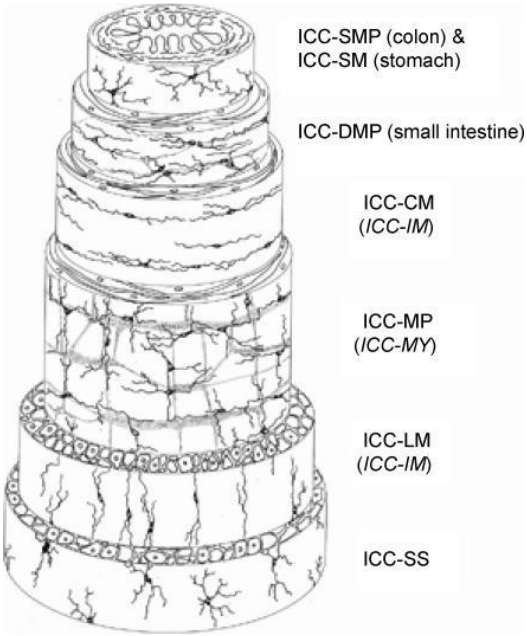

Figure 2. Schematic representation of the types of ICC located in different tissue layers of the GI tract. ICC-SMP and ICC-SM are seen at the interface between the submucosa and circular muscle layer in the colon and gastric pylorus, respectively. ICC-DMP are

associated with the deep muscular plexus located between the inner and outer circular muscle sublayers in the small intestine. ICC-CM and ICC-LM are found within the circular and longitudinal muscle layers, respectively. ICC-MP are associated with the myenteric plexus between the circular and longitudinal muscle layers. ICC-SS are found in the subserosal connective tissue space. ICC located in the myenteric (Auerbach's) plexus are designated as ICC-MP instead of ICC-MY or ICC-AP, to keep consistency with the abbreviation for ICC-DMP (deep muscular plexus) and ICC-SMP (submuscular plexus) and because of uncommon usage of the term Auerbach's plexus in the recent literature. ICC-CM and ICC-LM are separately designated, because some morphological and functional differences between them have not been ruled out. From Komuro 2006.

ICC is a myoid cell of mesenchymal origin that express c-Kit, and signaling via Kit receptor tyrosine kinase is necessary for normal development of ICC. After blockage of Kit receptors (with anti-Kit monoclonal antibody; ACK2), the phenotype of ICCs are modified (Fig. 3). Activation by ligand (Stem Cell Factor, SCF) is essential for the development of ICC (Maeda et al. 1992). Studies of Torihashi and colleagues showing that ICCs in the pacemaker region of the small intestine and longitudinal muscle cells of mice develop from the same Kit-immunopositive precursor cells, suggest inherent plasticity between the ICCs and Smooth Muscle Cells (SMCs) that is regulated by Kit-dependant cell signaling (Torihashi et al. 1999).

Significant reduction of density and constructional destruction of ICC with abnormal function have been suggested to be responsible for many GI motility disorders and diseases such as constipation, Chronic Intestinal PseudoObstruction, infantile hypertrophic pyloric stenosis and acquired megacolon (Vanderwinden & Rumessen 1999). Furthermore, a mutation of proto-oncogene *c-Kit* has been also reported in a sub-group of GI cancer such as colorectal carcinomas and GastroIntestinal Stromal Tumors (GIST) (Reed et al. 2002; Ördög et al. 2004; Yun et al. 2010).

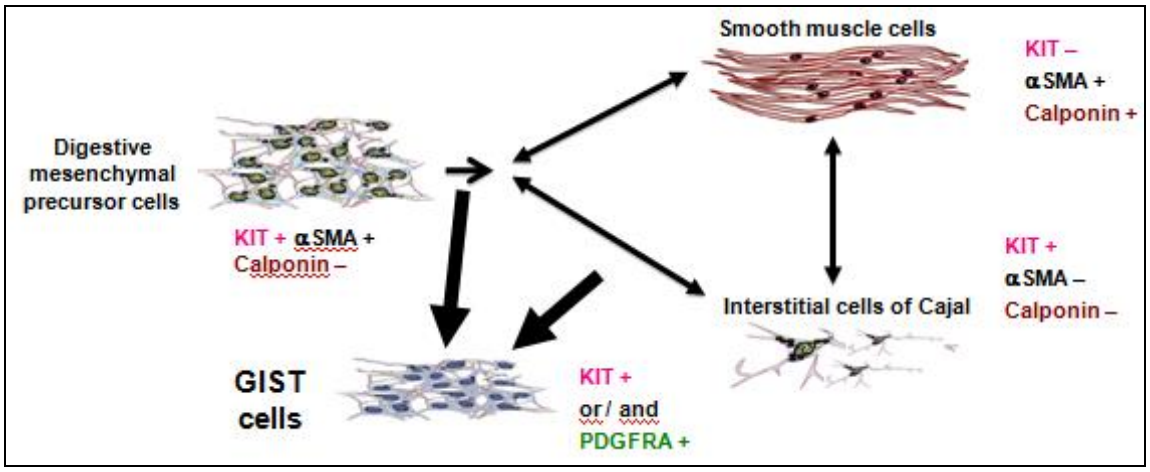

Figure 3. Schematic representation of the plasticity of ICCs. Kit signaling is essential for the maintenance of survival and proliferation of the mature ICCs. Moreover, ICCs might transdifferentiate to a type of alph-Smooth Muscle Actin (αSMA+) and Calponin (+) cells, a phenotype of Smooth Muscle Cells (SMCs), when there is a loss of function of Kit. ICC is widely accepted today as an essential target to be considered seriously in many abnormal GI motility diseases such as GIST.

Gastrointestinal stromal tumors (GISTs) are the most common primary mesenchymal neoplasms of the GI tract (Miettinen & Lasota 2006). They are thought to derive from or differentiate similar to the gastrointestinal pacemaker cells, ICCs (Kindblom et al. 1998). ICCs are innervated cells associated with Auerbach´s plexus that have autonomous pacemaker function and coordinate peristalsis throughout the GI tract. Recently, a popular hypothesis is that GISTs either arise from ICCs, or that they share a mesenchymal precursor cell, common of ICCs and SMCs. Tumors usually present as single nodules but they can consist of many nodules. They are usually fleshy and solid in consistency but can have central cystic degeneration (Rubin et al. 2007).

GISTs are highly resistant to conventional chemotherapy. However, a targeted therapy is now proposed. These tumors have activating mutation in two closely related receptor tyrosine kinases, KIT (75-80%) or Platelet-Derived Growth Factor Receptor Alpha (PDGFRA, 5-10%). These mutations lead to ligand-independent activation and signal transduction mediated by constitutively activated KIT or PDGFRA. Targeting these activated proteins with imatinib mesylate, a small-molecule tyrosine kinase inhibitor, has proven useful in the treatment of recurrent or metastatic GISTs and is now bending tested as an adjuvant or neoadjuvant. However, resistance to imatinib is a growing problem and

other targeted therapeutic such as sunitinib need to be developed in order to bring new therapeutic treatment (Rubin et al. 2007).

2 Historical overview of GIST

Gastrointestinal stromal tumors (GISTs) include the largest subset of mesenchymal neoplasms of the digestive tract. Over the past 10 years, this group of tumors has emerged from a poorly understood neoplasm to a well defined tumor entity.

On the basis of light microscopic descriptions in the 1930´s to 1950´s, stromal tumors of the GI tract were thought to be neoplasm's of smooth muscle origin. The first accurate description of mesenchymal neoplasms was in 1941 (Golden & Stout 1941). They were most often classified as leiomyoma, leiomyosarcoma, leiomyoblastoma or bizarre leiomyomas (Stout 1962; Appelman 1996). However, the advent of electron microscopy in the late 1960´s and early 1970´s revealed that only a few of them have convincing ultrastructural evidence of smooth muscle differentiation (Welsh & Meyer 1969; Franquemont 1995). In addition, the application of immunohistochemistry, which began in the 1980´s, clearly demonstrated that many of these tumors lack the features of smooth muscle differentiation and supported the electron microscopical evidence (Ricci 1987; Franquemont 1995).

The term "stromal tumor" was introduced in 1983 by Mazur and Clark, but it was not widely accepted until the early 1990´s, when it was discovered that most stromal tumors arising in the gastrointestinal tract express CD34 (Miettinen et al. 1995).

A little later, in 1984, Herrera et al (Herrera et al. 1984; Walker & Dvorak 1986; Herrera et al. 1989) introduced the concept of "plexosarcoma" to acknowledge the existence of a small subset of stromal tumors with autonomic neuronal differentiation which became better known as gastrointestinal autonomic nerve tumors (GANTs) (Lauwers et al. 1993). It is now established that gastrointestinal autonomic nerve tumor is a morphological variants of GIST (Lee et al. 2001).

The recognition of the central role of *C-KIT* mutations in the pathogenesis of GISTs (Hirota et al. 1998; Rubin et al. 2000) and in most cases the associated expression of KIT protein in these tumors has provided a reproducible genotypic and phenotypic marker (Kindblom et al. 1998). Therefore KIT (CD117 in the standardised terminology of leucocyte antigens) expression has emerged as a marker for discriminating GISTs from other mesenchymal gastrointestinal neoplasms and some have equated immunoreactivity for KIT as definition of GISTs (Miettinen & Lasota 2001).

In 2003, Heinrich and colleagues additionally identified *Platelet-Derived Growth Factor Receptor Alpha (PDGFRA)* gene mutations as an alternative pathogenetic event in GISTs lacking *KIT* gene mutations.

To date, approximately 85% of GISTs are reported to harbor activating mutations in KIT or the homologous receptor tyrosine kinase (RTK) gene, PDGFRA (Heinrich et al. 2003; Corless et al. 2004; Rubin et al. 2007; Corless et al. 2011).

Increased understanding of GIST biology has made this tumor a paradigm of molecularly targeted therapy in solid tumors and provides informative insights into the advantages and limitations of so-called targeted therapeutics.

3 Epidemiology

The exact incidence of GIST is hard to determine, as GISTs have only been properly recognized and uniformly diagnosed as an entity since the late 1990´s. However, the incidence of GIST is estimated to be approximately 10-20 per million people, per year. About 30-50% of GISTs have malignant evolution and metastases are observed in 50% despite initial surgical resection (Miettinen et al. 1999; Fletcher et al. 2002).

Recent population-based studies performed in Sweden (Nilsson et al. 2005), Holland (Goettsch et al. 2005), France (Nilsson et al. 2005), Rhône Alpes region in France (Cassier et al. 2010) and Iceland (Tryggvason et al. 2005) found respectively incidences of 14.5, 12.7, 15, 11.2 and 11 cases per million people per year. In Czech Republic and Slovakia the annual crude incidence between the 2001-2005 was 5.2 cases per million people. The annual European ASR (age-standardized rate) and World ASR were respectively 4.4 and 3.1 per million people (Brabec et al. 2009). These findings would translate into an annual incidence in Europe of around 8,000-9,000 cases and in the USA of around 4,000-5,000 cases per year (Liegl-Atzwanger et al. 2010). Nevertheless, the prevalence of GIST is probably higher, as many patients live with the disease for many years or develop small GISTs only detected at autopsy or if a gastrectomy is performed for another cause.

GISTs typically occur in older individuals over 50 years of age (Miettinen et al. 1999). The median ages in the larges series of GISTs of different locations have ranged between 55 years to 65 years. Some series show a male predominance, and others show equal gender distribution (Ueyama et al. 1992; Kim et al. 2005; Miettinen et al. 2005). GISTs are rare before the age of 40 years, and paediatric GISTs are observed but rare compared to the adult form (Miettinen & Lasota 2001).

Currently there are no known elements that indicate any association with geographic location, ethnicity, race or occupation (Stramatakos et al 2009).

The most common location of GIST is the stomach (50-60%) followed by small intestine (20-30%). Five to ten percent of GISTs arise from the colon and rectum, and less than 5% are located in the oesophagus. Other less common locations are those outside of the GI tract, like mesentery, retroperotoneum and omentum. However, there have been reported rare cases in the gallbladder, pancreas, liver and urinary bladder (Miettinen et al.

1999). In cases, where GIST occurs outside the GI tract, the tumors are known as Extra-GastroIntestinal Stromal Tumors (EGISTs) (Miettinen & Lasota 2001).

4 Clinical and pathological aspects

4.1 Clinical Features

The clinical presentation of GIST is erratic. Clinical symptoms associated with GIST include abdominal pain, fatigue, dysphagia, satiety and obstruction. Patients may present with chronic GI bleeding (causing anemia) or acute GI bleeding (caused by erosion through the gastric or bowel mucosa). Rupture of GIST into the abdominal cavity is rare and it causes life threatening intraperitoneal hemorrhage. Furthermore, only 70% of patients are symptomatic, while 20% are asymptomatic and 10% are detected at autopsy. The median tumor size in each of these categories was 8.9, 2.7 and 3.4 cm (Kim et al. 2005; Nilsson et al. 2005). Small GISTs mainly present as incidental findings during endoscopy, surgery or radiologic studies for other reasons.

In 50% of operated GISTs, metastases arise from the GI tract quite often 10-15 years after initial surgery and therefore long-term follow-up is required. On the other hand, distant metastases most commonly occurs in GIST tumors of peritoneum, omentum, mesenteric areas and liver, while in EGISTs tumors are rare. At this point, it is important to mention that rectal GISTs frequently metastasize to the lung (Corless et al. 2004; Agaimy et al. 2009). In addition, lymph nodes metastases are not common in GISTs.

4.2 Macroscopic features

GISTs present most often as well-circumscribed, highly vascular tumors associated with the stomach or the intestine. On gross examination, these tumors appear fleshy pink or tan-white and may show hemorrhagic foci, central cystic degenerative changes or necrosis (Coindre et al. 2005; Liegl-Atzwanger et al. 2010).

Figure 4. Typical gross appearance of a GIST. Surgical specimen of jejuna GIST: the blood clot on the right side revealed the tumor causing the mucosal ulceration. From Caterino et al. 2011.

4.3 Microscopic features and immunohistochemical Markers

Microscopic evaluation reveals three principal subtypes of GIST depending on the cytomorphology. Spindle cell GIST (Fig. 5A), accounting for approximately 70% of cases, is composed of cells with palely eosinophilic fibrillary cytoplasm, ovoid nuclei, and ill-defined cell borders, often with a syncytial appearance, arranged in short fascicles or whorls. GIST with epithelioid cell morphology (Fig. 5B), accounting for approximately 20% of cases, is compounded of round cells with eosinophilic to clear cytoplasm arranged in sheets and nests. Finally, approximately 10% of GISTs show mixed morphology, being composed of both spindle and epithelioid cells (Fig. 5C) (Corless et al. 2004; Miettinen & Lasota 2006). Occasional tumors have neuroendocrine-like features that resemble paraganglioma or carcinoid. A signet ring-like variant has also been described (Suster & Fletcher 1996). Uncommonly, some GISTs have a marked lymphocytic infiltrate (Shek et al. 1996).

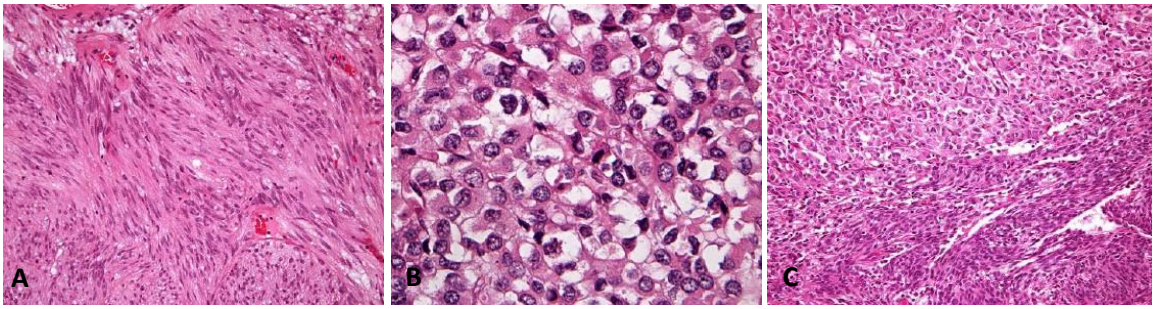

Figure 5. Hematoxylin and eosin stain of GIST composed of: (**A**) Spindle cells; (**B**) Epithelioid cells; (**C**) Mixed spindle cell and epithelioid cytomorphology. Adapted from Liegl-Atzwanger et al. 2010.

Obtaining adequate tumor tissue material for definitive diagnosis before surgical resection has been challenging. Because these tumors tend to be soft and friable, biopsy may cause tumor rupture and be associated with an increased risk for tumor dissemination. Tumors can have substantial histological variation, which necessitates a broad differential diagnosis and immunohistochemistry is often needed to verify diagnosis (Fletcher et al. 2002).

Approximately 95% are positive for KIT (CD117). In general, KIT staining in GISTs is strongly and diffusely positive, but is not necessarily uniform across different regions of the tumors. Staining may appear in a cytoplasmic (most common), membranous, or a concentrated dot-like perinuclear pattern. Some cases show combinations of these patterns. Epithelioid GISTs tend to have a weaker and patchier staining pattern that spindle cell GISTs.

Other commonly expressed markers include CD34 (60-70%), h-Caldesmon (60%), alpha Smooth Muscle Actin (αSMA; 30-40%), S100 (5%), Desmin (1-2%) and Keratin (1-2%) (Kindblom et al. 1998; Sarlomo-Rikala et al. 1998; Fletcher et al. 2002; Demetri et al. 2010).

However, about 5% of GISTs are truly negative for detectable KIT expression, the so-called "KIT-negative GISTs" (Fletcher et al. 2002; Medeiros et al. 2004; Debiec-Rychter et al. 2004). In a proportion of KIT-negative GISTs, the genotypic analysis shows mutations in the *PDGFRA* gene rather than *KIT*, in 10-15% of GISTs (Heinrich et al. 2003; Hirota et al. 2003; Corless et al. 2005). Many of these PDGFRA-mutant GISTs have an epithelioid morphology. Immunostaining with PDGFRA has been shown in this particular

setting to be helpful in discrimination between KIT-negative GISTs and other gastrointestinal mesenchymal lesions (Rossi et al. 2005; Peterson et al. 2006).

V600E BRAF mutations have been identified in 7% of adult GIST patients lacking *KIT or PDGFRA* mutations (known as wild-type GISTs). The *BRAF*-mutated GISTs show predilection for small bowel location and a high risk of malignancy. KIT protein is consistently over-expressed in these cases and there are no distinctive microscopic features that would differentiate them from *KIT*-mutated GISTs (Agaram et al. 2008; Antonescu 2011).

GISTs lacking *KIT* or *PDGFRA* mutations are a heterogeneous group, of with some have alternations in *HRAS* and *NRAS* gene or in the genes of *Succinate Dehydrogenase Complex*, but are mutch more rare (Corless et al. 2011).

Protein kinase C theta (PKCtheta) is a downstream effector in the KIT signalling pathway. It may play an important role in the diagnosis of KIT-negative GISTs, because it is expressed strongly in GISTs (Duensing et al. 2004; Kim et al. 2006).

DOG1 also known as TMEM16A or ANO1 is a calcium-dependent, receptor-activated chloride channel protein and seems to be expressed in GIST independent of mutation type (West et al. 2004; Espinosa et al. 2008). In a study of 1168 cases of GISTs, the overall sensitivity of DOG1 and KIT was nearly identical (94.4% and 94.7%, respectively) and a high concordance was seen between DOG1 and KIT immunohistochemistry (92.3% positivity for both) (Miettinen et al. 2009).

The experience with these novel immunomarkers is currently limited, and problems exist with the quality and availability of the commercial antibodies used to stain for them.

4.4 Prognostic Factors

Prediction of prognosis of primary tumors has been studied intensively. Tumor size and mitotic activity were two principal factors in the risk stratification system originally proposed by Fletcher and colleagues (2002), a tenet of which was that almost all gastrointestinal stromal tumors have malignant potential. Table 1 shows a revised version of the risk assessment scheme, which is based on several large series published by Mietinnen and colleagues (2006). This scheme includes anatomic site as a factor, since

small bowel stromal tumors carry a higher risk of progression than gastric stromal tumors of similar size and mitotic activity.

Table 1. Risk Stratification of Primary GIST by Mitotix Index, Size, and Site.

Tumor Parameters		***Risk for Progressive Disease* (%), Based on Site of Origin***			
Mitotic Rate	**Size**	**Stomach**	**Jejunum/Ileum**	**Duodenum**	**Rectum**
≤ 5 per 50 HPF	≤ 2 cm	None (0%)	None (0%)	None (0%)	None (0%)
	> 2, ≤ 5 cm	Very low (1.9%)	Low (4.3%)	Low (8.3%)	Low (8.5%)
	> 5, ≤ 10 cm	Low (3.6%)	Moderate (24%)	Insufficient data	Insufficient data
	> 10 cm	Moderate (10%)	High (52%)	High (34%)	High (57%)
> 5 per 50 HPF	≤ 2 cm	None†	High†	Insufficient data	High (54%)
	> 2, ≤ 5 cm	Moderate (16%)	High (73%)	High (50%)	High (52%)
	> 5, ≤ 10 cm	High (55%)	High (85%)	Insufficient data	Insufficient data
	> 10 cm	High (86%)	High (90%)	High (86%)	High (71%)

Data are based on long-term follow-up of 1055 gastric, 629 small intestinal, 144 duodenal, and 111 rectal GISTs. HPF = high-power field. Adapted from Miettinen & Lasota (2006).
*Defined as metastasis or tumor-related death.
†Denotes small numbers of cases.

Immunohistochemical markers may be of importance in predicting the malignant behavior of GISTs. Increased expression of cell cycle markers (PCNA, MIB-I or Ki-67) have been linked to a less favorable prognosis in larger studies (Singer et al. 2002).

4.5 Diagnosis

GISTs show a variety of differentiation spectrum, ranging from fully differentiated tumors with myoid, neural or ganglionic plexus phenotype to those with incomplete or mixed differentiation. Nowadays, by the means of immunohistochemistry, it has become clear that the GIST cells are closely related to the multi-potential mesenchymal stem cells. In table 2, differential diagnosis is being elucidated (Yan et al. 2008).

Table 2. Tumor types in differential diagnosis with GIST.

Leiomyoma
Leiomyosarcoma (LMS)
Schwannoma
Malignant Peripheral Nerve Sheath Tumor (MPNST)
Neurofibroma
Neuroendocrine tumor
Carcinoid
Carcinosarcoma
Fibromatosis or Desmoids tumor
Solitary fibrous tumor
Inflammatory fibroid polyp
Angiosarcoma
Clear cell sarcoma
Liposarcoma
Synovial sarcoma
Malignant mesothelioma
Dedifferentiated carcinoma
Sarcomatoid carcinoma
Metastatic melanoma

Adapted from Stamatakos et al. 2009.

Leiomyoma occurs chiefly in the oesophagus, colon, and rectum within the GI tract. It is the most common mesenchymal tumor of the oesophagus but is very rare in the stomach and nearly non-existent in the small intestine. The oesophageal leiomyomas present more often in males (2:1) and occur at a younger age than GISTs, with the median age of 30-35 years. Although they are usually 1-3cm in diameter, some leiomyomas have reached a large size (more than 500g and 10cm) (Seremetis et al. 1976; Miettinen et al. 2000). Similar tumors rarely occur in the stomach, especially in the cardia. Histologically, leiomyomas are paucicellular spindle cell tumors with low or moderate cellularity and slight if any mitotic activity. Focal nuclear atypia may be present. The cells have elongated nuclei and eosinophilic, fibrillary, often clumped cytoplasm. Calcifications are sometimes

present. Oesophageal leiomyomas are typically strongly positive for both Desmin and αSMA and are negative for CD34 and KIT and *KIT* mutations (Miettinen et al. 2000).

Leiomyomas of the muscular mucosae of the colon and rectum are small bining tumors that are typically incidental finding at colorectal endoscopy in older adults. These tumors merge with smooth muscle of the muscularis mucosae and small, usually less than 1cm. They are composed of well-differentiated smooth muscle cells that are positive for αSMA and Desmin and negative for KIT and CD34 (Miettinen et al. 2000).

Leiomyomas resembling the uterine ones may be attached to the external aspect of the sigmoid and rectum. Similar to uterine leiomyomas, these tumors are composed of well-differentiated, Desmin and αSMA positive cells that are typically also positive for the Estrogen receptor and negative for KIT (Miettinen et al. 2000).

Leiomyosarcomas (LMSs) are well-differentiated malignant smooth muscle tumors and typically occur in older individuals. In contrast to GISTs, LMSs seem to be more often intraluminal polypoid tumors, possibly suggesting their origin from the inner smooth muscle layers or from the muscularis mucosae of the colon (Miettinen et al. 2000). Histologically, LMSs are composed of well-differentiated SMCs with cigar-shaped nuclei and well-differentiated cytoplasm. They are negative for KIT and CD34 and are positive for αSMA and usually for Desmin (Miettinen et al. 2001). The lack of *KIT* mutations in these tumors suggests that LMSs are not extreme phenotypic variants of GISTs but have a different pathogenesis.

Computing tomography (CT) or endoscopy and Magnetic resonance imaging (MRI) scans will help to determine extent and spread of disease.

4.5.1 GIST and NeuroFibromatosis type I (NF1)

The occurrence of multiple small GISTs in the small bowel, other than in the setting of disseminated sporadic GIST, is significantly associated with NF1. These GISTs show spindle cell morphology, are usually mitotically inactive, and express KIT, usually in the absence of *KIT* and *PDGFRA* mutations (Andersson et al. 2005; Miettinen et al. 2006). Clinically, they are usually benign. In rare cases, clinically malignant GISTs in association with multiple benign tumor nodules have been described (Miettinem et al. 2006; Liegl-Atzwanger et al. 2010).

4.5.2 Paediatric GISTs

Approximatelly 1-2% of GISTs occur in the paediatric age group. Peadiatric GISTs are associated with a marked female predominance, are preferentially located in stomach, and show mainly epithelioid morphology. Although these tumors consistently express KIT protein, the majority lack *KIT* or *PDGFRA* mutations (Prakash et al. 2005; Miettinen et al. 2005; Janeway et al. 2007).

Unlike adults GISTs, these tumors quite often spread to lymph nodes. Interestingly, paediatric *KIT* wild-type GISTs lack the typical cytogenetic deletions seen in adult *KIT*-mutant GISTs and progress to malignancy without acquiring large-scale chromosomal aberrations (Janeway et al. 2007). The difference between paediatric *KIT* wild-type and adult GISTs of the stomach is further demonstrated by their separate clustering by gene expression profiling (Prakash et al. 2005), and it is very likely that these tumors are a separate clinicopathologic entity. In the pediatric wild-type GIST group, time to tumor progression was significantly longer on sunitinib than on prior Imatinib treatment, indicating that this patient group could benefit from sunitinib as first-line treatment (Heinrich et al. 2008; Janeway et al. 2009).

4.5.3 Famillial GISTs

Several heritable mutations in exon 8, exon 11, exon 13 and exon 17 of *KIT* and in exon 12 of *PDGFRA* have been identified in some families. The penetrance in these kindreds is high, and most affected family members will develop one or more GISTs during their life spam. The mean age of onset (44 years) is younger than that of sporadic GISTs (around 60 years) without gender difference. Most of these GISTs follow a benign course, and their morphology does not differ from that of their sporadic counterparts (Nishida et al. 1998; Isozaki et al. 2000; Kang et al. 2007).

The first to be reported was a Japanese family in which a deletion of one of two consecutive valine residues (codon 559 and 560, GTTGTT) was traced through three generations. Development of multiple GISTs was found in a 60-year-old Japanese woman (Fig. 6, case 5). Her nephew (case 10) also suffered from multiple benign GISTs. Analysis of the family pedigree revealed many family members suffering from symptoms

attributable to development of multiple GISTs (Fig. 6) includind case 9 (a niece of case 5) who underwent surgery for benign and malignant GISTs (Nishida et al. 1998).

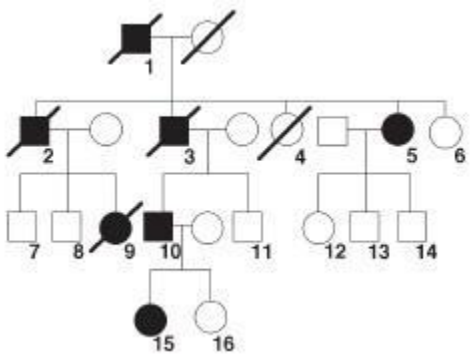

Figure 6. A family with multiple GISTs and mutation of the *KIT* gene. Family pedigree; filled symbols indicate family members with either intestinal obstruction or the *KIT* mutation or both. Squares, males; circles, females; symbols with a dash, dead cases. Adapted from Nishida et al. 1998.

4.5.4 GISTs in association with Carney´s triad and Carney´s dyad (Carney-Stratakis syndrome)

GISTs are part of Carney´s triad (gastric GIST, paraganglioma, and pulmonary chondroma) (Carney & Stratakis 2002) and Carney´s dyad (paraganglioma, gastric GIST) (Pasini et al. 2008), and these GISTs are *KIT/PDGFRA* wild-type. The genetic basis for Carney´s triad is not known, although it is thought to be sporadic rather than familial. In both conditions, the presence of multiple gastric GISTs is common. Carney´s dyad is transmitted as an autosomal dominant trait, and recently Pasini and colleagues (2008) demonstrated, in a subset of these GISTs, germline mutations of the genes coding for *Succinate Dehydrogenase subunits B*, *C*, or *D*, implying that other molecular mechanisms, rather than *KIT/PDGFRA* mutations, may play a role in the pathogenesis of GISTs in this setting (Pasini et al. 2008).

Recently, Zhang and colleagues (2010) reported a study of 104 GISTs in Carney triad, emphasizing the differences from sporadic GISTs. The clinical features of the triad include occurrence at a young age, female predilection, tumors multifocality, slow growth, frequent metastasis (often to lymph nodes), lack of response to Imatinib treatment, and

fatal outcome. In addition, this subset of GISTs occurs mainly in the gastric antrum, shows predominantly epithelioid morphology, and lack *KIT*, *PDGFRA*, or *SDH* mutations (Pasini et al. 2008). Interestingly, there is no correlation between conventional risk assessment and tumor behavior and, even with metastatic disease, clinical behavior is unpredictable (Liegl-Atzwanger et al. 2010).

5 Oncogenic kinase mutations in GIST

5.1 Receptor tyrosine kinase

Since the discovery of the first receptor tyrosine kinase (RTK) more than a quarter of a century ago, many members of this family of cell surface receptors have emerged as key regulators of critical cellular processes, such as proliferation and differentiation, cell survival and metabolism, cell migration and cell cycle control (Ullrich & Schlessinger 1990; Blume-Jensen & Hunter 2001).

Humans have 58 known RTKs, which fall into twenty subfamilies (Fig. 7). All RTKs have a similar molecular architecture, with a ligand-binding region in the extracellular domain, a single transmembrane helix, and a cytoplasmic region that contains the protein tyrosine kinase (TK) domain plus additional carboxy (C-) terminal and juxta-membrane regulatory regions.

The overall topology of RTKs, their mechanism of activation, and key components of the intracellular signaling pathways that they trigger are highly conserved in evolution from the nematode Caenorhabditis elegans to humans, which is consistent with the key regulatory roles that they play.

Furthermore, numerous diseases result from genetic changes or abnormalities that alter the activity, abundance, cellular distribution, or regulation of RTKs. Mutations in RTKs and aberrant activation of their intracellular signaling pathways have been causally linked to cancers, diabetes, inflammation, severe bone disorders, arteriosclerosis and angiogenesis. These connections have driven the development of a new generation of drugs that block or attenuate RTK activity (Lemmon & Schlessinger 2010).

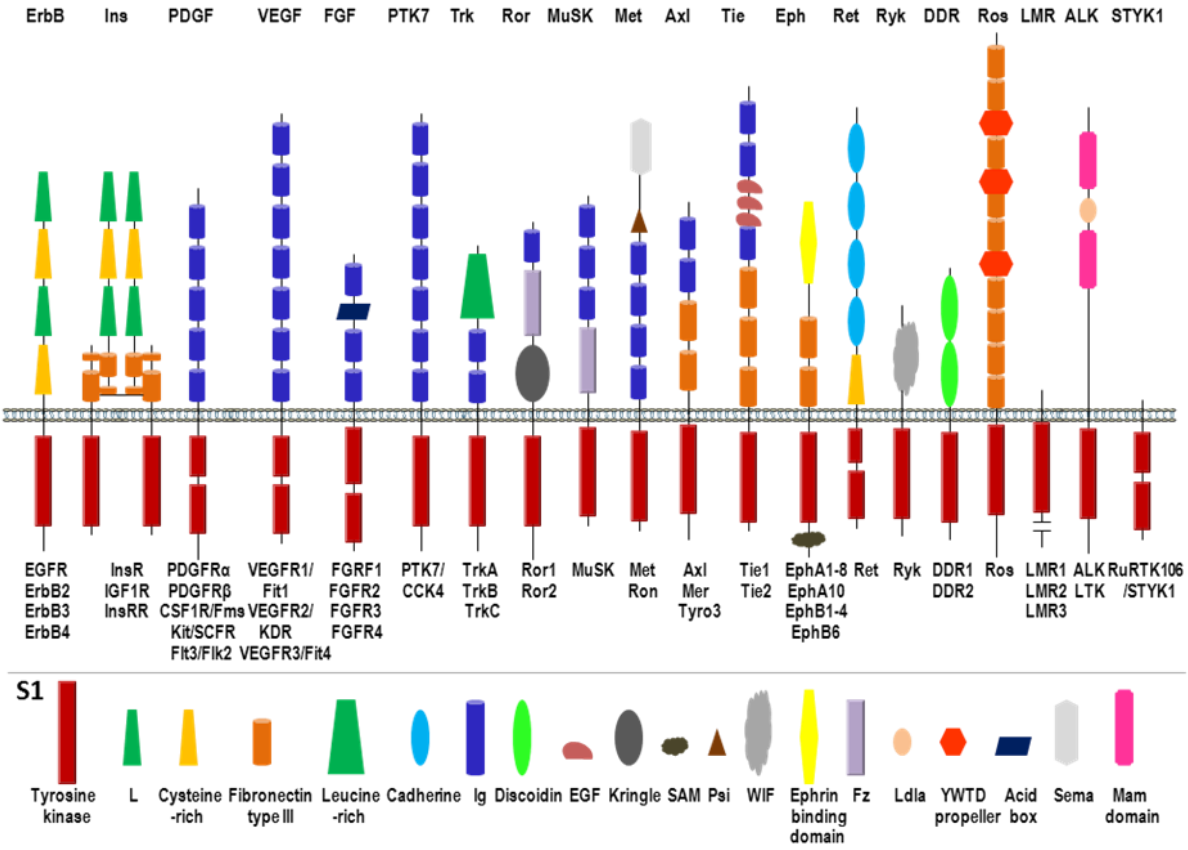

Figure 7. Human receptor tyrosine kinase families contain 20 subfamilies, shown here schematically with family members listed beneath each receptor. Structural domains are marked according to the key presented in Supplementary Figure **S1**. Adapted from Lemmon & Schlessinger 2010.

Type III receptor tyrosine kinase is a family of kinases sharing a structure that consists of five extracellular immunoglobulin-like domains, a transmembrane domain and a split kinase domain. KIT is a member of this family that includes PDGFRA and PDGFRB, as well as macrophage Clony-Stimulating-Factor 1 Receptor (CSF1R) and Fms-Like Tyrosine kinase 3 (FLT3) (Hanks et al. 1998).

5.1.1 KIT

KIT, a 145-kDa transmembrane glycoprotein is located on the proximal long arm of chromosome 4, and is the normal cellular homologue of the viral oncoprotein v-KIT. It is a member of the receptor tyrosine kinase subclass III family. This RTK receptor has an

extracellular (EC) ligand-binding domain containing five immunoglobulin-like (Ig-like) repeats, a single transmembrane domain, a juxtamembrane domain (JM), and two cytoplasmic kinase domains (TK I: ATP-binding pocket; and TK II: kinase activation loop; Fig. 8A) (Besmer et al. 1986; Stenman et al. 1989).

KIT is normally expressed by hematopoietic progenitor cells, mast cells, germ cells, ICCs, and also by certain human tumors (Tarn et al. 2005).

The KIT ligand, stem cell factor (SCF) is a homodimer of two four-helix bundles. Each SCF molecule binds to one molecule of KIT through contacts with the first three (of five) Ig-like domains in the KIT EC region. Binding of SCF to KIT results in receptor homodimerization, activation of the tyrosine kinase activity, and resultant phosphorylation of several signalling substrates known to promote cell growth and survival (Fig. 8B) (Blume-Jensen et al. 1991; Lemmon et al. 2010). Alternatively, oncogenetic KIT mutations in these receptors result in ligand-independent kinase activation (Fig. 8C).

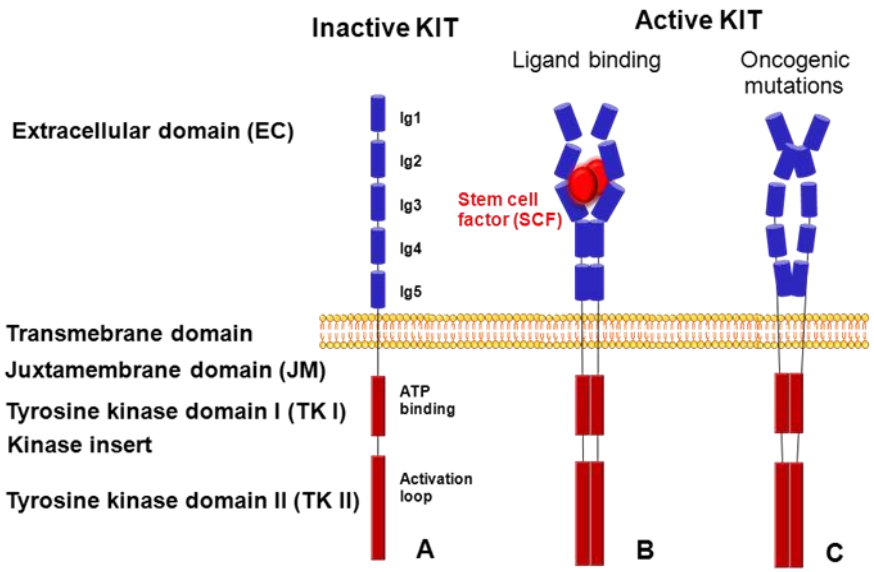

Figure 8. KIT structure, dimerization and kinase activation. (**A**) Schematic structure of KIT receptor; (**B**) Activation of KIT receptor occurs through the binding of extracellular ligands SCF (stem cell factor) that cause receptor dimerization; (**C**) Oncogenic mutations in this receptor can cause ligand-independant receptor activation. Adapted from Chen et al. 2004; Yuzawa et al. 2007; Liegl-Atzwanger et al. 2010; Lemon & Schlessinger 2010; Corless et al. 2011.

As first reported by two groups in 1998, 95% of GISTs are immunohistochemically positive for the receptor tyrosine kinase KIT (also known as CD117 in the standardized terminology of leukocyte antigens), and this remains a crucial diagnostic marker for these tumors. At the same time, Hirota and colleagues published their groundbreaking discovery of KIT mutations in GISTs (Hirota et al. 1998; Kindblom et al. 1998).

5.1.1.1 KIT gene mutations

It is now established that 70-80% of GISTs harbour a *KIT* gene mutation (Fig. 9), that these mutations lead to the constitutive activation of the kinase and that mutant KIT is a clinically important therapeutic target in GISTs (Hirota et al. 1998; Rubin et al. 2001).

The most common primary mutations in KIT affected the juxtamembrane domain that is encoded by exon 11. Two-thirds of GISTs harbor mutations in exon 11, which disrupt the normal jextamembrane secondary structure that prevents the kinase activation loop from swinging into the active conformation (Mol et al. 2004). These mutations include in-frame deletions, insertions and substitutions, or combinations of these. The deletions are associated with a shorter progression-free and over-all survival in comparison to the other exon 11 mutations (Singer et al. 2002; Corless et al. 2004). In particular, deletions involving codon 557 and/or codon 558 are associated with malignant behavior (Wardelmann et al. 2003).

Aside from exon 11 mutations, between 7% and 10% of GISTs have a mutation in an extracellular domain that is encoded by exon 9. These mutations are thought to mimic the conformational change that the extracellular KIT receptor undergoes when SCF is bound. Importantly, the kinase domain in exon 9-mutant KIT is essentially the same as in wild-type KIT, and this has an effect on inhibitor sensitivity. Also important is that these mutations occur in tumors that arise in the small and large intestine, but they are rarely seen in gastric GISTs, and their gene expression profile differs from that of exon 11-mutant tumors (Antonescu et al. 2004).

Mutations in the activation loop (which is encoded by exon 17) of the kinase are uncommon, and they stabilize the active conformation. Primary mutations, such as K642E in the ATP-binding region (encoded by exon 13), are also uncommon (Lasota et al. 2008).

Secondary mutations are concentrated in two regions of the KIT kinase domain (Fig. 9). One is the ATP-binding pocket, encoded by exons 13 and 14, mutations of witch directly interfere with drug binding. The second is the activation loop, where mutations can stabilize KIT in the active conformation and thereby hinder drug interaction. Compounding the problem, almost all of the secondary exon 17 or 18 *KIT* mutations can also serve as primary activation mutations, thus potentially increasing kinase activity. By contrast, the secondary ATP-binding pocket mutations do not cause intrinsic kinase activation (Tamborini et al. 2004; Liegl et al. 2008).

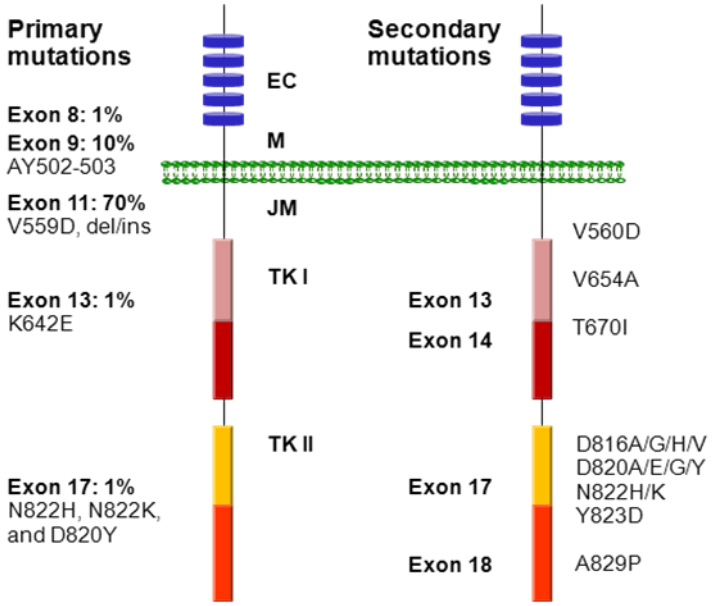

Figure 9. KIT receptor tyrosine kinase and distribution of primary and secondary mutations in GIST. EC, Extracellular domain; M, Membrane; JM, Juxtamembrane domain; TK I, Tyrosine kinase domain I; TK II, Tyrosine kinase domain II. Adapted from Gajiwala et al. 2009; Corless et al. 2011.

By immunohistochemistry, KIT is detected at the surface of GIST cells, but strong staining is commonly observed in the cell cytoplasm and is sometimes concentrated in a perinuclear, dot-like pattern (Pauls et al. 2005). Xiang and colleagues (2007) have observed that *KIT* with an exon 17 mutation (D816V) is concentrated in the Golgi of transfected A375 cells. Furthermore, mutant KIT that has been further modified with a Golgi-localization motif retains its ability to activate downstream signaling, raising the interesting possibility that signaling from mutant *KIT* can occur directly from the Golgi.

Preliminary studies of signal transduction in GISTs demonstrate a somewhat homogenous pattern of signal transduction activation. Tumor extracts from *KIT*-mutant GISTs demonstrate evidence of activation of downstream signaling pathways (Fig. 11), including the MAPK pathway (which consists of RAF, MEK and MAPK), the PI3K-AKT pathway and signal transducer and activator of transcription 1 and 3 (STAT1 and STAT3), and p70/85S6K (Rubin et al. 2001; Corless et al. 2004). In contrast, the JNK and STAT5 pathways are not activated (Heinrich et al. 2003). Using specific inhibitors of KIT, MEK1/2, PI3K or mTOR, it has been shown that activation of the PI3K/mTOR, but not the MEK/mitogen-activated protein kinase pathway, is essential to KIT-mediated oncogenic signalling in GISTs. Correspondingly, selective inhibitor of the PI3K/mTOR pathway reduces proliferation and increases apoptosis (Corless et al. 2004).

5.1.2 PDGFRA

Platelet-Derived Growth Factor Receptors (PDGF-R) are cell surface tyrosine kinase receptors for members of the platelet-derived growth factor (PDGF) family. PDGF-R are important factors regulating cell proliferation, cellular differentiation, cell growth, development and many diseases including cancer (Williams 1989; Heldin 1992). There are two forms of the PDGF-R, alpha and beta each encoded by a different gene. These two receptor isoforms dimerize upon binding the PDGF dimer, leading to three possible receptor combinations, namely -αα, -ββ and -αβ. The α-receptore binds all three forms of PDGF, whereas the β-receptor binds only PDGF ββ. The extracellular region of the receptor consists of five immunoglobulin-like domains while the intracellular part is a tyrosine kinase domain (Yarden et al. 1986; Kawagishi et al. 1995).

Human *alpha-Platelet Derived Growth Factor Receptor* (*HGMW*-approved symbol *PDGFRA*) gene spans approximately 65 kb and contains 23 exons (Kawagishi et al. 1995). PDGFRA is normally expressed in the digestive musculature into fibroblast-like cells, cells closely associated to ICC and myenteric ganglionic cells (c-Kit-negative fibroblast-like cells express platelet-derived growth factor receptor alpha in the murine gastrointestinal musculature (Iino et al. 2009; Kurahashi et al. 2011).

PDGFRA is activated in approximately 8% of GISTs that harbor mutations in the *PDGFRA* juxtamembrane domain (encoded by exon 12), the ATP-binding domain

(encoded by exon 14) or the activation loop (encoded by exon 18) (Fig. 10). Consistent with their extensive functional overlap, *KIT* and *PDGFRA* mutations are mutually exclusive in GISTs (Heinrich et al. 2003; Hirota et al. 2003). Altogether, about 85 % of gastrointestinal stromal tumors have mutation in one of these two kinase genes.

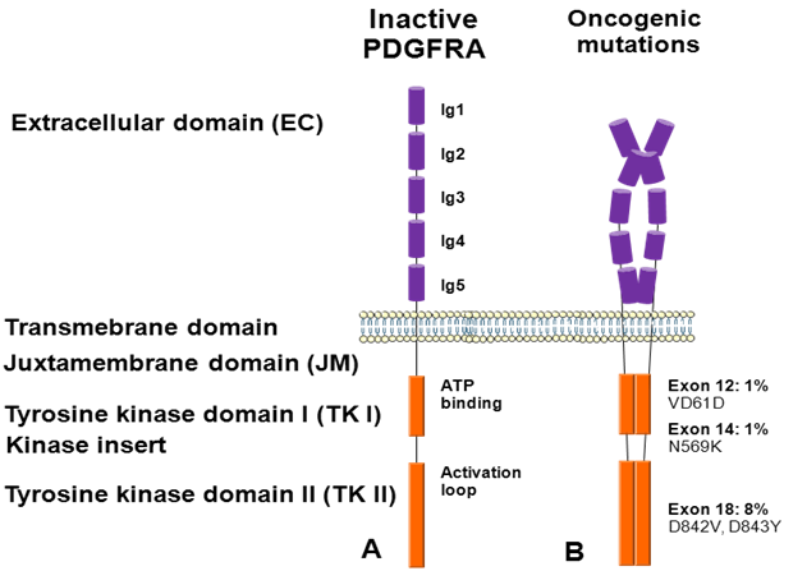

Figure 10. PDGFRA schematic structure. (**A**) Schematic structure of PDGFRA receptor tyrosine kinase; (**B**) Oncogenic mutations in this receptor can cause ligand-independant receptor activation. Adapted from Corless et al. 2011; Liegl-Atzwanger et al. 2010.

5.2 Oncogenic signaling in *KIT* and *PDGFRA*-mutant GISTs

Dimerization of KIT or PDGFRA proteins at the cell surface through binding of stem cell factor (SCF) or one of three forms of PDGF, mutational activation, leads to autophosphorylation (P) of tyrosine residues. The uncontrolled RTK activity results in the activation of PI3K-AKT and MEK-MAPK pathways accompanied by relatively low level signal transducer and activation of transcription (STAT) 1 and STAT3 activations, leading to alterations in cell cycle, protein translation, metabolism, and apoptosis (Fig. 11) (Rubin et al. 2001; Corless et al. 2004).

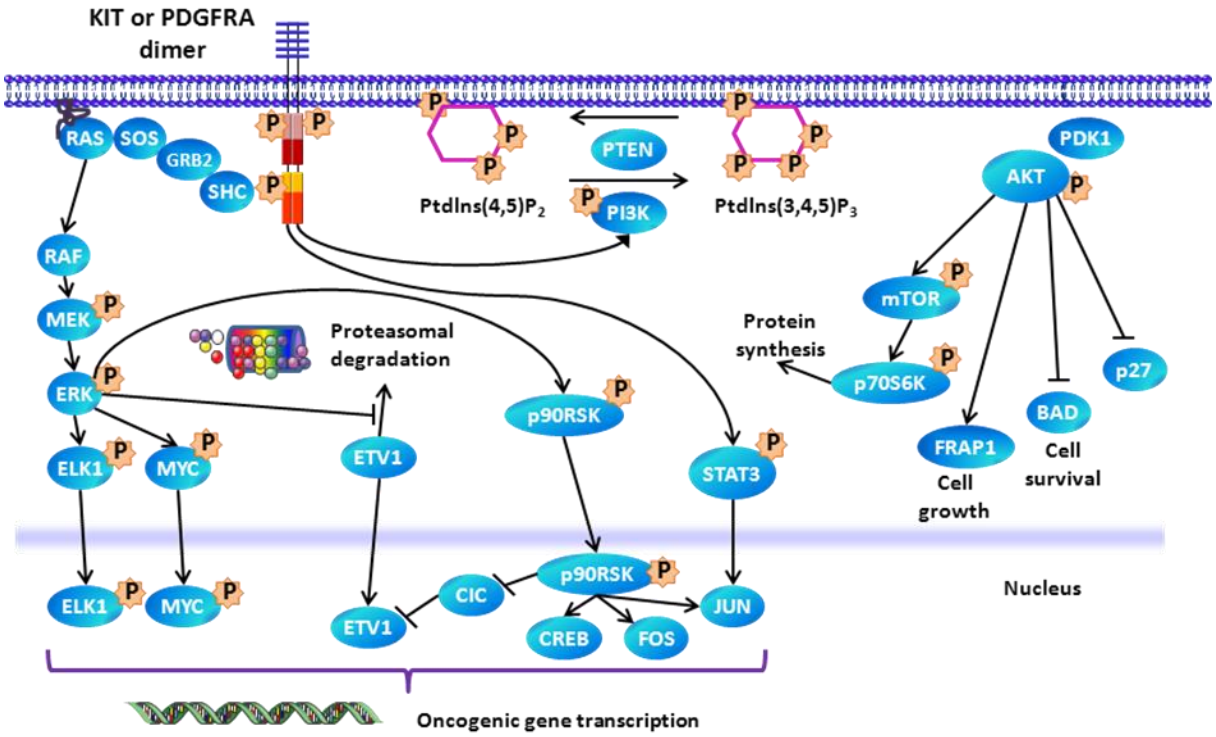

Figure 11. Oncogenic signaling in *KIT* and *PDGFRA*-mutant GISTs. Dimerization of KIT proteins at the cell surface, through the binding of stem cell factor (SCF) or mutational activation, leads to autophosphorylation (P) of tyrosine residues. Phosphotyrosines provide docking sites for a complex of proteins (SHC, GRB2 and SOS) that activated RAS. In thurn, RAS activates the MAPK cascade (RAF, MEK and ERK), leading to changes in gene expression through MYC and ELK1. In addition, the activation of p90RSK by ERK leads to the activation of CREB, increased transcriptional activity of FOS and JUN, and the downregulation of capicua (CIC), which is a transcription suppressor of ETS translocation variant 1 (ETV1) (Chi et al. 2010; Dissanayake et al. 2011). Signal transducer and activator of transcription 3 (STAT3) phosphorylation by KIT also promotes JUN transcription. Proteasomal degradation of ETV1 a crucial developmental regulator of ICCs and GISTs, is regulated by the activity of ERK. Kinase activity of mutated *KIT* (or *PDGFRA*) induces the activation of ERK and thereby decreases the degradation of ETV1 in GIST. Finally, activation of PI3K by KIT leads to the conversion of phosphatidylinositol-4,5-bisphosphate (Ptdlns(4,5)P_2) to the triphosphate (Ptdlns(3,4,5)P_3) form that allows docking of PDK1 and AKT at the membrane. Phosphorylation of AKT then leads to alterations in protein translation, metabolism and apoptosis through mediators, mTOR and p70S6K. PTEN is a phosphatase (and tumor suppressor) that

converts Ptdlns(4,5)P_2 back to (Ptdlns(3,4,5)P_3. Adapted from Rubin et al. 2007; Liegl-Atzwanger et al. 2010; Corless et al. 2011.

These data will doubtless be useful in the development of new targeted therapies for GISTs.

5.3 Other driver mutations

Approximately 15% of GISTs do not have a detectable mutation in either *KIT* or *PDGFRA*. In other respects these so-called "wild-type" GISTs are clinically indistinguishable from *KIT*-mutant or *PDGFRA*-mutant GISTs, as they have an identical morphology, express high levels of KIT and occur anywhere in the gastrointestinal tract. Phosphorylated KIT is detectable in these tumors, suggesting that KIT is still activated (Duensing et al. 2004), but the mechanism of this activation is unclear.

However, recent studies have revealed that wild-type GISTs are a heterogeneous group and display various oncogenic mutations. For example, the *BRAF V600E* substitution that is common in papillary thyroid carcinoma and melanoma is present in up to 13% of wild-type GISTs (Hostein et al. 2010; Antonescu 2011). *HRAS* and *NRAS* gene mutations also occur, but are much more rare. Because BRAF and RAS proteins are constituents of the MAPK signaling cascade, they can result in KIT-independant growth stimulation (Fig. 12A), and are possible causes of resistance to KIT and PDGFRA kinase inhibitors (Corless et al. 2011).

Defects in the Succinete DeHydrogenase (SDH) complex of respiratory chain complex II have recently been identified in wild-type GISTs (Fig. 12B). This complex, which is comprised of four subunits (SDHA, SDHB, SDHC and SDHD), oxidizes succinate to fumarate as part of the mitochondrial Kreb's cycle. Germline mutations in *SDHB*, *SDHC* or *SDHD* increase the risk not only of the development of GIST, but also of the development of paragangliomas (known as Carney-Stratakis syndrome). Interestingly, some wild-type GISTs lacking *SDH* gene mutation show either a marked reduction or an absence of SDHB protein expression by immunohistochemistry, and a corresponding loss of respiratory chain complex II enzymatic activity (Janeway et al. 2011). However, *SDHB*, *SDHC* and *SDHD* mRNA levels are comparable to those in *KIT*-mutant GISTs, which

suggests that SDHB downregulation occurs at the level of protein translation (Corless et al. 2011).

The tumorigenic mechanisms of SDH loss-of-function in GISTs remain to be studied, but it is possible that the resulting elevation of succcinate levels may negatively regulate prolyl hydroxylase. This enzyme is an important regulator of Hypoxia-Inducible Factor 1α (HIF1α) levels, and HIF1α is a transcriptional activator of Insulin-like Growth Factor 2 (IGF2) and Vascular Endothelial Growth Factor (VEGF) (Fig. 12C). In keeping with this model, VEGF expression is higher in wild- type GISTs than in *KIT*-mutant GISTs (Antonescu et al. 2004).

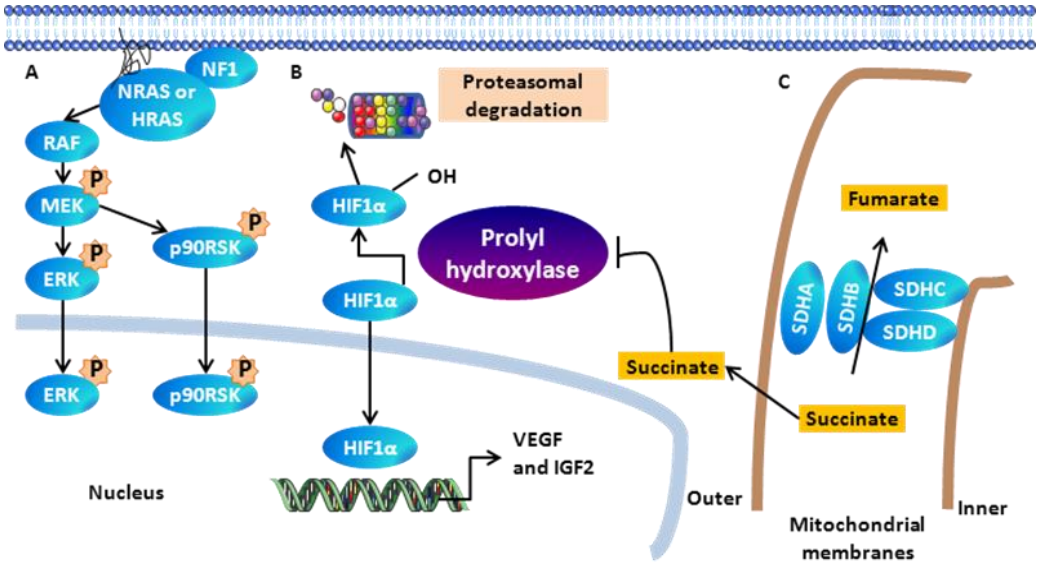

Figure 12. Oncogenic signaling in wild-type GISTs. (**A**) Mutations in NeuroFibromin 1 (NF1), *RAS* or *BRAF* can all increase signalling through the MAK cascade; (**B**) The Succinate Dehydrogenase (SDH) complex is comprised of four subunits, two of which (SDHC and SDHD) are anchored in the inner mitochondrial membrane. SDHA and SDHB coordinate the oxidation of succinate to fumarate as part of the Kreb´s cycle. Loss of SDH complex activity owing to mutational inactivation of any of the SDH subunits leads to the cytoplasmic accumulation of succinate, which downregulates prolyl hydroxlase. This enzyme negatively regulates Hypoxia-Inducible factor 1α (HIF1α): through its hydroxylation by the prolyl hydroxlase conducts to its proteasomal degradation; (**C**) Therefore, increased succinate levels lead to increased levels of HIF1α, which can enter the nucleus and activate the transcription of VEGF and IGF2. Adapted from Corless et al. 2011.

Approximately 50% of wild-type GISTs show high expression of Insulin-like Growth Factor 1 Receptor (IGF1R). Whether this correlates with SDH complex activity remains to be determined, but it is possible that an IGF autocrine loop is sustained in part by loss of SDH and upregulation of IGF2 expression (Corless et al. 2009). IGF1R signals through both the MAKP and the PI3K-AKT pathways.

It is estimated that 7% of patients with neurofibromatosis type I (NF1) develop one or more GISTs. Most arise in the small intestine and they do not readily metastasize. The majority of these GISTs are wild-type for *KIT* and *PDGFRA*, but they show either somatic mutation or loss of the remaining wild-type *NF1* allele (Anderssonn et al. 2005; Miettinen et al. 2006; Kang et al. 2007).

Unlike GISTs in adults, those that arise in paediatric patients (approximately 1-2% of all GISTs) are rarely positive for *KIT* or *PDGFRA* mutations. These tumors, which often metastasize but which tend to grow slowly, have a different gene expression signature from adult type GISTs (Janeway et al. 2007; Agaram et al. 2008).

5.4 Chromosomal and molecular alterations during GIST progression

Although oncogenic kinase mutations have an important role in the development of GISTs, other genetic events are important in their clinical progression. Approximately two-thirds of GISTs demonstrate either monosomy of chromosome 14, or partial loss of 14q (Fukasawa et al. 2000; Heinrich et al. 2003; Corless et al. 2011). Interestingly, these chromosome 14 abnormalities are observed both in *KIT*-mutant and in *PDGFRA*-mutant GISTs (Wozniak et al. 2007). Loss of the long arm of chromosome 22 is observed in approximately 50% of GISTs (Bergmann et al. 1998; Heinrich et al. 2003; Wozniak et al. 2007). Losses on chromosomes 1p, 9p, 11p and 17p are successively less common than 14q and 22q losses, but are more significantly associated with malignancy (Gunawan et al. 2007). Looses on chromosomes 10, 13q and 15q have also been reported in GISTs (Gunawan et al. 2007; Ylipaa et al. 2011). Gain on chromosome 8q, 3q and 17q are associated with metastatic behavior (Ylipää et al. 2011).

Ylipää and colleagues (2011) conducted a comprehensive, high-resolution, whole-genome array comparative genomic hybridization analysis to map the recurrent copy number aberrations in 42 GISTs (Fig. 13). They also proposed a new tumor-progression

genetic staging system termed genomic instability stage (GIS) to complement the current GIST staging system, which is based on tumor size, mitotic index (MI), and *KIT* and/or *PDGFRA* mutations.

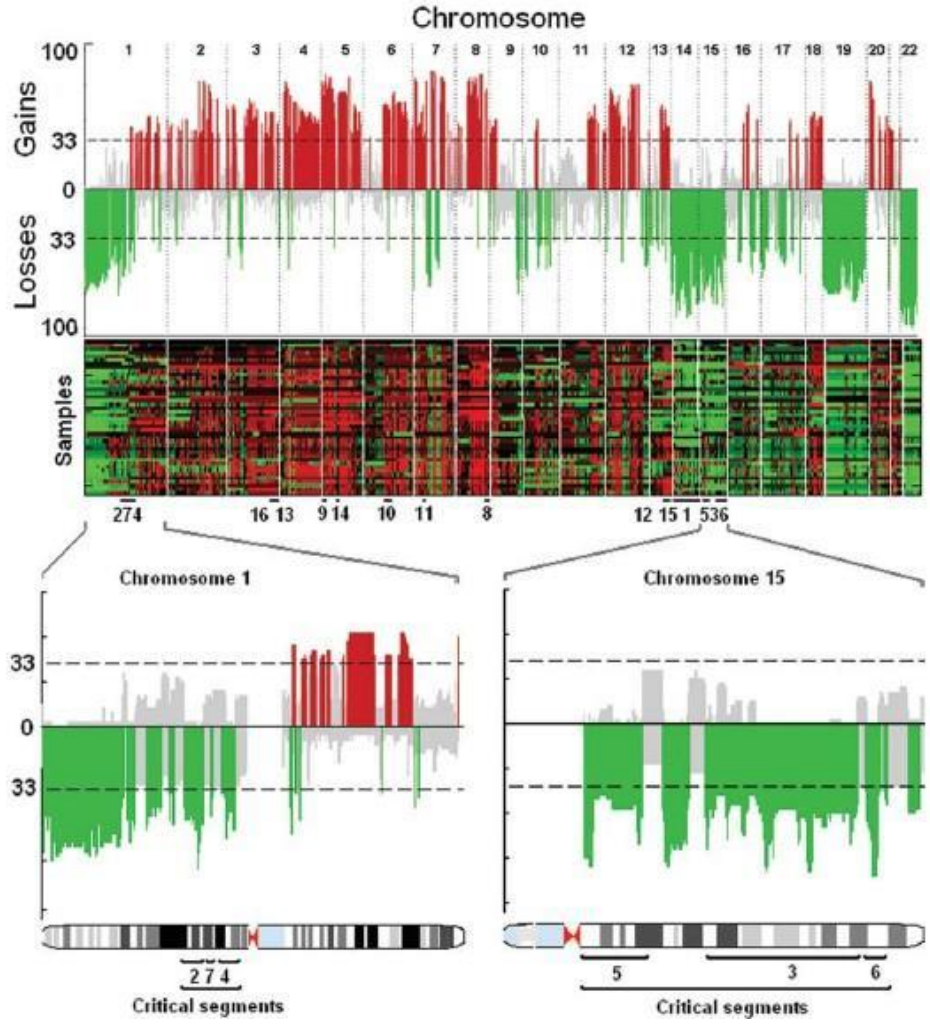

Figure 13. Skyline plots and heat maps of signature gene copy number aberrations for GISTs. The recurrence of copy number aberrations throughout the genomes is shown both in skyline plots and heat maps. The value on the y-axis of each skyline plot is the percentage of patients who had tumors that had gains (positive axis; red) or losses (negative axis; green) in corresponding genomic loci. The probes are aligned evenly in chromosome order on the x-axis. The dashed line indicates the threshold for a significant number of patients whose tumors share the same aberration (14 patients for GIST). The significance threshold is computed with the use of a permutation test. Recurrence rates that exceed this threshold are deemed significantly recurrent and are color-coded to emphasize

the locations. Gray color represents a no significant amount of aberration in the locus. The lower plots in highlight chromosomes 1 and 15, both of which contain 3 critical segments. Critical segments are contiguous genomic regions of recurrent aberration that harbor at least 1 dosage-sensitive, survival-affecting gene. Losses in 1p, 14q, 15q, and 22q are markedly more common in GIST. Adapted from Ylipää et al. 2011.

6 Human cell lines and animal models in research of GIST

6.1 Animal models in research

Research workers usually use laboratory animals as models (Fig. 14) of humans or some other target species. The research involves a long-term objective, such as developing a new drug for diabetics, screening a particular compound for human toxicity, studying a gene or mutation found in both animals and humans or studying a fundamental process such as gene transcription. The short-term objective is to use the animal model in experiments to determine how it responds to the treatments.

Animal models representing specific taxonomic groups in the research and study of developmental processes are also referred to as model organisms. There are three main types of animal models Homologous, Isomorphic and predictive. Homologous animals have the same causes, symptoms and treatment options as would humans who have the same disease. Isomorphic animals share the same symptoms and treatments.

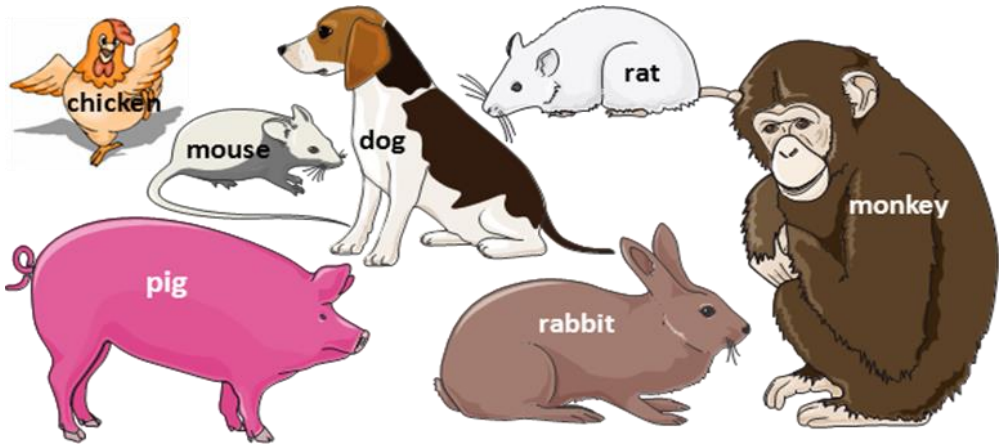

Figure 14. Animal models. Animals, from chicken, mouse, rats, rabbit, dogs, pig to monkeys, have the same organs (heart, lungs, brain etc.) and organ systems (gastrointestinal, respiratory, cardiovascular, nervous systems etc.) which perform the same functions in pretty much the same way. The similarity means that nearly 90% of the veterinary medicines that are used to treat animals are the same as, or very similar to, those developed to treat human patients.

If it is a faithful model of humans, then humans should respond in the same way. Animals, and other models, are used because the research cannot be done on humans for practical or ethical reasons.

6.2 Human GIST cell lines

To examine the relevance of c-KIT signaling in the pathobiology of GIST, Tuveson and colleagues established a GIST cell line, GIST882, from a patient with metastatic GIST. Both the primary GIST and the GIST882 cell line expressed *c-KIT* allele with an exon 13 missense mutation, resulting in a single amino acid substitution, K642E, in the proximal part of the split tyrosine kinase domain (Tuvenson et al. 2001). This GIST cell line was first reported, and to this day human GIST882 Imatinib sensitive cell line is used (Deneubourg et al. 2011).

In 2002, Taguchi and colleagues published study of GIST cell line, GIST-T1. It has a heterogenic 57-bp deletion in exon 11 to produce a mutated c-KIT, which results in constitutive activation of c-KIT (Taguchi et al. 2002; Jin et al. 2006).

Inhibition of KIT oncoproteins by Imatinib induces clinical responses in most GIST patients. However, many patients develop Imatinib resistance due to secondary KIT mutations. Heat shock protein 90 (HSP90) protects KIT oncoproteins from proteasome-mediated degradation, and Bauer and colleagues therefore did preclinical validations of the HSP90 inhibitor, 17-allylamino-18-demethoxy-geldanamycin (17-AAG), in an Imatinib-sensitive GIST cell line (GIST882) and in novel Imatinib-resistant GIST lines that are either dependent on (GIST430 and GIST48) or independent of (GIST62) KIT oncoproteins (Bauer et al. 2006).

In the literature, we can also see GIST cell line with the *PDGFRA D842V* mutation (Heinrich et al. 2012).

6.3 Animal models in research of GISTs

In this part we would like to highlight the importance and usefulness of mice or mouse models in biological and cancer research by using the Kit receptor tyrosine kinase as an example.

In 2005, a mouse model of GIST has been developed by a knock-in gene targeting strategy, which introduced a *Kit* gene K641E mutation, originally identified in sporadic human GISTs and in the germ line of familial GIST syndrome patients (Rubin et al. 2005). Homozygous and heterozygous *Kit* K641E mice develop gastrointestinal pathology with complete penetrance and all *Kit* K641E homozygotes die by age 30 weeks due to gastrointestinal obstruction by hyperplasic interstitial cells of Cajal (ICC) or GISTs. Heterozygous mice have less extensive ICC hyperplasia and smaller GISTs, suggesting a dose-response relationship between oncogenic activated Kit and ICC proliferation (Rubin et al. 2005). In addition to ICC hyperplasia and GISTs, homozygous *Kit* K641E mice exhibit loss-of-function Kit phenotypes, including white coat color, decreased numbers of dermal mast cells, and sterility, indicating that despite its oncogenic activity the mutant form cannot accomplish many activities of the wild-type gene. *Kit* K641E reproduces the pathology associated with the familial GIST syndrome and thus is an excellent model to study Kit pathway activation, ICC biology, GIST pathogenesis, and preclinical validations of GIST therapies and mechanisms of drug resistance (Rubin et al. 2005; Deneubourg et al. 2011).

In the literature we can see a few studies based on cell transplantation in animal models. For example, Bernex and colleagues analyzed spatial and temporal patterns of c-kit-expressing cells in $W^{lacZ/+}$ and W^{lacZ}/ W^{lacZ} mouse embryos (1996). They specifically marked the *c-kit*-expressing cells and followed their fate during embryogenesis. A mutation was introduced by gene targeting at the W/Kit locus in mouse embryonic stem cells. The *lacZ* reporter gene was inserted into the first exon of *c-kit*, thus creating a null allele, called W^{lacZ}. The lacZ expression reflects normal expression of the c-kit gene in $W^{lacZ/+}$ embryos. The comparison of the patterns of lacZ-expressing cells between $W^{lacZ/+}$ and W^{lacZ}/W^{lacZ} embryos allowed us to detect where and when melanoblasts, primordial germ cells and hematopoietic progenitors failed to survive in the absence of Kit. Therefore, ICCs do not depend on Kit expression during embryogenesis. These results indicate that the function if the *c-kit* gene is only required for the postnatal development of the ICC (Bernex et al. 1996). In 2003, Sommer and colleagues published study wherever

heterozygous mutant $Kit^{V558\Delta}/+$ mice reproduce human familial GISTs for the study of the role and mechanisms of Kit in neoplasia (Sommer et al. 2003).

Olson and Soriano have generated conditional knock-in mice with mutations in PDGFRA that drive increased kinase activity under the control of the endogenous PDGFRA promoter. In embryos, increased PDGFRA signaling leads to hyperplasia of stromal fibroblasts, which disturbs normal smooth muscle tissue in radially patterned organs. In adult mice, elevated PDGFRA signaling also increases connective tissue growth, leading to a progressive fibrosis phenotype in multiple organs. Increased PDGFRA signaling in an Ink4a/Arf-deficient genetic background leads to accelerated fibrosis, suggesting a new role for tumor suppressors in attenuating fibrotic diseases. These results highlight the role of PDGFRA in normal connective tissue development and homeostasis and demonstrate a pivotal role for PDGFRA signaling in systemic fibrosis diseases (Olson & Soriano 2009).

Studies engaged of gastrointestinal neoplasms and GISTs behavior in the digestive tract in rats (Mukaisho et al. 2006; Fujimoto et al., 2006), dogs (Frost et al. 2003; Maas et al. 2007), horses (Hafner et al. 2001; Haga et al., 2008), ibex (Velarde et al., 2008), guinea pigs (Frantisek et al. 2008), rhesus macaque (Bielefeldt-Ohmann et al. 2005) and chimpanzee (Saturday et al., 2005).

7 Treatment of GastroIntestinal Stromal Tumor

The main treatment for localized GISTs is surgical resection. The goal of surgery is complete gross resection with preservation of an intact pseudocapsule. These tumors should be handled carefully to avoid tumor rupture, which confers a very high risk of intra-abdominal dissemination. In a large retrospective series, patients whose complete resection was complicated by tumor rupture had significantly shortened survival compared with patients who had complete resection without tumor rupture (Shiu et al. 1982; Ng et al. 1992).

Generally, segmental tumor resection is recommended with the goal of obtaining negative microscopic margins. However, simple enucleation of the tumor should be avoided. In skilled hands, laparoscopic surgery can be especially from the stomach. This approach decreases morbidity and shortens hospital stay and has local recurrence rates similar to open procedures (Shiu et al. 1982; Nguyen et al. 2006).

Metastasis typically presents with tumors isolated in the peritoneal cavity or the liver, or both. Historically, the median survival of patients with advanced GISTs was between 10 and 20 months (Joensuu et al. 2002). Before the pre-TKI era, treatment options were extremely limited for patients with unresectable or metastatic gastrointestinal stromal tumors. These tumors respond poorly (0% - 27%) to conventional cytotoxic chemotherapy agents and radiation therapy (Dematteo et al. 2002; Demetri et al. 2010).

7.1 Target therapy of GISTs

Targeted therapy is a type of medication. More precisely targeted cancer therapies are drugs or other substances that block the growth and spread of cancer by interfering with specific molecules involved in tumor growth and progression. Because scientists often call these molecules “molecular targets,” targeted cancer therapies are sometimes called “molecularly targeted drugs,” “molecularly targeted therapies,” or other similar names. By focusing on molecular and cellular changes that are specific to cancer, targeted cancer therapies may be more effective than other types of treatment, including chemotherapy and radiotherapy, and less harmful to normal cells (NCI Dictionary of Cancer Terms, 2012).

Now is targeted therapy the first choice of treatment for GIST that cannot be removed completely with surgery.

7.1.1Targeted therapy of GISTs with Imatinib mesylate

Imatinib mesylate (STI571, Gleevec) is a 2-phenylpyrimidine (Fig. 15) derivative that blocks the binding of adenosine triphosphate to ABL kinase. Developed by Dr. Brian Druker in collaboration with Novartis Pharma, this drug has received worldwide attention for its effectiveness against chronic myelogenous leukemia (CML). The BCR-ABL fusion gene product of the Philadelphia chromosome in CML is responsible for driving tumor proliferation (Mauro et al. 2002).

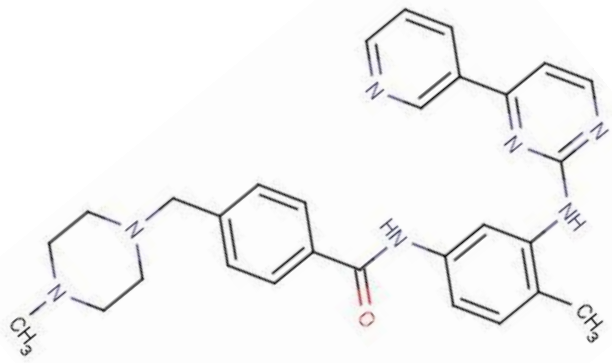

Figure 15. Chemical structure of Imatinib mesylate. Molecular formula: $C_{29}H_{31}N_7O$. From Drug Bank, 15.6. 2012.

Imatinib is not entirely specific for ABL and has significant inhibitory activity against related tyrosine kinases ARG (ABL-related kinase), PDGFRA, PDGFRB, and KIT (Fig. 16). Two important observations made in 1999 suggested that Imatinib might be effective against GISTs. The first was that Imatinib could block the in vitro kinase activity of both wild-type KIT and a mutant KIT isoform commonly found in GISTs (point mutation in exon 11) (Heinrich et al. 2000). The second observation was that Imatinib inhibited the growth of a GIST cell line containing a KIT gene mutation (Tuveson et al. 2001). In part, on the basis of these preclinical findings, a patient with GIST metastatic to the liver was granted compassionate use of Imatinib mesylate in March 2000. Within a matter of weeks, metastases in this patient decreased in size by up to 75%, and six of 28

hepatic lesions were no longer detectable on follow-up MRI scans after 8 months of therapy. This clinical response correlated with a near complete inhibition of [^{18}F]fluorodeoxyglucose PET uptake on position emission tomography scan, and a post-treatment biopsy showed a marked decrease in tumor cellularity and extensive myxoid degeneration (Fig. 17). Although CT shows greater anatomic detail, PET can reveal small metastases and establish baseline metabolic activity, which can later aid assessment of therapy effectiveness. Imatinib was well tolerated in this patient, and all cancer-related symptoms disappeared (Joensuu et al. 2001).

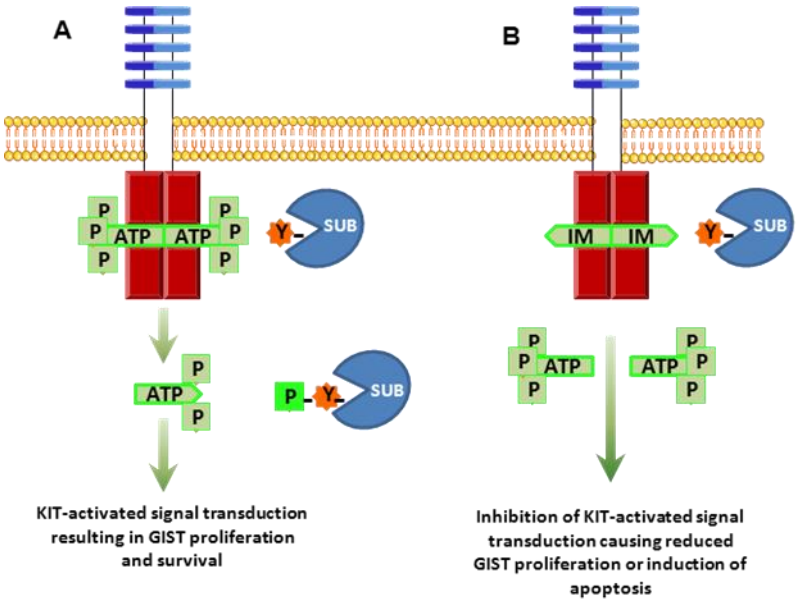

Figure 16. Mechanism of action of Imatinib Mesylate. (**A**) Normally, ATP binds to the active site of KIT or PDGFRA where it donates a phosphate to either KIT or PDGFRA, resulting in autoactivation, or to substrate molecules (SUB), resulting in activation of signal transduction; (**B**) Imatinib is a competitive inhibitor, binding to the same site as ATP, thus preventing phosphorylation of downstream substrates and resulting in inhibition of KIT or PDGFRA signalling. Adapted from Rubin et al. 2007.

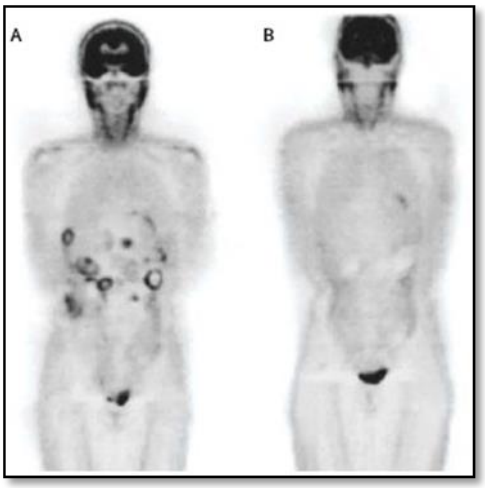

Figure 17. PET studies with 18F-fluorodeoxyglocose in a patient with gastrointestinal stromal tumor with intra-abdominal dissemination. The study shown in (**A**) was done before Imatinib therapy. Note the increased PET signal in the right renal pelvis, indicative of hydronephrosis. After 4 weeks of therapy with Imatinib (**B**), metabolic activity, as shown by loss of PET signal, was lost in the tumor nodules and the right kidney. From Rubin et al. 2007.

The success in treating the first GIST patient with Imatinib quickly led to a multicenter trial (CSTIB2222) that included the Dana-Farber Cancer Institute, Fox-Chase Cancer Center, Oregon Health & Science University Cancer Institute, and the University of Helsinki (Demetri et al. 2002). In all, 147 patients with advanced, unresectable and KIT-positive GIST were enrolled. Patients were randomly assigned to either 400 mg or 600 mg per day in a single oral dose; patients on 400 mg were allowed to go to 600 mg if their tumor progressed. With a minimum follow-up of 6 months, partial responses were observed in 54% of patients, and an additional 28% had stable disease. Disease progression was seen in only 14% of patients during initial follow-up.

Similar results were reported for the European Organization for Research and Treatment of Cancer Soft Tissue and Sarcoma Group phase I study of Imatinib for patients with advanced soft tissue sarcomas, including GISTs (Van Oosterom et al. 2001). Forty patients, of whom 36 had GISTs, were treated with dose levels from 400 mg to 1,000 mg daily, with therapy continuing until progression, unacceptable toxicity, or patient refusal to proceed. A dose of 500 mg bid resulted in dose-limiting toxicities (mostly nausea and vomiting) in five of eight patients. Substantial activity was seen only in the GIST patients, with 19 (53%) of 36 patients having a partial response and only seven failing therapy

during 9 months of follow-up. By contrast, none of the four patients with non-GIST sarcomas had a demonstrable response to Imatinib.

On the basis of the results of the CSTIB2222 trial and the European Organization for Research and Treatment of Cancer trial, Imatinib was approved by the US Food and Drug Administration for the treatment of unresectable and metastatic GIST on February 1, 2002. Preliminary reports from ongoing phase III trials of Imatinib for GIST treatment in both Europe and the United States confirm the phase II results (Benjamin et al. 2003). Trials of adjuvant and neoadjuvant treatment of GISTs with this drug are also underway. There are several excellent reviews that provide additional details on the use of Imatinib in the clinical management of GISTs (Demetri 2002; Joensuu et al. 2002; Corless et al. 2004).

7.1.1.1 Optimal dose of Imatinib

Several separate clinical studies have assessed the efficacy of Imatinib mesylate dose levels. Two randomised, phase III trials to compare the efficacy of 400 mg of Imatinib given either once or twice a day were done in Europe and Australasia, and North America (Tab. 3). The trial designs were intentionally similar except that the primary endpoints differed (progression free survival in the European Organisation for Research and Treatment of Cancer (EORTC) trial (Benjamin et al. 2003) in Australasia and overall survival in the US National Cancer Institute (NCI) trial) (Verweij et al. 2004).

Table 3. Clinical studies of Imatinib for advanced unresectable gastrointestinal tumors.

	Phase	***Patients enrolled***	***Dose***	***Objective response****	***Tumor control†***
EORTC[1]	I	36	400-800 mg	63%	90%
EORTC[2]	II	27	400 mg twice a day	71%	89%
EORTC-AustralAsian[3]	III	473	400 mg once a day	50%	82%
EORTC-AustralAsian[4]	III	473	400 mg twice a day	54%	86%
US-Finnish[5]	II	73	400 mg once a day	66%	83%
US-Finnish[5]	II	74	600 mg once a day	66%	83%
US-Canadian[6]	III	345	400 mg once a day	48%	75%

US-Canadian[6]	III	349	400 mg twice a day	48%	74%

*Complete responses plus partial responses. †Complete response plus partial response plus stable disease. [1]van Oosteterom et al. 2001; [2]Verweij et al. 2003; [3]Verweij et al. 2004; [4]Benjamin et al. 2003; [5]von Mehren et al. 2002; [6]Rankin et al. 2004. From Rubin et al. 2007.

The results of the meta-analysis of 1640 patients from both trials showed that treatment with high-dose Imatinib (400 mg, twice daily) results in a small but significant PFS advantage compared with standard-dose Imatinib (400 mg/d) (Tab.3; Fig. 18). Besause of the crossover design, it is not surprising that no OS advantage was seen, in that the patients randomized to 400 mg/d crossed over to 800 mg at progression (MetaGIST 2010). Statistically significant evidence shows that the relative benefit of high-dose Imatinib depends on the mutation type (Fig. 18), and that starting Imatinib at a daily dose of 800 mg will prolong median PFS in patients with KIT exon 9 mutations. However no evidence shows that this will improve survival.

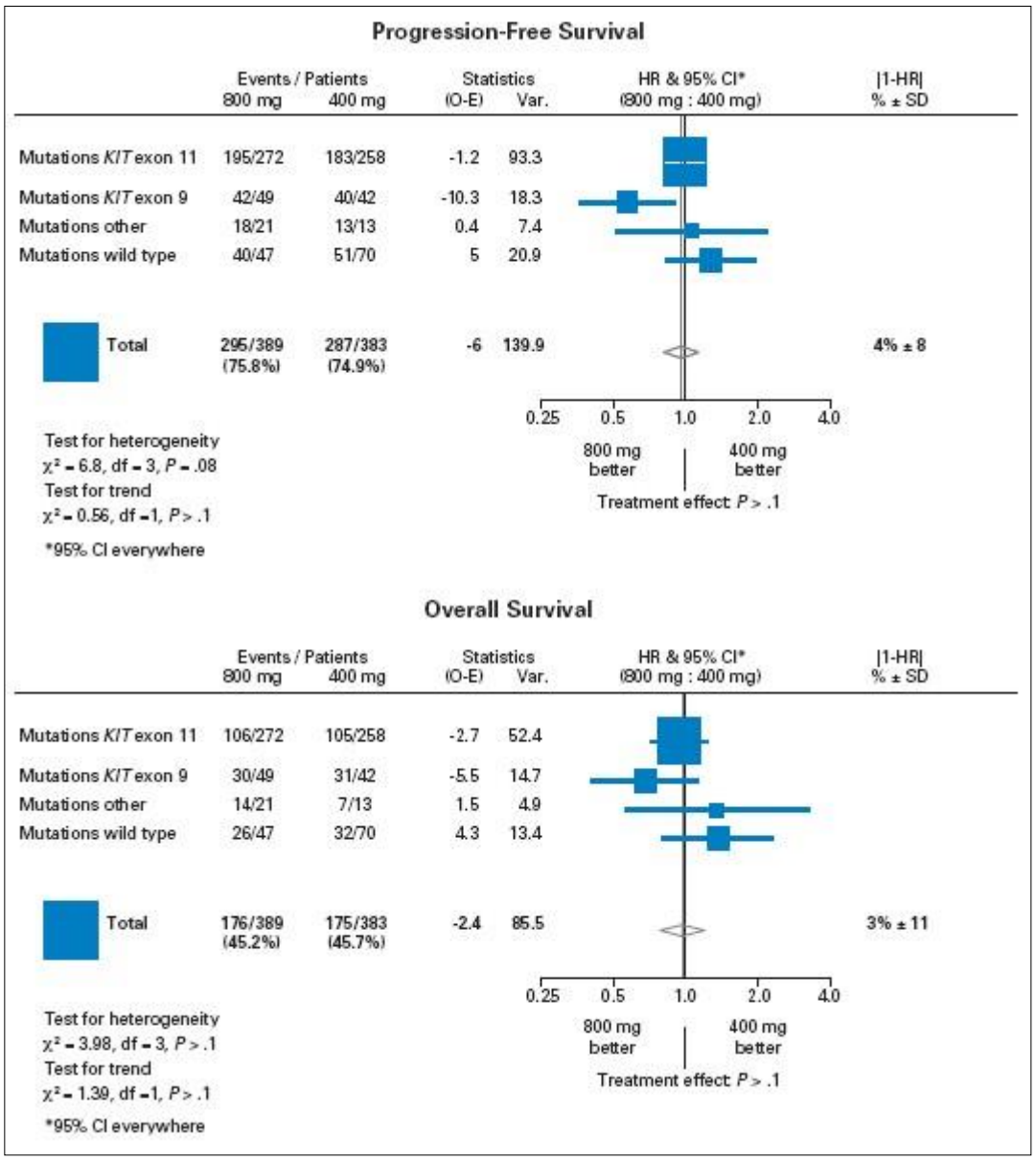

Figure 18. Forest plots of results of treatment comparison in all mutation subgroups. N, number of patients; O, events; E, expected; HR, hazard ratio; SD, standard deviation. From MetaGIST 2010.

7.1.1.2 Toxicity profile of Imatinib

The toxicity profile of Imatinib is generally better than that of traditional chemotherapy. Fluid retention, diarrhea, nausea, fatigue, muscle cramps, abdominal pain, and rash are the most common nonhematologic toxicities reported in clinical trials (Guilhot et al. 2004). The side-effect profile may improve with prolonged therapy.

A study that reviewed common toxicities noted that 13% of patients had grade 3 or higher anaemia and 7% had neutropenia of that severity. About a third of patients had grade 2 or higher oedema, or fatigue, about fifth had nausea or diarrhoea, and a sixth had skin rash of similar severity (Van Galabbeke et al. 2006). Toxicity was generally dose-related and risk factors included increasing age and female gender, possibly related to decreased Imatinib clearance in these patient groups. A risk calculator is available for assessing individual patient´s risk of Imatinib toxicity (Van Galabbeke et al. 2006).

Serious side effects (e.g. lung toxicity, LFT abnormalities are seen in fewer than 5% of patients. Recent reports suggest that concomitant administration of steroids and imatinib in patients with LFT abnormalities may allow patients to receive therapy (Ferrero et al. 2006).

Patients with large bulky tumors may have a 5% risk for tumor hemorrhage not associated with thrombocytopenia. These patients should be monitored closely for evidence of a decline in haemoglobin in the first 4 to 8 weeks of Imatinib. Asymptomatic bleeding can be monitored closely while Imatinib is continued. However, acute large decreases in haemoglobin of than 3 g/dL may require temporary withholding of Imatinib until haemoglobin has stabilized or transfusion if patients are symptomatic. Surgical intervention should be considered if bleeding does not resolve. Emergency surgery may also be required in patients who have other complications (bowel obstruction, abscess). Patients on long-term Imatinib may develop anemia that may be multifactorial (iron deficiency, chronic disease, B12 deficiency, folate deficiency, suppression of hematopoiesis by the TKI) (Demetri et al. 2010).

Although symptoms improved with dose reduction or interruption, response to antidepression medications was not consistent. Further studies are needed to evaluate the incidence and risk factors of depression in patients treated with Imatinib. Patients should undergo routine screening for depressive symptoms and suicidal ideations (Demetri et al. 2010).

7.1.1.3 KIT and PDGFRA mutation status predicts response to Imatinib

One of the questions addressed by the CSTIB2222 trial of Imatinib therapy for advanced GIST was whether there is a relationship between target kinase mutations and tumor response. Corless and colleagues proposed that GISTs be classified according to molecular

context of the tumor and provides a quick reference for other syndromes with which it may be associated (Tab. 4) (2004).

Table 4. Molecular Classification of GIST.

GIST Type	**Comments**
Sporadic GIST	
***KIT* mutation**	
Exon 11	Best response to Imatinib
Exon 9	Intermediate response to Imatinib
Exon 13	Sensitive to Imatinib in vitro; clinical responses observed
Exon 17	Sensitive to Imatinib in vitro; clinical responses observed
***PDGFRA* mutation**	
Exon 12	Sensitive to Imatinib in vitro; clinical responses observed
Exon 18	D842V has poor response to Imatinib; other mutations are sensitive
Wild type	Poor response to Imatinib
Familial GIST	
KIT exon 11 (V559A, delV559, W557R)	Skin pigmentation, urticaria pigmentosa, mastocytosis
KIT exon 13 (K642E)	No skin pigmentation or mastocytosis
KIT exon 17 (D820Y)	No skin pigmentation or mastocytosis; abnormalities in esophageal peristalsis
GIST with paraganglioma	Autosomal dominant; endocrine symptoms common
Pediatric GIST	
Sporadic	*KIT* mutations much less frequent than in adults
Carney´s triad	Gastric GIST with pulmonary chondroma and/or paraganglioma; female or male ratio = 7:1; no *KIT* mutations identified
NF1-relared GIST	No KIT mutations identified

From Corless et al. 2004.

To the extent that this classification is useful in identifying patients in whom initial Imatinib therapy is likely fail or in identifying kindreds with possible germline KIT mutations, it is obvious that there will be an increasing role for mutation screening in newly diagnosed GISTs.

7.1.1.4 Responses in experimental systems

The above clinical results are mirrored by cellular models of Imatinib sensitive GIST. These *KIT*-mutant GIST cell lines derived from human tumor specimens typically retain substantial sensitivity to the inhibitory effects of Imatinib on KIT kinase activity, unless they are subjected to carcinogen-induced mutagenesis. Imatinib treatment of these cell lines induces a strong anti-proliferative effect, leading some cells to go undergo apoptosis through a mechanism that is dependent on histone H2AX, highlighting the requirement of these cell for oncogenic KIT signaling, a phenomenom that is often referred to as oncogene addiction (Weinstein 2002; Liu et al. 2007). However, many cells simply become quiescent through nuclear p27-mediated exit from the cell cycle, as well as by upregulation of autophagy. Even after prolonged exposure, the removal of Imatinib from the culture system allows the cells to resume proliferation (Liu et al. 2007; Gupta et al. 2010).

It is possible, however, to induce apoptosis in quiescent GIST cells by using Imatinib-synergistic treatments such as ABT-737 (a BCL-2 inhibitor) or RNA interference directed against the pro-apoptotic BCL-2 family member, BIM (Gordon & Fisher 2010; Reynoso et al. 2011). In addition, inhibition of the autophagy survival pathway by small interfering (siRNA) against *ATG7* or *ATG12*, or chloroquine inhibition of lysosomal acidification, can also induce apoptosis in GIST cells that are quiescent during Imatinib treatment (Gupta et al. 2010). These data suggest that some form of combination therapy might improve that ability of current Tyrosine Kinase Inhibitors (TKIs) to kill GIST cells.

Therefore, TKI therapy can control the growth and survival of differentiated GIST cells that account for most of the cellular composition of clinical GIST lesions, but this therapy may not control or eradicate the GIST stem cell and progenitor cell pool (Bardsley et al. 2010).

7.1.1.5 Imatinib resistance

Targeting of KIT in GIST by TKI has been a considerable success, however, approximately 10-15% of tumors demonstrate primary resistance to Imatinib (progression within 6 months) and an additional 40-50% of tumors develop secondary drug resistance (progression within 2 years) (Nilsson et al. 2009; Gramza et al. 2009).

Four mechanisms of Imatinib resistance were identified (Fletcher et al. 2003):

1. Target resistance due to mutation – a new KIT or PDGFRA point mutation and protein activation, superimposed on the original mutation in that gene.
2. KIT genomic amplification with overexpression of the KIT oncoprotein, without a new point mutation.
3. Target modulation – activation of an alternate receptor tyrosine kinase protein, accompanied by loss of KIT oncoprotein expression.
4. Functional resistance – KIT or PDGFRA activation, outside the juxtamembrane hotspot region, in the absence of a secondary point mutation.

All these mechanisms were involved in late resistance, but only 4. was seen in primary resistance.

7.1.1.5.1 Primary resistance

Approximately 10-15% of patients with GISTs have primary resistance, which is defined as progression within the first 6 months of treatment. One of the interesting observations that has emerged from the Phase II trials, and which was confirmed in the Phase III trials, is that tumors response to Imatinib correlates with the underlying kinase genotype (Heinrich et al. 2003; Debiec-Rychter et al. 2004; Heinrich et al. 2008). The probability of primary resistance to Imatinib for *KIT* exon 11, *KIT* exon 9 and wild-type GISTs is 5%, 16% and 23%, respectively (Heinrich et al. 2003).

The most common PDGFRA mutation in GISTs, D842V, is strongly resistant to the effects of Imatinib (Heinrich et al. 2003; Hirota et al. 2003; Corless et al. 2005). This mutation favors the active conformation of the kinase domain and consequently disfavours imatinib binding (Heinrich et al. 2003; Gajiwala et al. 2009; Biron et al. 2010). This has

been corroborated by clinical results, as patients with PDGFRA D842V-mutant GISTs have low response rates and very short progression-free survival and overall survival during Imatinib treatment.

Wild-type GISTs include tumors with mutations downstream of KIT (Hostein et al. 2010; Janeway et al. 2011), hence these subsets of wild-type GISTs might respond better to other targeted agents, such as VEGFR inhibitors for paediatric or SDH-mutant GIST, and BRAF or MEK inhibitors for BRAF-mutant GIST (Janeway et al. 2009).

7.1.1.5.2 Secondary resistance

After an initial benefit from Imatinib, the vast majority of patients eventually develop disease progression or secondary resistance. The resistance may manifest in a number ways, including growth of a nodule within a pre-existing, clinically quiescent lesion, the development of one or more new nodules, or widespread expansion of lesions throughout the liver or abdominal cavity. It is now established that acquired mutations in *KIT* or *PDGFRA* account for most secondary resistance, and that these mutations occur almost exclusively in the same gene and allele as the primary oncogenic driver mutation (Antonescu et al. 2005; Chen et al. 2004; Heinrich et al. 2006).

In a Phase II Imatinib study for advanced GISTs, 67% of the patients whose tumor showed Imatinib resistance had a new, or secondary, mutation in KIT. Secondary mutations of KIT have not been reported in wild-type GISTs, suggesting that KIT activation is not the primary driver of tumor growth in these cases (Heinrich et al. 2006). Unlike primary mutations that activate KIT, which are predominantly in the juxtamembrane regions that are encoded by exons 9 and 11, the secondary mutations were concentrated in two regions of the KIT kinase domain, which is the domain that is a targeted by Imatinib. One is the ATP-binding pocket, encoded by exons 13 and 14, mutations of which directly interfere with drug binding. The second is the activation loop, where mutations can stabilize KIT in the active conformation and thereby hinder drug interaction. Compounding the problem, almost all of the secondary exon 17 or 18 *KIT* mutations can also serve as primary activation mutations, thus potentially increasing kinase activity. By contrast, the secondary ATP-binding pocket mutations do not cause intrinsic kinase activation (Antonescu et al. 2005; Heinrich et al. 2006; Agaram et al. 2007; Liegl et al. 2008).

Drug resistance has also been observed in PDGFRA-mutant GISTs, in which the most common is an acquired D842V mutation (activation loop) (Heinrich et al. 2006). However, there have been no reliable reports of a secondary *KIT* mutation arising in a GIST with a primary *PDGFRA* mutation, or vice versa, during treatment with Imatinib.

Additional studies using more sensitive assays have identified secondary mutations in more than 80% of drug-resistant GIST lesions (Liegl et al. 2008).

Although secondary mutations in *KIT* are the most common cause of acquired resistance to Imatinib therapy, there are other potential causes for GIST growth in the face of TKI therapy. For example, there can be downregulation or loss of *KIT* and *PKCθ* expression, which is associated with a marked increase in cyclin D1 and JUN levels (Duensing et al. 2004; Corless et al. 2011). Overexpression of *IGF1R* has been shown in GISTs lacking primary *KIT* or *PDGFRA* mutations, and the inhibition of *IGF1R* may kill GIST cells independently of *KIT* mutation status (Tarn et al. 2008; Corless et al. 2009). Focal adhesion kinase (FAK) may also have a role in the growth and survival of Imatinib-resistant GIST cells (Sakurama et al. 2009). In addition, an Imatinib-resistant GIST cell line and two patients with *KIT*-negative GISTs were observed to have overexpression of the tyrosine kinase AXL, which activates similar pathways to KIT (Mahadevan et al. 2007).

7.1.2 Alternative targeted therapies for GIST

Unfortunately, most patients will not respond to Imatinib dose escalation, forcing a switch to an alternative KIT and PDGFRA TKI. Such salvage agents include sunitinib, soraferin, vatalanib, masitinib, nilotinib and dasatinib, as well as other investigational inhibitors (Tab. 5). Although all of these agents are KIT and PDGFRA inhibitors, most of them, in contrast to imatinib, also target VEGFR1 and VEFGR2 (Demetri 2011), hence these agents have the potential to decrease tumor growth by the inhibition of angiogenesis, as well as by the direct inhibition of KIT and PDGFRA.

Table 5. New therapies being tested for the treatment of GISTs.

DRUG	***TARGETS***	***TRIAL INFORMATIONS***
Tyrosine kinase inhibitors		
Imatinib	KIT and PDGFRA	FDA approved
Sunitinib	KIT, PDGFRA and VEGFR	FDA approved
Nilotinib	KIT and PDGFRA	Phase III (ClinicalTrials.gov ID: NCT 00785785)
Dasatanib	KIT and PDGFRA	Phase II (NCT00568750)
Sorafenib	KIT, PDGFRA and VEGFR	Phase II (NCT01091207)
Regorafenib	KIT, PDGFRA and VEGFR	Phase III (NCT01271712)
Vatalanib	KIT, PDGFRA and VEGFR	Phase II (NCT00117299)
Masitinib (AB1010)	KIT and PDGFRA	Phase III (NCT00812240)
Pazopanib	KIT, PDGFRA and VEGFR	Phase II (NCT01323400)
Crenolanib	PDGFRA	Phase II (NCT01243346)
HSP90 inhibitors		
STA-9090	HSP90	Phase II (NCT01039519)
AT-13387	HSP90	Phase II (NCT01294202)
AUY922	HSP90	Phase II (NCT01404650)
Monoclonal antibodies		
IMC-3G3 (Olaratumab)	PDGFRA	Phase II (NCT01316263)
Bevacizumab	VEGFR	Phase III (NCT00324987)
mTOR inhibitor		
Everolimus	mTOR	Phase II (NCT00510354)
Other		
Perisine	AKT (PI3K pathway)	Phase II (NCT00455559)
NKp30	Natural cytotoxity receptor	

FDA, US Food and drug Administration; GISTs, gastrointestinal stromal tumors; HSPP90, heat shock protein 90; PDGFRA, platelet-derived growth factor receptor-α; VEGFR, vascular endothelial growth factor receptor. From Corless et al. 2011.

Sunitinib id US Food and Drug Administration (FDA)-approved for the treatment of patients with GISTs with progression on Imatinib (Demetri et al. 2006) but biochemical evidence suggests that the range of activity of sunitinib against secondary Imatinib-resistant kinase mutations is suboptimal.

Nilotinib is a drug that is structurally similar to Imatinib and that has limited activity against ATP-binding pocket mutations and activation loop mutations and that therefore display minimal efficacy in Imatinib-resistant cells. Correspondingly, nilotinib has shown limited activity in patients with Imatinib-resistant GISTs in Phase II clinical trial, whereas a sorafenib analogue (regorafenib) provided a remarkable 10-month median progression-free survival, prompting Phase III trial that is currently underway (George et al. 2011).

Even with newer drugs such as regorafenib (also approved by the FDA), resistance develops over time, suggesting that escape from ATP-competitive inhibitors of KIT and PDGFRA is inevitable. Interestingly, a new class of non-ATP mimetic kinase inhibitors (known as switch pocket kinase inhibitors, such as DP-2976) have shown high potency when tested in vitro against Imatinib-resistant KIT mutants (Heinrich et al. 2010; Eide et al. 2011). This class of drug, which suppresses the conformational switch to the activated form of KIT, represents a novel alternative in the battle against TKI resistance.

There is evidence that the PI3K-mTOR signaling pathway is one of the most important pathways in the growth of GIST cells (Bauer et al. 2007), and multiple medications targeting this pathway are in the clinical development. There are also ongoing efforts to test HSP90 inhibitors in the treatment of TKI-resistant GISTs (Tab. 5).

In theory, an inhibitor “cocktail” could not only prevent secondary resistance from emerging, but might also knock out GIST stem cells and thereby eradicate the disease. However, it can be challenging to combine small-molecule inhibitors for simultaneous treatment, as many of these drugs are metabolized by shared cytochrome P450 pathways (for example, CYP3A4). In particular, combining drugs that inhibit or that induce pathways that are responsible for the metabolism of a co-administered drug can be difficult, if not impossible (Reichardt et al. 2005; Schoffski et al. 2007).

7.2 Conclusion of treatment

Achievements in the treatment of GISTs during the past decade are the direct result of a growing understanding of their molecular biology. The high frequency *KIT* and *PDGFRA* mutations in these tumors makes them sensitive to kinase inhibitors such as Imatinib, but resistance develops in most cases. The risk of relapse following surgical resection may be estimated now using 5 parameters: 1) mitotic rate, 2) tumor size, 3) tumor site, 4) tumor rupture, and 5) the nature of the primary mutation. Risk models based on the first 2, 3, 4, and 5 risk factors have been proposed (Blay et al. 2012). These risk models are used by physicians to decide for an adjuvant treatment with Imatinib. Patients with tumors at high risk of relapse are considered for adjuvant treatment. The threshold level for high risk varies according to the prognostic classification. Physician decision has also to be adapted to the clinical context (age, comorbidities) and require a careful discussion with the patient. In addition, Sunitinib was second drugs approved by the FDA and EMA in 2012.

Metastasis typically presents with tumors isolated in the peritoneal cavity or the liver, or both. Historically, the median survival of patients with advanced GISTs was between 10 and 20 months. Before the pre-TKI era, treatment options were extremely limited for patients with unresectable or metastatic gastrointestinal stromal tumors. These tumors respond poorly (0% - 27%) to conventional cytotoxic chemotherapy agents and radiation therapy.

An immediate research goal is to develop new inhibitors that can inhibit secondary activation loop mutations that confer cross-resistance to all clinically available TKIs. In addition, the development of effective combination therapy is likely to improve tumor control. To date, our therapeutic approach to GISTs is focused on gain-of-function kinase mutations, but ongoing high-throughput genomic studies are likely to identify additional drivers and modifiers of GIST biology that can be targeted.

8 Mechanisms regulating the development of the digestive muscles

Gastrointestinal development requires regulated differentiation of visceral smooth muscle cells (SMCs) and their contractile activities. Gastrointestinal SMC developement and remodeling involves post-transcriptional modification of messenger RNA. Only a few studies have investigated the molecular mechanisms controlling visceral mesenchyme differentiation into SMCs.

Basides transcriptions, which represents the first step of gene expression, many post-transcriptional events regulate the final fate of messenger RNAs (mRNAs) in eukaryotic cells and determine their spatiotemporal pattern of expression. RNA-protein complexes control multiple steps of this proces, including mRNA cellular localization, splicing, translational regulation, or mRNA degradation (Notarnicola et al. 2012). Moreover, postregulatory RNA events are involved in the control of differentiation and remodeling of smooth muscle tissues, such as heart and vessels, suggesting that visceral smooth muscle development and plasticity could be regulated similary.

Recently was showen, that the microRNA miR-145 is strongly expressed in gut smoth muscle and regulates its developement (Zeng et al. 2009). Modulation of miR-145 levels results in gut smooth muscle and epithelium maturation defects (Fig. 19).

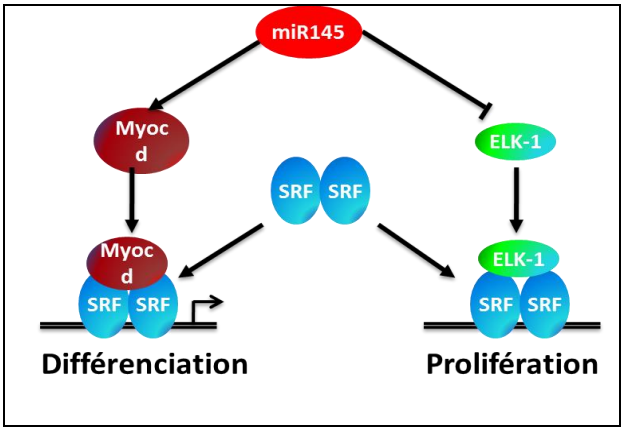

Figure 19. miR-145 functions in gut smooth muscle. miR145 is involved in the regulation of serum response factor. SRF cofactor needs to act. In association with myocardin stimulates the differentiation of SMC and in combination with ELK1 it stimulates their proliferation. MiR145 expression in SMC allows the stimulation of the expression of the

myocardin, but also inhibits the expression of ELK1, thus reinforcing the differentiation of SMCs (Zeng et al. 2009).

Another example, in our laboratory we identified RBPMS2 (RNA-Binding Protein with multiple splicing 2) as a new marker of visceral SMC remodeling. Ectopic expression of RBPMS2 in primary culture of diferentiated SMCs triggers an increase of their priloferative rate and hinders their contractile function (Notarnicola et al., 2012), more information you can found in the chapter 10.2 Expression and function of RBPMS2 in GI tract.

9 RNA-binding proteins

RNAs in cells are associated with RNA-binding proteins (RBPs) to form RiboNucleoProtein (RNP) complex. RBPs are essential players in post-transcriptional control of RNAs (Fig. 20), which, along with transcriptional regulation, is a major way to regulate patterns of gene expression during development. Post-transcriptional control can occur at many different steps in RNA metabolism, including splicing, polyadenylation, mRNA stability, mRNA localization and translation (Curtis et al. 1995; Lee & Schedl 2006; Lukong et al. 2008). Eukaryotic cells encode a large number of RBPs (thousands in vertebrates), each of which has unique RNA-binding activity and protein-protein interaction characteristics (Glisovic et al. 2008; van Kouwenhove et al. 2011).

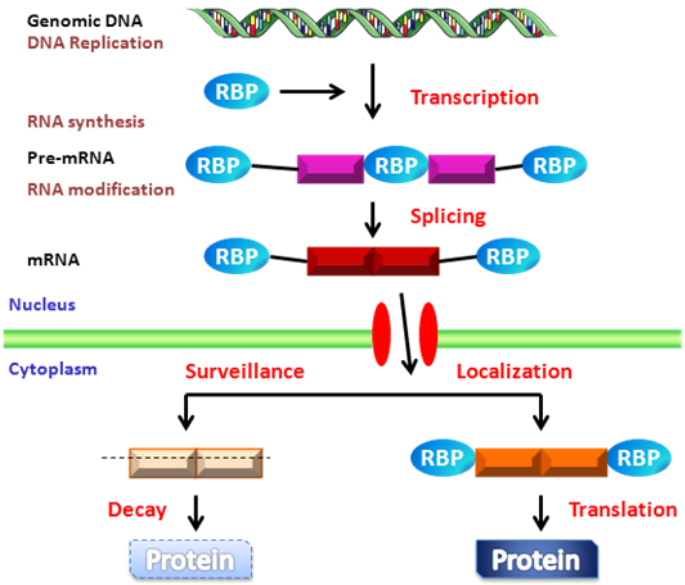

Figure 20. Multifunctionality of RBP in RNA metabolism. RNA undergoes several steps of regulation from transcription to translation such as splicing, localisation, surveillance, decay and translation. RBP binds to RNA and regulated multiple steps of RNA metabolism. Adapted from Glisovic et al. 2008; Kim et al. 2009.

Thus, altered expression and dysfunction of RBPs are implicated in the development of various diseases including cancer (Cooper et al. 2009). For example, if RBPs are mutated or overexpressed in cancer cells, they might associate with many incorrect target RNA molecules due to altered target affinity, which might lead to

formation of aberrant RNPs in cancer cells (Fig. 21). Moreover, related to GISTs, Delahaye and colleagues correlated that alternative splicing isoform expression of natural killer (NK) cell receptor NKp30 affect the prognosis of GIST patients independently from *KIT*- mutation (2011).

If RBPs or RBP binding elements are mutated in cells, processes of RNA metabolism would be changed as aberrant alternative splicing, unregulated decay, malfunctioning surveillance, mislocalization and unregulated translation of target RNAs. Such aberrant RNA molecules could generate aberrant and pathogenic proteins (Kim et al. 2009).

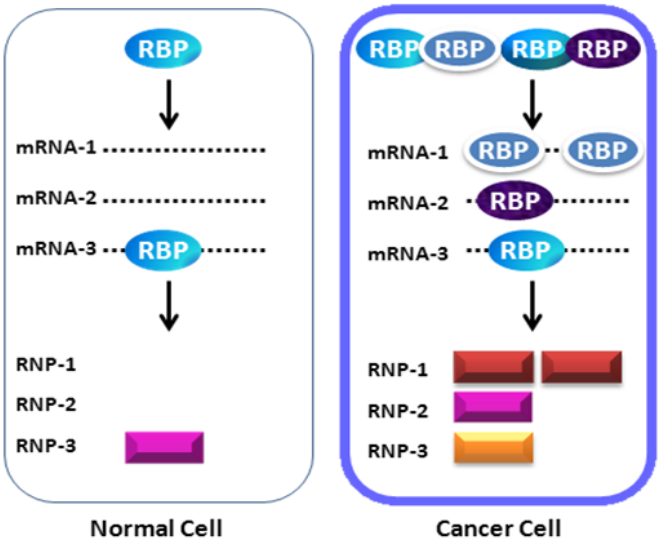

Figure 21. Aberrant formation of RiboNucleoProtein (RNP) complexes in cancer cells. RNA-binding proteins (RBPs) bind their target RNAs and from specific RNPs in normal cells. However, altered expression or overexpression of a RBP changes the affinity of that RBP to the target RNA molecules, so as to associate with wrong target RNA molecules and from aberrant RNPs in cancer cells. Adapted from Kim et al. 2009.

9.1 RNA-binding domains of RNA-binding protein (RBP)

The discovery of the heterogeneous nuclear RiboNucleoProteins (hnRNP) and other pre-mRNA/mRNA-binding proteins ted to the identification of the first amino acid motifs and functional domains that confer binding to RNA (Burd & Dreyfuss 1994). RBPs contain

one or, more often, multiple RNA-binding domains. Some well-characterized RNA-Binding Domain (RBD, also known as RNP domain and RNA recognition motif, RRM); K-homology (KH) domain (type I and type II); RGG (Arg-Gly-Gly) box; Sm domain; DEAD/DEAH box; zinc finger (ZnF, mostly C-x8-X-x5-X-x3-H); double stranded RNA-Binding Domain (dsRBD); cold-shock domain; Pumilio/FBF (PUF or Pum-HD) domain; and the Piwi/Argonaute/Zwille (PAZ) domain (Fig. 22) (Lunde et al. 2007). Using these motifs, bioinformatic analyses revealed that eukaryotic genomes encode a large number of RBPs.

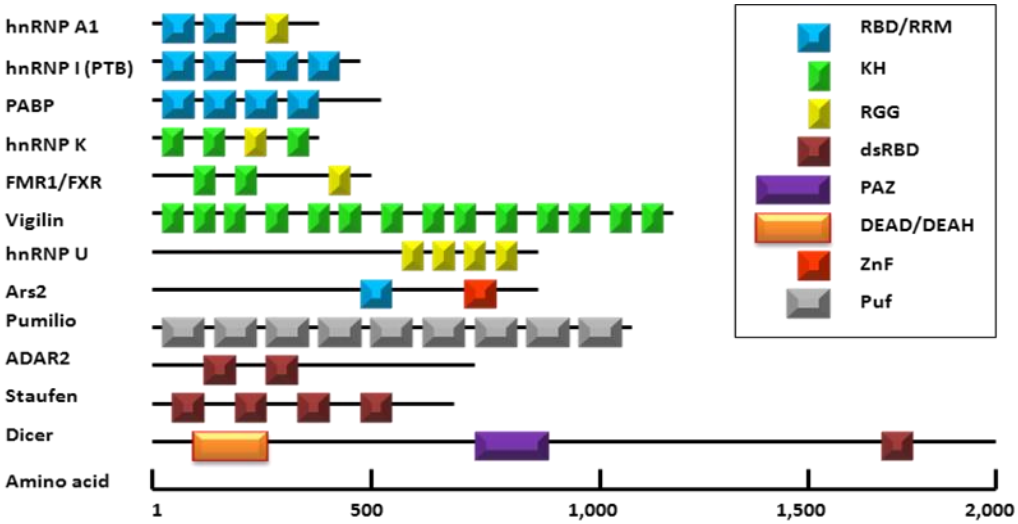

Figure 22. RNA-binding domains of RBPs. Often, several RNA-binding domains are found within one RB. Different RNA-binding domains include the RNA-binding domain (RBD/RRM), K-homology (KH) domain, RGG (Arg-Gly-Gly) box, double stranded RNA-binding somain (dsRBD), Piwi/Argonaute/Zwille (PAZ) domain, RNA helicase DEAD/DEAH box, RNA-binding zinc finger (ZnF) and Puf RNA-binding repeats (Puf). All are presented as colored boxes. Adapted from Glisovic et al. 2008.

However, it is likely that the number of RBPs is much higher, since there are probably other RNA-binding domains that remain to be uncovered. Why do eukaryotes need so many – hundreds and perhaps thousands of – RBPs? One possible explanation is that as eukaryotes evolved highly specific post-transcriptional processes to fine-tune gene expression, a concomitant expansion of the number of RBPs needed to function in these processes has occurred (Anantharaman et al. 2002). For example, in both vertebrates and

plants, the emergence of alternative splicing during evolution drove the need for a corresponding increase in the number of RBPs (Anantharaman et al. 2002).

9.1.1 The RNA Recognition Motif (RRM)

The RNA Recognition Motif (RRM), also known as the RNA-Binding Domain (RDB) or RiboNucleoProtein domain (RNP), was first identified in the late 1980´s when it was demonstrated that mRNA precursors (pre-mRNAs) are always found in complex with proteins (Dreyfuss et al. 1988). RRM-containing proteins are involved in most post-transcriptional gene expression processes (i.e. mRNA and rRNA processing, RNA export and stability) (Dreyfuss et al. 2002).

Genomic sequencing projects recently showed that the RRM is found abundantly in all life kingdoms, including prokaryotes and viruses although at lower abundance than in eukaryotes. In eukaryotes, the RRM is one of the most abundant protein domains. To date, a total of 6056 RRM motifs have been identified in 3541 different proteins (Bateman et al. 2002). In humans, 497 proteins containing at least one RRM have been identified. Assuming about 20 000 – 25 000 human genes, the RRM would therefore be present in about 2% of gene products (Hudson et al. 2004) and is the most extensively studied RNA-binding domain, both in terms of structure and biochemistry (Maris et al. 2005).

The largest group of single strand RNA-binding proteins is the eukaryotic RNA recognition motif (RRM) family. This motif of about 90 amino acids is known to bind single-stranded RNAs (Dreyfuss et al. 1988). In addition, this motif contains an eight amino acid RNP-1 consensus sequence (Bandziulis et al. 1989). RRM proteins have a variety of RNA binding preferences and functions, and include heterogeneous nuclear RiboNucleoProteins (hnRNPs), proteins implicated in regulation of alternative splicing (SR, U2AF, Sxl), protein components of small nuclear RiboNucleoProteins (U1 and U2 snRNPs), and proteins that regulate RNA stability and translation (PABP, La, Hu) (Query et al. 1989). The RRM in heterodimeric splicing factor U2 snRNP auxiliary factor (U2AF) appears to have two RRM-like domains with specialised features for protein recognition (Kielkopf et al. 2004). The motif also appears in a few single stranded DNA binding proteins.

The typical RRM consists of four anti-parallel beta-strands and two alpha-helices arranged in a beta-alpha-beta-beta-alpha-beta fold with side chains that stack with RNA bases (Fig. 23). Specificity of RNA binding is determined by multiple contacts with surrounding amino acids. A third helix is present during RNA binding in some cases (Birney et al. 1993).

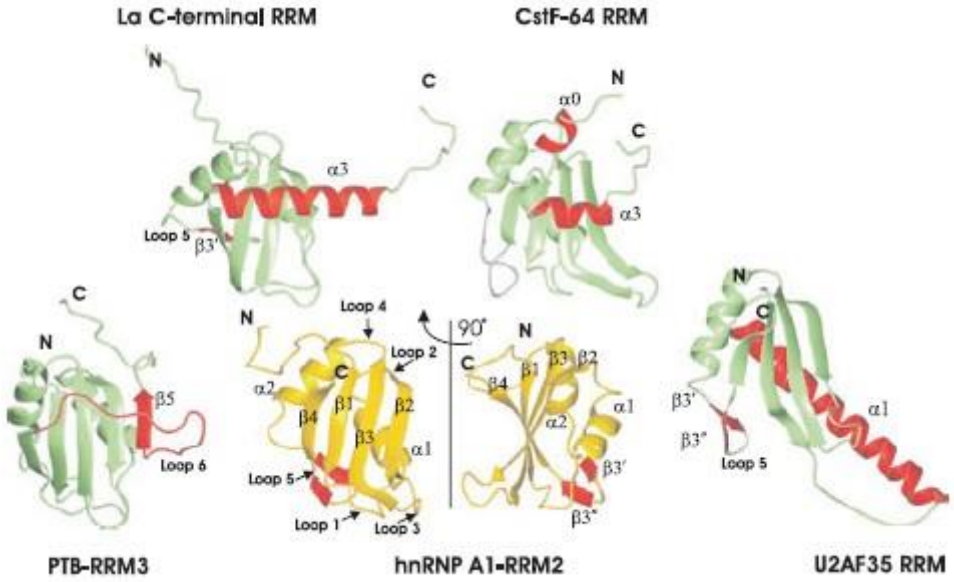

Figure 23. hnRNPA1 RRM 2, a typical RRM fold and its structural variations as illustrated by these different protein structures: hnRNPA1 RRM 2, PTB RRM 3, La C-terminal, Cst64 RRM and U2AF35. From Maris et al. 2005.

Structural data also show that RRMs have the capacity to interact using all the elements composing their structure (i.e. β-strands, loops, α-helices) explaining certainly the high conservation of this motif during evolution (Cléry et al. 2008).

Human proteins containing this RRM: A2BP1; ACF; BOLL; BRUNOL4; BRUNOL5; BRUNOL6; CCBL2; CGI-96; CIRBP; CNOT4; CPEB2; CPEB3; CPEB4; CPSF7; CSTF2; CSTF2T; CUGBP1; CUGBP2; D10S102; DAZ1; DAZ2; DAZ3; DAZ4; DAZAP1; DAZL; DNAJC17; DND1; EIF3S4; EIF3S9; EIF4B; EIF4H; ELAVL1; ELAVL2; ELAVL3; ELAVL4; ENOX1; ENOX2; EWSR1; FUS; FUSIP1; G3BP; G3BP1; G3BP2; GRSF1; HNRNPL; HNRPA0; HNRPA1; HNRPA2B1; HNRPA3; HNRPAB; HNRPC; HNRPCL1; HNRPD; HNRPDL; HNRPF; HNRPH1; HNRPH2; HNRPH3; HNRPL; HNRPLL; HNRPM; HNRPR; HRNBP1; HSU53209; HTATSF1;

IGF2BP1; IGF2BP2; IGF2BP3; LARP7; MKI67IP; MSI1; MSI2; MSSP-2; MTHFSD; MYEF2; NCBP2; NCL; NOL8; NONO; P14; PABPC1; PABPC1L; PABPC3; PABPC4; PABPC5; PABPN1; POLDIP3; PPARGC1; PPARGC1A; PPARGC1B; PPIE; PPIL4; PPRC1; PSPC1; PTBP1; PTBP2; PUF60; RALY; RALYL; RAVER1; RAVER2; RBM10; RBM11; RBM12; RBM12B; RBM14; RBM15; RBM15B; RBM16; RBM17; RBM18; RBM19; RBM22; RBM23; RBM24; RBM25; RBM26; RBM27; RBM28; RBM3; RBM32B; RBM33; RBM34; RBM35A; RBM35B; RBM38; RBM39; RBM4; RBM41; RBM42; RBM44; RBM45; RBM46; RBM47; RBM4B; RBM5; RBM7; RBM8A; RBM9; RBMS1; RBMS2; RBMS3; RBMX; RBMX2; RBMXL2; RBMY1A1; RBMY1B; RBMY1E; RBMY1F; RBMY2FP; RBPMS; **RBPMS2**; RDBP; RNPC3; RNPC4; RNPS1; ROD1; SAFB; SAFB2; SART3; SETD1A; SF3B14; SF3B4; SFPQ; SFRS1; SFRS10; SFRS11; SFRS12; SFRS15; SFRS2; SFRS2B; SFRS3; SFRS4; SFRS5; SFRS6; SFRS7; SFRS9; SLIRP; SLTM; SNRP70; SNRPA; SNRPB2; SPEN; SR140; SRRP35; SSB; SYNCRIP; TAF15; TARDBP; THOC4; TIA1; TIAL1; TNRC4; TNRC6C; TRA2A; TRSPAP1; TUT1; U1SNRNPBP; U2AF1; U2AF2; UHMK1; ZCRB1; ZNF638; ZRSR1; ZRSR2; eIF4B.

10 RNA-binding protein with multiple splicing 2 (RBPMS2)

10.1 Characterization of RBPMS2

Gerber and colleagues have isolated in a screen for novel sequences expressed during embryonic heart development a gene which encodes a putative RNA-binding protein (1999). This gene has been named *hermes* (HEart, RNA recognition Motif Expressed Sequence) and recently named as RBPMS2 (for RNA Binding Protein with Multiple Splicing 2) (Fig. 24). RBPMS2 contains one unique RNA recognition motif (RRM) (Gerber et al. 1999; Wilmore et al. 2005). Human *RBPMS2* gene is localized in chromosome 15 (Fig. 25).

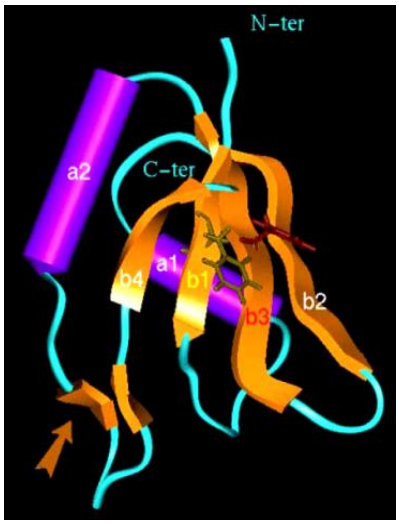

Figure 24. Three-dimensional structure of RNA-binding protein with multiple splicing 2 gene-encoded RRM. Display of the six secondary structure elements $\beta_1\alpha_1\beta_2\beta_3\alpha_2\beta_4$ of the modelled structure. Amino acid side chains are shown for the most conserved aromatic residues from β_3 strand (Phe 44; in red) and from β_1 strand (Phe 6; in yellow) respectively. The brown arrow points to conserved elements in the loop between α2 and β4. From Thion & Erard 2002.

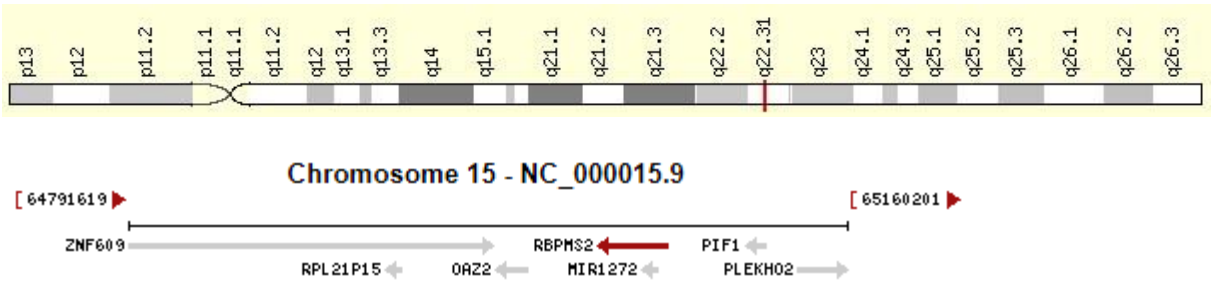

Figure 25. Localization RBPMS2 in chromosome 15. From NCBI and genetic card on 07.08.2012

The *hermes* sequence is closely related to three genes: *Drosophila couch potato* (*cpo*), *C. elegans mec-8*, and the human gene *RBP MS type 1* (Fig. 26). Expression of *hermes* at high levels in the developing heart begins at approximately the time of differentiation and is maintained throughout development. The timing of expression suggests a role for Hermes in post-transcriptional regulation of myocardial gene expression (Gerber et al. 1999).

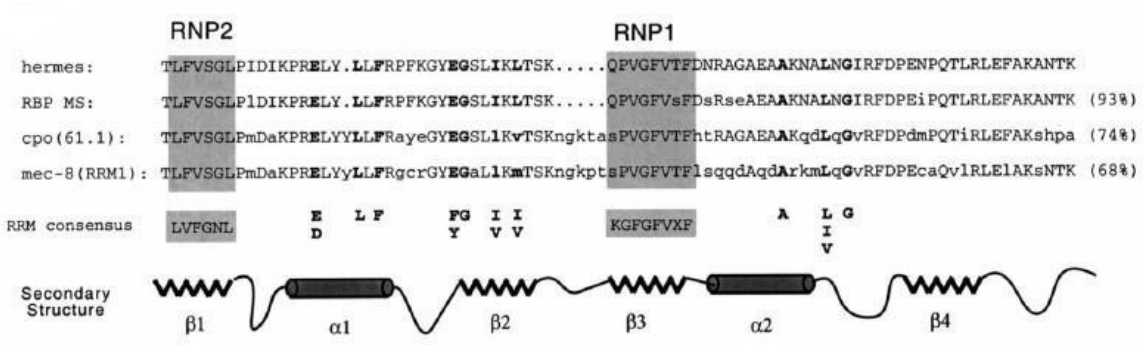

Figure 26. Comparison of the RNA recognition motif (RRM) domains. RRM domains contained in *hermes*, *RBP MS (Werner syndrome locus*, humain gene*), couch potato* (*cpo*, *Drosophila* gene) and the firs RRM of *mec-8 (C. elegans* gene). The RNP1 and RNP2 regions are shaded and RRM consensus residues (Burd & Dreyfuss 1994) are in bold. A diagram showing the secondary structure is aligned with the RRM sequences. From Gerber et al. 1999.

In addition to transcriptional control, an important and often overlooked aspect of gene regulation occurs at the post-transcriptional level. Post-transcriptional regulation may be achieved at numerous steps in the RNA metabolism pathway, including pre-mRNA

processing (capping, splicing and polyadenylation), RNA transport, RNA localization, translational regulation and RNA stability (Day & Tuite 1998).

10.2 Expression and function of RBPMS2 in GI tract

First report presenting the expression of *Hermes* in the developing gastrointestinal system was published by Wilmore and colleagues, 2005. Hermes expression was observed in the foregut, midgut, and hindgut of the stage 25 (approximately 4.5-5 days of incubation) chicken embryo, and was confined to the mesoderm of the gut and was absent from the endoderm (Wilmore et al. 2005).

In our laboratory we investigated the expression and function of the RNA-binding protein RBPMS2 in the developing chick gastrointestinal tract. RBPMS2 expression in the chick gastrointestinal mesenchymal layer is regulated temporally because it is high at E4–E6 (approximately 4-6 embryonic days of incubation) and then progressively is reduced at a later stage. This dynamic expression pattern corresponds to the progression of visceral undifferentiated mesenchymal cells into differentiated SMCs (Fig. 27). Only few genes have such a dynamic expression pattern in visceral SMC precursors. αSMA is expressed as early as RBPMS2, but then is maintained also in differentiating SMCs, when calponin, smooth muscle myosin heavy chain, and myocardin also are expressed. These data identify RBPMS2 as a marker of undifferentiated visceral SMCs (Notarnicola et al. 2012).

We then showed that sustained RBPMS2 expression hinders visceral SMC differentiation in vivo and in SMC primary cultures through up-regulation of Noggin expression that leads to inhibition of the Bone Morphogenetic Protein (BMP) signaling pathway. Previous studies showed that exogenous stimulation of BMP activity could prevent dedifferentiation of vascular SMCs in cell culture, suggesting that BMP activation is essential for modulating the vascular SMC phenotype (Lagna et al. 2007). Our findings confirm this observation in vivo and suggest that Noggin is a key regulator during visceral SMC development and also may be involved in the phenotypic regulation of SMCs in culture (Fig. 28).

We also found differences between the action of RBPMS2 and Noggin mainly in SMC primary cultures. Indeed, RBPMS2, but not Noggin, overexpression induced SMC proliferation and transient repression of SMA expression. Therefore, in addition to the

Noggin-BMP axis, RBPMS2 might regulate other pathways that contribute to the dedifferentiation and increased proliferation of visceral SMCs, thus dissociating the effect on proliferation from the effect on differentiation (Notarnicola et al. 2012).

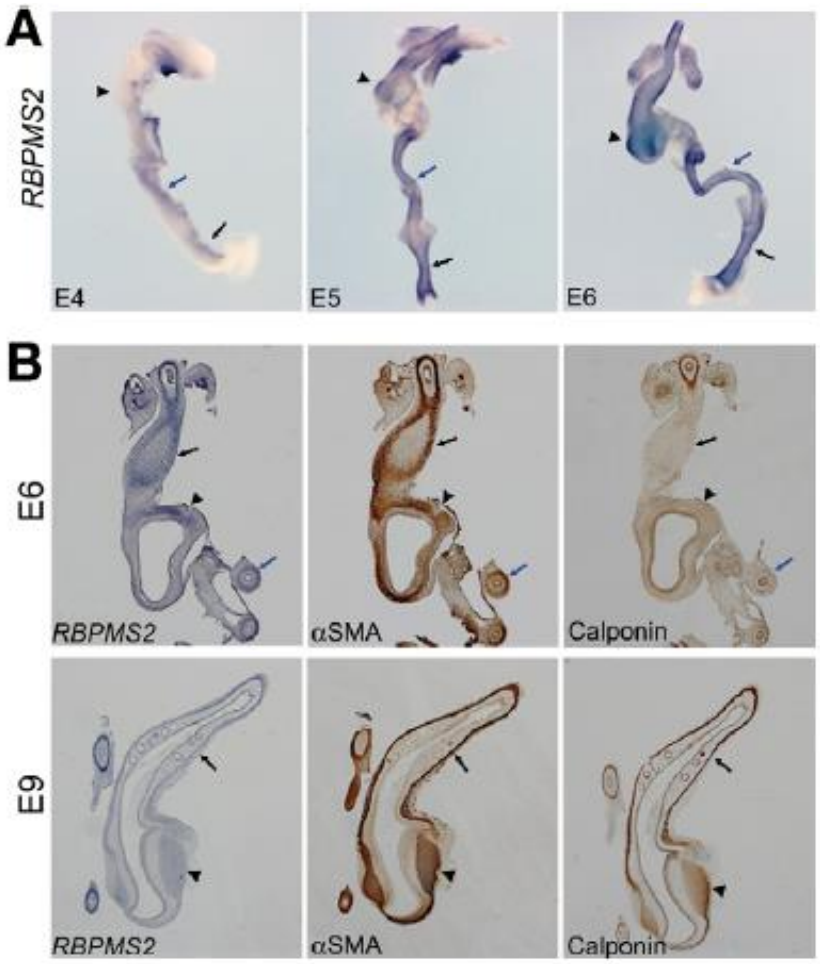

Figure 27. Dynamic expression of RBPMS2 in chick gastrointestinal mesenchyme. (**A**) Whole-mount in situ hybridization of E4, E5, and E6 gastrointestinal tracts using the RBPMS2 riboprobe. Arrows, arrowheads, and blue arrows indicate the colon, developing stomach, and small intestine, respectively. (**B**) Serial longitudinal sections of E6 (upper panels) and E9 (lower panels) stomachs analyzed by in situ hybridization with the RBPMS2 riboprobe and by immunohistochemistry with anti-SMA and anticalponin antibodies. Arrows, arrowheads, and blue arrows indicate the anterior glandular stomach, posterior muscular stomach, and duodenum, respectively.

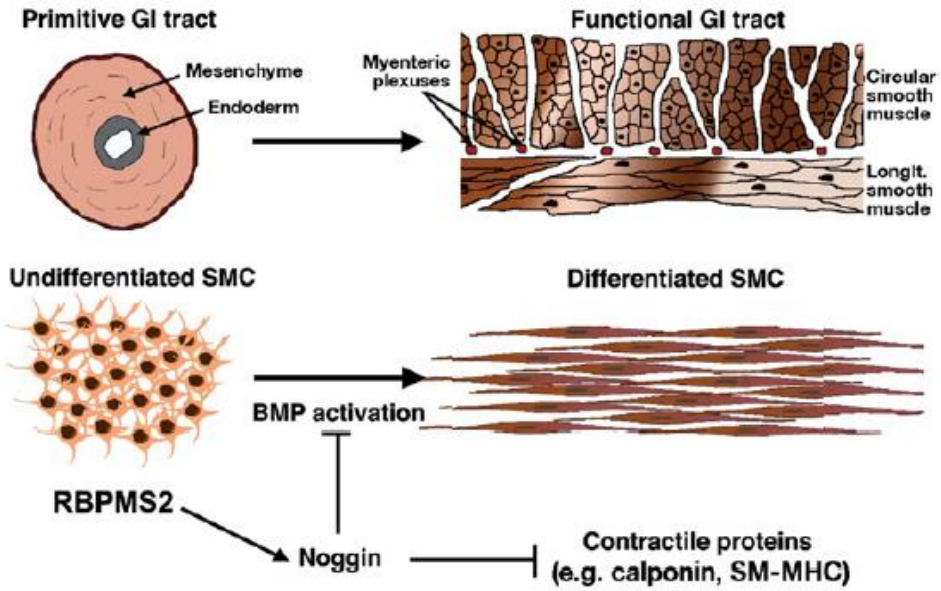

Figure 28. Model of the gastrointestinal SMC development regulated by the RBPMS2 and BMP pathways. RBPMS2 regulates the early stage of SMC differentiation through the control of the expression of the BMP inhibitor Noggin and the inhibition of contractile proteins. From Notarnicola et al. 2012.

We showed that RBPMS2 and Noggin overexpression in differentiated SMCs hinders their differentiation associated with myocardin up-regulation. Indeed, recently, Yin and colleagues reported that myocardin accumulation inhibits its own function and that proteosomal degradation of myocardin is required for its full transcriptional activity (2011). Similarly, we show that myocardin accumulation results in a reduction of calponin expression (a marker of differentiated SMCs). In addition, RBPMS2 and Noggin misexpression led to up-regulation of the SRF target gene FHL2, which interacts with SRF and inhibits induction of smooth muscle contractile genes by SRF (Philippar et al. 2004). Altogether, these results support the notion that activation of the RBPMS2/Noggin pathway inhibits SMC contractile genes through functional alteration of the myocardin/SRF pathway (Notarnicola et al. 2012).

In summary, in our laboratory we identified RBPMS2 as a new marker of visceral SMC remodeling that could be useful for the characterization of smooth muscle alteration in visceral myopathies. RBPMS2 transcripts were up-regulated in patients with Chronic Pseudo Obstruction syndrome (CIPO), and alterations in RBPMS2 function might be involved in digestive motility disorders (Notarnicola et al. 2012).

10.3 RBPMS2 in cancer cells

Human embryonic stem (hES) cells possess unlimited self-renewal and pluripotency and thus have the potential to provide an unlimited supply of different cell types for tissue replacement. The hES-T3 cells with normal female karyotype were first differentiated into embryoid bodies and then induced to generate the pancreatic islet-like cell clusters, which expressed pancreatic islet cell-specific marker of insulin, glucagon and somatostatin.

The expression profiles of microRNAs and mRNAs from the pancreatic islet-like cell clusters were analyzed and compared with those of undifferentiated hES-T3 cells and differentiated embryoid bodies. MicroRNAs negatively regulate the expression of protein-coding mRNAs. The pancreatic islet-like cell clusters were found to exhibit very high expression of microRNAs as miR-199a, which down-regulated the expression of RBPMS2 (Chen et al. 2010).

Therefore, this microRNAs and their target gene is very likely to play important regulatory roles in the development of pancreas and/or differentiation of islet cells (Chen et al. 2010).

AIM OF THE RESEARCH

The aim of my thesis work was to investigate the espression and the function of the RNA-Binding Protein with Multiple Splicing 2, RBPMS2 in human normal and tumoral gastrointestinal musculature. For these aims, we develipped two studies listed below:

Specific objectives of the study 1 include:

1. *In situ* hybridization of smooth muscle layers sections from normal rectum and GIST samples.
2. Clinicopathological features and *RBPMS2* mRNA expression in the adult GIST cohort.
3. Characterization of the home-made anti-human RBPMS2 antibody by immunofluorescence and western blotting.
4. RBPMS2 protein expression in the adult GIST cohort.
5. Regulation of RBPMS2 expression in GIST cell line.

Specific objectives of the study 2 include:

1. The development and characterization of a human Colonic Smooth Muscle Cells (hCSMC) line.
2. The impact of ectopic expression of RBPMS2 in hCSMC line on their differentiation and proliferation status.
3. Creation and characterization of stable hCSMC line expressing RBPMS2.
4. Identify protein partner of RBPMS2.

RESULTS

STUDY I

RBPMS2 expression in GISTs

(Hapkova et al., *Exp Mol Pathol*. 2013 Apr;94(2):314-21. doi: 10.1016/j.yexmp.2012.12.004. Epub 2013 Jan 4.)

High expression of the RNA-Binding Protein RBPMS2 in gastrointestinal stromal tumors

Ilona Hapkova [a,b], Josef Skarda [c], Caroline Rouleau [a,d], An Thys [e], Cécile Notarnicola [a], Maria Janikova [c], Florence Bernex [a], Miroslav Rypka [b], Jean-Marie Vanderwinden [e], Sandrine Faure [a], Jaroslav Vesely [b], Pascal de Santa Barbara [a,*]

[a] *INSERM U1046, Université Montpellier 1, Université Montpellier 2, Montpellier, France*
[b] *Department of Pathophysiology, Faculty of Medicine and Dentistry, Palacky University, Olomouc, Czech Republic*
[c] *Department of Clinical and Molecular Pathology, Faculty of Medicine and Dentistry, Palacky University and University Hospital, Olomouc, Czech Republic*
[d] *CHU Montpellier, Service d'Anatomie Pathologique, Montpellier, France*
[e] *Laboratory of Neurophysiology, Faculty of Medecine, Université Libre de Bruxelles, Brussels, Belgium*

Keywords: Gastrointestinal Stromal Tumors (GIST), RNA-Binding Protein, RBPMS2, KIT, Smooth muscle cells, Interstitial Cell of Cajal.

* Corresponding author at: INSERM U1046, 371 Avenue Doyen Giraud, 34295 Montpellier, France. Fax: 33 467 415 231.

E-mail address: Pascal.de-Santa-Barbara@inserm.fr (P. de Santa Barbara).

1 Abstract

Gastrointestinal stromal tumors (GISTs) are the most common mesenchymal neoplasms of the gastrointestinal tract and are often associated with *KIT* or *PDGFRA* gene mutations. GIST cells might arise from the interstitial cells of Cajal (ICCs) or from a mesenchymal precursor that is common to ICCs and smooth muscle cells (SMCs). Here, we analyzed the mRNA and protein expression of RNA-Binding Protein with Multiple Splicing-2 (RBPMS2), an early marker of gastrointestinal SMC precursors, in human GISTs (n=23) by in situ hybridization, quantitative RT-PCR analysis and immunohistochemistry. The mean *RBPMS2* mRNA level in GISTs was 42-fold higher than in control gastrointestinal samples ($p<0.001$). *RBPMS2* expression was not correlated with *KIT* and *PDGFRA* expression levels, but was higher in GISTs harboring *KIT* mutations than in tumors with wild type *KIT* and *PDGFRA* or in GISTs with *PDGFRA* mutations that were characterized by the lowest *RBPMS2* levels. Moreover, *RBPMS2* levels were 64-fold higher in GIST samples with high risk of aggressive behavior than in adult control gastrointestinal samples and 6.2-fold higher in high risk than in low risk GIST specimens. RBPMS2 protein level was high in 87% of the studied GISTs independently of their histological classification. Finally, by inhibiting the KIT signaling pathway in GIST882 cells, we show that *RBPMS2* expression is independent of KIT activation. In conclusion, RBPMS2 is up-regulated in GISTs compared to normal adult gastrointestinal tissues, indicating that RBPMS2 might represent a new diagnostic marker for GISTs and a potential target for cancer therapy.

2 Introduction

Gastrointestinal stromal tumors (GISTs) are the most common mesenchymal neoplasms of the gastrointestinal tract (Corless et al., 2011) and are highly resistant to conventional chemotherapy and radiotherapy. These tumors are characterized by the presence of activating mutations in *KIT* (75-80% frequency) or *Platelet-Derived Growth Factor Receptor Alpha* (*PDGFRA*) (5-10% of tumors), two genes encoding receptors for growth factors that are normally activated only in specific situations (Hirato et al., 1998). Imatinib mesylate, a small-molecular tyrosine kinase inhibitor that targets phosphorylation/activation of KIT and PDGFRA and also constitutively activated KIT and

PDGFRA proteins, has proven efficient in GIST treatment (Joensuu et al., 2001; Tuveson et al., 2001); however, resistance to such therapy is increasing. Therefore, the development of new-targeted therapies is strongly encouraged (Renouf et al., 2009).

It is now largely documented that post-regulatory RNA events play crucial roles in modulating differentiation and remodeling of smooth muscle tissues (Xin et al., 2009; Notarnicola et al., 2012). RNA-protein complexes control multiple steps of this process, including mRNA cellular localization, splicing, translational regulation and degradation (St Johnston, 2005). For instance, the expression of an alternative splicing isoform of the natural killer (NK) cell receptor NKp30 correlates with the prognosis of GISTs, independently from the *KIT* mutations (Delahaye et al., 2011).

Moreover, RNA-binding proteins (RBPs), which play important roles in regulating RNA metabolism, may also be deregulated in diseases, particularly in cancers during the initiation and progression phases (van Kouwenhove et al., 2011). The RNA Recognition Motif (RRM) proteins form a large RBP family which includes also RNA-Binding Protein for Multiple Splicing-2 (RBPMS2), an early marker of gastrointestinal smooth muscle precursor cells that we identified recently (Notarnicola et al., 2012). We showed that ectopic expression of *RBPMS2* in differentiated SMCs hinders their ability to contract, favors their proliferation and leads to their dedifferentiation, demonstrating that RBPMS2 expression must be tightly regulated to avoid SMC dedifferentiation (Notarnicola et al., 2012).

These results and the fact that GISTs are thought to arise from Interstitial Cells of Cajal (ICCs) or from a mesenchymal precursor that is common to ICCs and smooth muscle cells (SMCs) (Sanders et al., 2006; Le Guen et al., 2009; Faure and de Santa Barbara, 2011) prompted us to examine the mRNA and protein expression of RBPMS2 in different categories of human adult GISTs and in the GIST882 cell line. We found that RBPMS2 is up-regulated in GISTs compared to normal adult gastrointestinal tissues.

3 Material and Methods

3.1 Tumor samples and KIT and PDGFRA mutational analysis

Paraffin-embedded tumor samples from primary GISTs of 23 adult patients before Imatinib treatment were collected in the *Department of Clinical and Molecular Pathology* of the Olomouc University Hospital (Olomouc, Czech Republic). The risk of clinically aggressive behavior was evaluated according to the consensus approach published by Fletcher and coworkers (Fletcher et al., 2002). Control samples were normal gastrointestinal tissue specimens isolated from adult epithelial-derived tumors. For *KIT* and *PDGFRA* mutational analysis, genomic DNA was extracted from the paraffin-embedded GIST samples using the QIAamp DNA FFPE Tissue Kit (Qiagen). Specific PCR primers were used to analyze *KIT* exons 9, 11, 13 and 17 and *PDGFRA* exons 12, 13, 17 and 18 as previously described (Willmore-Payne et al., 2005). The GIST tissue microarray (DAA1, SuperBioChips Laboratories) contained 48 GIST and 9 normal adult gastrointestinal tissue samples. The microarray GIST samples were KIT-positive by immunodetection, but their *KIT* mutation status was unknown.

3.2 RNA isolation and quantitative RT-PCR

Total RNA was extracted from paraffin-embedded GIST samples using the High Pure RNA Paraffin kit (Roche Diagnostic). For quantitative RT-PCR analysis, gene expression levels were measured using the LightCycler technology (Roche Diagnostics). PCR primers (Table 6) were designed using the LightCycler Probe Design software 2.0. Each sample was assayed in three independent experiments in triplicate. Expression levels were determined with the LightCycler analysis software (version 3.5) relative to standard curves. Data were represented as the mean level of gene expression relative to the expression of the reference gene *HPRT* (Roche Diagnostic). For cell culture experiments, RNA isolation was done with the RNeasy Mini kit (Qiagen) and quantitative RT-PCR was performed using Power Sybergreen (Applied biosystems). Data were represented as the mean level of gene expression relative to the expression of the reference genes *ABL*, *TTC1* and *UBC* for the comparison of *RBPMS2* expression between different cell lines and *GAPDH* and *ACTIN* for GIST882 cells, which were treated with either Imatinib or U0126.

Table 6. Primers used for quantitative RT-PCR amplification of selected human genes.

Target transcript	Forward primer (5'-3')	Reverse primer (5'-3')	Amplicon size (bp)
KIT	CCT TTG CTG ATT GGT TTC G	AGG AAG TTG TGT TGG GTC TA	162
TMEM16A	GCT TCC GCA GGG AGG AGT A	TCG TCG GCA TCT TCA GT	162
RBPMS2	CTC CCA TGC TGC GTT CA	GGG TGG TGT CAG AGG AAG	92
PDGFRA	ATG TGC CAG ACC CAG AT	CCC TCA CTG TTG TGT AAG GTT	139
HPRT	TGT AAT GAC CAG TCA ACA GGG	TGA CCA AGG AAA GCA AAG TCT G	136
Calponin	AGA AGT ATG ACC ACC AGC	CAG CCC AAT GAT GTT CCG	406
αSMA	TTC AAT GTC CCA GCC ATG TA	GAA GGA ATA GCC ACG CTC AG	222
Desmin	AGG AGA TGA TGG AAT ACC GAC	TTT GCT CAG GGC TGG TTT	351
SM22	GCA GTC CAA AAT CGA GAA GA	CTG TTG CTG CCC ATC TGA AG	503
PCNA	CTC CAT CCT CAA GAA GGT GTT	GGT GTC GAA GCC CTC AG	151

3.3 Production of anti-RBPMS2 antibodies and cell culture

The anti-human RBPMS2 rabbit polyclonal antibody was raised using a synthetic peptide corresponding to the C-terminus of human RBPMS2 (SSDTTQQGWKYRQ) (Figure 30A). Anti-RBPMS2 antibodies were purified using protein A-sepharose and were tested by ELISA (Biotem, France). The human GIST cell line GIST882 was maintained in DMEM (GIBCO) supplemented with 10% Fetal Bovine Serum (FBS), 2% Penicilline-Streptomycin (Lonza) and incubated with 1 μM of Imatinib (inhibitor of KIT activity) (LC Laboratory) or 5 μM of U0126 (MEK inhibitor) (Sigma-Aldrich), as previously described (Gromova et al., 2011). The human Embryonic Kidney 293 (HEK293) cell line was grown in DMEM supplemented with 10% FBS and transfected, using JetPEiTM (Polyplus, France), with 5 μg of a construct in which the full length human *RBPMS2* cDNA was subcloned in the pCS2 vector with an in frame N-terminal HA tag and the CMV promoter. Cells were analyzed after 24h. For western blot analyses, cells were lysed and protein extracts (20 μg) were separated on 10% polyacrylamide gels (Bio-Rad Laboratories), transferred onto nitrocellulose membranes (Amersham Hybond-ECL) and incubated with anti-RBPMS2 (home-made), anti-Tubulin (Abcam) and anti-HA (Santa Cruz

Biotechnologies) primary antibodies overnight. After several washes, membranes were incubated with the relevant horseradish peroxidase-conjugated secondary antibodies (Perkin Elmer). Detection was performed by chemiluminescence (Santa Cruz Biotechnologies) on Kodak films. Tubulin expression served as a loading control.

3.4 Immunohistochemistry and in situ hybridization

Immunofluorescence and immunohistochemistry analysis of paraffin-embedded GIST sections were performed as described (Rouleau et al., 2009; Rouleau et al., 2012). Briefly, sections were deparaffinized with Histoclear (VWR, France) and rehydrated through a series of graded alcohols to PBS. For immunodetection, heat-induced antigen retrieval was carried out in 10 mM sodium citrate solution (pH9.0). Endogenous peroxidases were inactivated by incubation in 3% H_2O_2 (Sigma-Aldrich) for 30 minutes. Anti-RBPMS2 (home-made), -Ki67 (NeoMarker), -αSMA (Sigma-Aldrich), -CD34 (Clinisciences), -S100 (Clinisciences), -KIT (Zymed), -Desmin (Euromedex) and -TMEM16A (also called DOG1) (Abcam) primary antibodies were used. Specific mouse or rabbit anti-IgG biotinylated secondary antibodies were used with the avidin-peroxidase reagent (Vector) and antibody reactions were detected with 3,3′-Diaminobenzidine (Sigma-Aldrich). As control, each GIST sections were tested without primary antibodies. Hematoxylin and Eosin (H&E) staining was performed according to standard procedures. *In situ* hybridization experiments using paraffin sections were carried out as described (Come et al., 2006; Notarnicola et al., 2012). Anti-sense riboprobes were generated by PCR amplification of human *RBPMS2* cDNA using specific primer sets and subcloned in pGEM T Easy Vector (Promega, France) as previously published (Notarnicola et al., 2012). Images were acquired using a Nikon-AZ100 stereomicroscope and a Carl-Zeiss AxioImager microscope.

3.5 Statistical analysis

Statistical analysis was carried out using the Mann-Whitney test as previously described (Notarnicola et al., 2012).

4 Results

4.1 RBPMS2 transcripts are detected in adult GISTs

To determine whether the RNA-binding protein RBPMS2 was expressed in GISTs, we first analyzed by *in situ* hybridization a commercial tissue microarray that included 48 KIT-positive GISTs (from low to high risk) and 9 normal adult gastrointestinal tissues (Fig. 29). The level of *RBPMS2* transcripts was very low in smooth muscles of normal adult gastrointestinal tissues (black arrows, Fig. 29). Conversely, *RBPMS2* was strongly expressed in 36 of the 48 GIST samples (75%), independently of their localization and the risk of aggressive behavior (red arrows, Fig. 29).

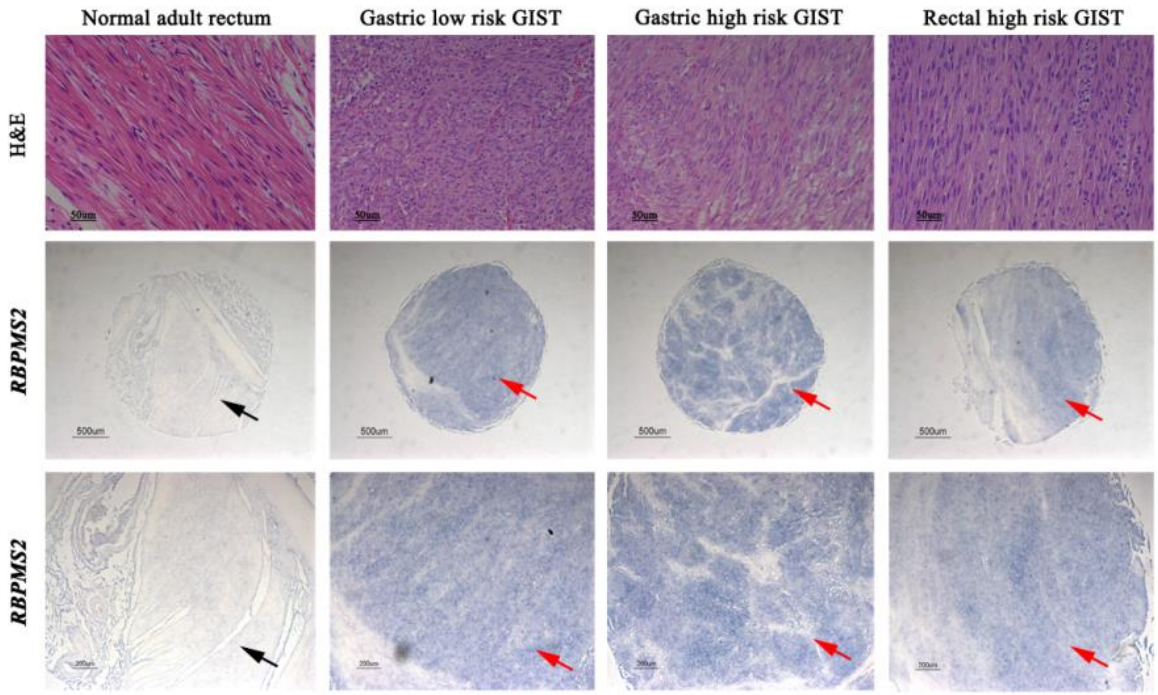

Figure 29. Expression of *RBPMS2* transcripts in adult normal rectum and GIST samples. Hematoxylin-eosin (H&E) staining (upper panels) and *in situ* hybridization of smooth muscle layers sections from normal rectum and GIST samples (middle and lower panels show different magnifications of the same sections) with an anti-human *RBPMS2* riboprobe. *RBPMS2* transcripts are not detected in adult normal rectal musculature (arrows), whereas they are strongly expressed in tumor cells (red arrows). Bars, 50 µm (upper panels), 500 µm (middle panels) and 200 µm (lower panels).

4.2 Clinicopathological features of the GIST cohort

Due to the limited clinical data and the absence of information on the *KIT* and *PDGFRA* mutational status for the GISTs included in the microarray and in order to better characterize RBPMS2 expression in GISTs, we analyzed GIST samples from a cohort of patients from Olomouc University Hospital. The group included 16 males and 7 females (male/female ratio: 1.44) with a mean age of 63.4 years (range: 36 to 81 years) who had exclusively primary GISTs located in the esophagus (n=4), stomach (n=5), small intestine (n=8), rectum (n=3), abdomen (n=2) and soft tissues (n=1) (Table 7). All GISTs included in this study were characterized by using classical histopathological and immunohistochemical approaches with anti-KIT, -SMA, -CD34, -Desmin, -S100 and -TMEM16A (DOG-1) antibodies (Fig. 2A; and data not shown). GISTs were divided in spindle (n=11), epithelioid (n=4) and mixed cell (epithelioid and spindle) (n=8) tumors based on the cell morphology (Table 7). Mitotic cells were detected with the anti-Ki67 antibody (summary in Fig. 30A) and tumors were classified as low risk (n=10) or high risk (n=13) as previously described (Miettinen and Lasota, 2006). *KIT* and *PDGFRA* mutational analysis was available for 21 GISTs and showed that 10 tumors (47.6%) had *KIT* mutations (three GISTs with *KIT* mutations in exon 9, six tumors with mutations in exon 11 and one tumor with a mutation in exon 13), four (19%) had a *PDGFRA* mutation (one missense and two silent mutations in exon 18 and one missense mutation in exon 12) and seven (33.4%) had wild type (WT) *KIT* and *PDGFRA* (Table 7). Quantitative RT-PCR analysis of *KIT* and *PDGFRA* expression levels indicated, as previously published, that in all the analyzed GIST samples (n=20) *KIT* and *PDGFRA* were up-regulated in comparison to normal gastrointestinal samples of adult colon, stomach and small intestine (Figs. 30B and 30C).

Table 7. Summary of the clinical and morphological features, risk assessment, *KIT* and *PDGFRA* mutational status as well as KIT and RBPMS2 expressions in the GIST cohort.

Patient	Sex	Age (y)	Site	Morphology	Size (mm)	Risk	*KIT* or *PDGFRA* mutations	*KIT* RT-PCR	*RBPMS2* RT-PCR	RBPMS2 IHC
1	M	73	Small intestine	Spindle	90x100x110	High Risk	Exon 9 ins AY502-503 *KIT*	+++	+++	++
2	M	73	Soft tissue	Epithelioid	12x5x12	High Risk	Exon 9 ins AY502-503 *KIT*	+++	+++	+++
3	M	74	Duodenum	Spindle	70x75x85	High Risk	Exon 9 ins AY502-503 *KIT*	++	++	+++
4	M	71	Small intestine	Spindle	14x5x14	Low Risk	Exon 11 V559D *KIT*	++	+++	+++
5	M	60	Rectum	Spindle	35x20x15	Low Risk	Exon 11 V559D *KIT*	-	++	++
6	M	71	Stomach	Mixed	15x12x10	High Risk	Exon 11 del/ins *KIT*	+++	+++	+
7	M	77	Esophagus	Spindle	22x18x40	High Risk	Exon 11 del/ins *KIT*	+++	+++	++
8	M	74	Rectum	Spindle	80x75x60	Low Risk	Exon 11 del/ins *KIT*	+	+++	++
9	M	66	Stomach	Spindle	9x5x5	Low Risk	Exon 13 K642E *KIT*	++	+++	NA
10	F	67	Stomach	Epithelioid	43x47x35	High Risk	E12 V561D *PDGFRA*	+	++	++
11	F	62	Stomach	Mixed	NA	Low Risk	Exon 18 D842Y *PDGFRA*	++	+++	NA
12	F	58	Colon	Mixed	10x10x10	Low Risk	Exon 18 silent mutation V824V *PDGFRA*	++	++	++
13	M	36	Recto-peritoneum	Mixed	65x45x42	Low Risk	Exon 18 silent mutation V824V *PDGFRA*	+	++	+
14	F	70	Esophagus	Mixed	50x30x30	Low Risk	WT	+++	+++	++
15	M	48	Esophagus	Spindle	35x25x20	High Risk	WT	+	+	++
16	M	61	Stomach	Spindle	45x25x10	Low Risk	WT	++	+++	NA
17	M	42	Small intestine	Mixed	40x30x20	High Risk	WT	+++	+++	+
18	M	60	Duodenum	Mixed	40x32x22	Low Risk	WT	++	+++	+
19	M	81	Rectum	Mixed	1x3x15	High Risk	WT	+	++	++
20	F	55	Recto-peritoneum	Epithelioid	90x70x50	High Risk	WT	+++	+++	++
21	M	65	Small intestine	Epithelioid	12x8x8	High Risk	NA	NA	NA	++
22	F	55	Small intestine	Spindle	150x13x110	High Risk	NA	NA	NA	+
23	F	60	Stomach	Spindle	50x40x50	High Risk	Exon 11 del/ins *KIT*	NA	NA	+

4.3 RBPMS2 is strongly expressed in malignant GISTs

We then analyzed the levels of *RBPMS2* transcripts in this GIST cohort and in gastrointestinal control samples by quantitative RT-PCR. In most of the analyzed GIST samples (19 of 20) *RBPMS2* expression level was higher than in control samples (Fig. 30D; Table 7) and the mean *RBPMS2* level in GISTs was 42-fold higher than in control samples ($p<0.001$) (Fig. 30E). The level of *KIT* and *PDGFRA* did not significantly correlated with the amount of *RBPMS2* expression in the tumors (compare Figs. 30B and 30C and Fig. 30D; data not shown). Conversely, *RBPMS2* expression was higher in GISTs harboring *KIT* mutations than in tumors with wild type *KIT* and with wild type *KIT* or *PDGFRA* mutations (Fig. 30F). GISTs with *PDGFRA* mutations were characterized by the lowest *RBPMS2* expression levels (Fig. 30F). Finally, *RBPMS2* levels were 64-fold higher in GIST samples with high risk of aggressive behavior than in adult control digestive samples (Fig. 30G) and 6.2-fold higher in high risk than in low risk GISTs (Fig. 30G).

A

Immunohistochemistry	Positive, n (%)	Negative, n (%)	NA, n (%)	Total, n
KIT (CD117)	22 (96)	1 (4)	0 (0)	23
TMEM16A	16 (69.5)	4 (17.5)	3 (13)	23
CD34	15 (65)	4 (17.5)	4 (17.5)	23
SMOOTH MUSCLE ACTIN	9 (39)	8 (35)	6 (26)	23
DESMIN	2 (9)	12 (52)	9 (39)	23
S100	7 (30)	10 (44)	6 (26)	23

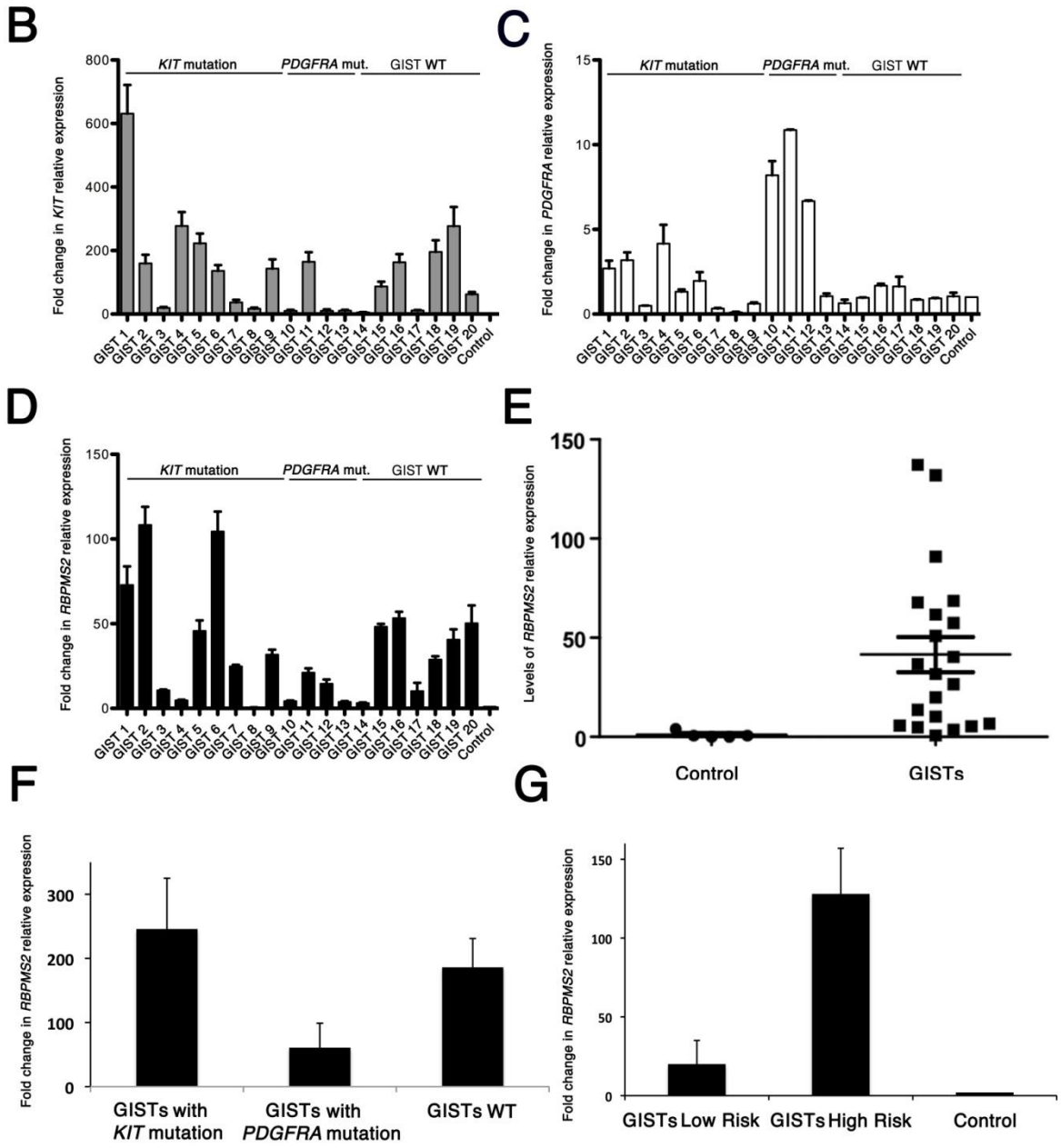

Figure 30. Clinicopathological features and *RBPMS2* mRNA expression in the adult GIST cohort. (**A**) Results of immunohistochemical staining for KIT (CD117), TMEM16A, CD34, αSMA (Smooth Muscle Actin), DESMIN and S100 (n=23 GIST samples). (**B** and **C**) *KIT* (**B**) and *PDGFRA* (**C**) expression level by quantitative RT-PCR in GIST samples (n=20) and in normal samples from different regions of the gastrointestinal tract as controls (n=5). *KIT* and *PDGFRA* mut., GIST samples with a mutation in *KIT* or *PDGFRA*; GIST WT, GIST samples with wild type *KIT* or *PDGFRA*; NA, not available. (**D**) *RBPMS2* transcript level was determined by quantitative RT-PCR in GIST (n=20) and in non-tumor samples from different regions of the gastrointestinal tract (n=5, control). GIST WT, GIST samples with wild type *KIT* or *PDGFRA*; *KIT* and *PDGFRA* mut., GIST samples with a mutation in *KIT* or *PDGFRA.* (**E**) Comparison of the *RBPMS2* transcript levels in the GIST and non-tumoral samples described in A with the Mann-Whitney test ($p<0.001$). (**F**) Mean expression level of *RBPMS2*, *KIT* and *PDGFRA* in GISTs that were classified based on their *KIT* and *PDGFRA* mutational status. (**G**) Mean expression level of *RBPMS2*, *KIT* and *PDGFRA* in GISTs that were classified according to the risk of aggressive behavior.

4.4 RBPMS2 protein is highly expressed in adult GISTs

In order to examine RBPMS2 protein expression, we generated antibodies directed against the C-terminus of human RBPMS2 (Fig. 31A). The efficiency and the specificity of these anti-RBPMS2 antibodies were confirmed by western blot and immunofluorescence analyses in HEK293 cells that express HA tagged RBPMS2 (Figs. 31B, and 31C). In western blots, the anti-RBPMS2 antibody identified a single band of 27kDa, corresponding to the predicted size of human RBPMS2 fused to the HA tag (Fig. 31B, lane 3; data not shown). In addition, this band was also detected with the anti-HA antibody (Fig. 31B). Moreover, the anti-RBPMS2- and –HA antibodies both detected an epitope localized in the cytoplasmic compartment of such cells (Fig. 31C). Finally, the RBPMS2 signal was specifically lost when the anti-RBPMS2 antibody was pre-incubated with the RBPMS2 C-terminal peptide used to produce the antibody (data not shown). We then examined the expression of RBPMS2 by immunohistochemistry in control gastrointestinal and GIST samples (Figs. 31D-F). RBPMS2 was faintly but reproductively detected in the gastrointestinal musculature with the exception of the myenteric plexus (arrow, Fig. 31D). In contrast, it was strongly detected in 87% of the analyzed GIST samples (Fig. 31D,

representative GIST sample, and Fig. 31E) and its expression level was comparable in spindle, epithelioid and mixed cell tumor variants (Fig. 31F).

A

human RBPMS2 protein

MSNLKPDGEHGGSTGTGSGAGSGGALEEEVRTLFVSGLPVDIKPRELYLLFRPF
KGYEGSLIKLTARQPVGFVIPDSRAGAEAAKNALNGIRFDPENPQTLRLEFAKA
NTKMAKSKLMATPNPSNVHPALGAHFIARDPYDLMGAALIPASPEAWAPYPLY
TTELTPAISHAAFTYPTATAAAAALHAQVRWYPSSDTTQQGWKYRQFC

B

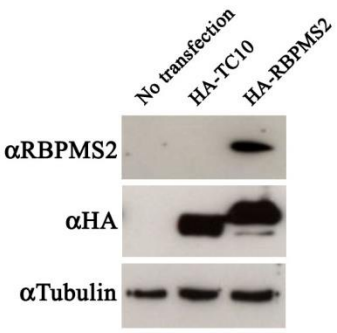

C

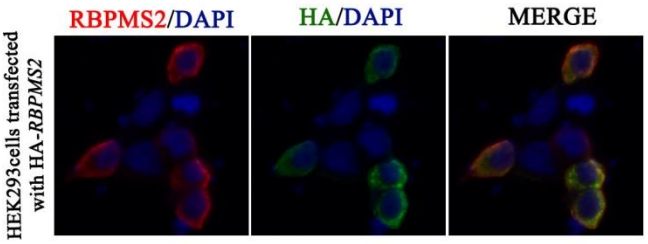

D

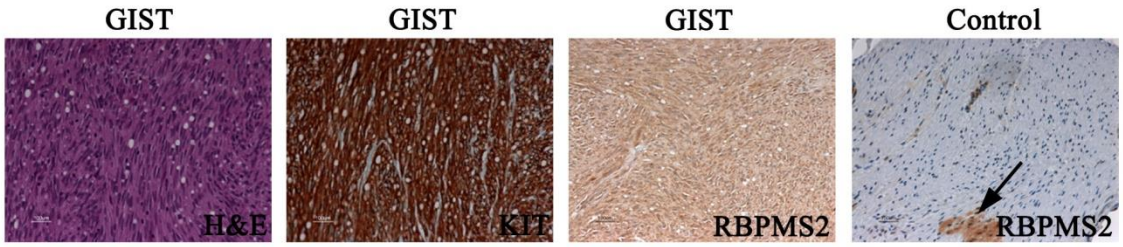

E

Immunohistochemistry	Positive, n (%)	Negative, n (%)	NA, n (%)	Total, n
KIT (CD117)	22 (96)	1 (4)	0 (0)	23
RBPMS2	20 (87)	0 (0)	3 (13)	23

F

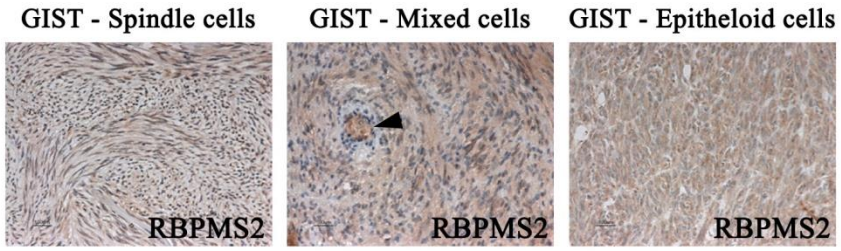

Figure 31. RBPMS2 protein expression in adult GISTs. Characterization of the anti-human RBPMS2 antibody by immunofluorescence and western blotting (**A**-**C**). (**A**) Sequence of the human RBPMS2 protein (amino acids 1-209). Amino acids 195-207 of the C-terminus (in red) correspond to the sequence of the synthesized peptide used for producing the anti-RBPMS2 antibody. (**B**) Western blot analysis of HEK293 cells following transfection of empty vector (lane 1), the HA-TC10 (lane 2) or the HA-RBPMS2 construct (lane 3). 20 μg of whole protein extracts were processed for each condition. Tubulin (50 kDa) was used as loading protein control. HA-RBPMS2 was detected as a 27kDa band with both anti-HA and anti-RBPMS2 antibodies. In addition, lower band corresponding to a Cterminal product of degradation was observed with only anti-HA antibodies. (**C**) HEK293 cells were transfected with the HA-RBPMS2 construct and then processed for immunofluorescence analysis using mouse anti-HA and anti-RBPMS2 primary antibodies and anti-mouse Alexa488 and anti-rabbit Alexa555 IgG, respectively. Nuclei were stained with Hoechst. Cytoplasmic localization of the signal is observed with both antibodies. (**D**) Representative example of RBPMS2 protein expression in a colonic, high risk GIST sample. Histological staining (H&E) and labeling with anti-KIT (CD117) and anti-RBPMS2 antibodies. In normal colon (control), RBPMS2 is expressed in vessels and the enteric myenteric plexus (arrow), but not in visceral SMCs. (**E**) Summary of KIT (CD117) and RBPMS2 protein expression in the GIST cohort (n=23). NA, not available. (**F**) Analysis of the expression of RBPMS2 in the GIST samples that were classified based on their morphological features (spindle, mixed and epithelioid cells). Arrowhead shows vessels.

4.5 RBPMS2 expression and regulation in GIST882 cells

To position RBPMS2 in the KIT signaling pathway in GISTs, we first compared *RBPMS2* expression in GIST882 (a GIST cell line homozygous for the oncogenic *KIT* mutation K641E with strong *KIT* expression and high level of KIT activity) (Tuveson et al., 2001), HeLa and 1321N1 (human astrocytoma) cells as well as in two prostate cancer cell lines (PC3 and LNCaP). *RBPMS2* mRNA level was relatively high in GIST882 and HeLa cells in comparison to 1321N1 cells and the two prostate cancer cell lines (Fig. 32A). Then GIST882 cells were treated with 1 μM of Imatinib (a specific inhibitor of KIT activity) (Tuveson et al., 2001) or with 5 μM of U0126 (a selective inhibitor of MEK which is a

downstream effector of the KIT signaling pathway) for 6, 24 and 48 h (Figs. 32B, and 32C) and *RBPMS2* expression was determined by quantitative PCR. No significant changes in *RBPMS2* mRNA levels were observed following addition of Imatinib or U0126 in the culture medium (Figs. 32B and 32C).

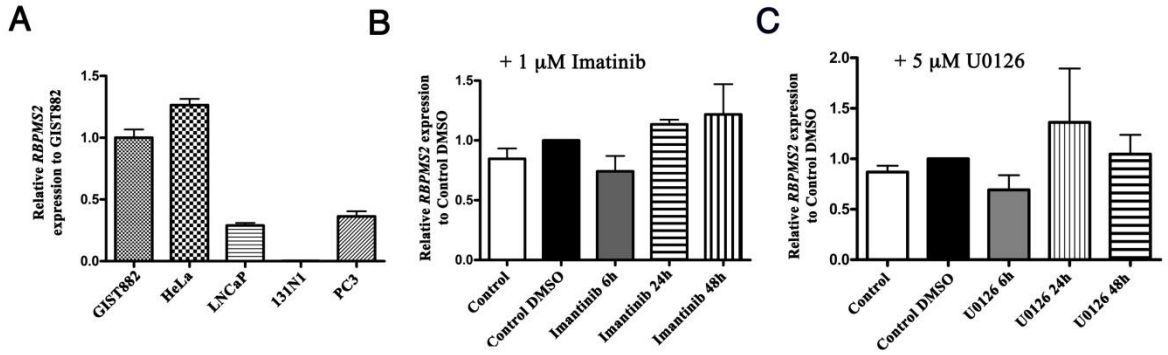

Figure 32. *RBPMS2* mRNA expression and regulation in the GIST882 cell line. (**A**) Analysis of *RBPMS2* expression by quantitative RT-PCR in GIST882, HeLa, LNCaP, 1321N1 and PC3 cells. *RBPMS2* is strongly expressed in GIST882 and HeLa cells, weakly in LNCaP and PC3 prostate cancer cells and undetectable in 1321N1 astrocytoma cells. (**B**) Analysis of *RBPMS2* transcript level in GIST882 cells upon incubation with 1 μM of Imatinib (inhibitor of KIT activity) or with DMSO alone (control DMSO) for 6, 24 and 48 h. *RBPMS2* transcript level is not influenced by inhibition of KIT activity. Control, untreated cells. (**C**) Analysis of *RBPMS2* transcript level in GIST881 cells following incubation with 5 μM of U0126 (inhibitor of MEK activity) or with DMSO alone (control DMSO) for 6, 24 and 48h. *RBPMS2* transcript level is not influenced by MEK inhibition. Control, untreated cells.

5 Discussion

In this study we analyzed the expression of the RNA-binding protein RBPMS2 in a cohort of GIST samples that were classified according to their *KIT*/*PDGFRA* mutational status, risk of aggressive behavior and histological pattern (spindle, epithelioid and mixed cell phenotype).

We found that RBPMS2 mRNA and protein expression was significantly higher in GIST samples than in control gastrointestinal tissues, particularly in high risk tumors. The levels of *KIT* and *PDGFRA* did not significantly correlate with the amount of *RBPMS2* expression. However, *RBPMS2* mRNA levels were higher in GISTs harboring *KIT* mutations than in tumors with *PDGFRA* mutations or with wild type *KIT* and *PDGFRA*. This difference could be due to the different origins of *KIT* and *PDGFRA* expressing cells and would suggest that *RBPMS2* and *KIT* expression are linked. However, in the GIST882 cell line that carries the KIT mutation K641E and shows high KIT activity we did not observe a correlation between *RBPMS2* expression and KIT activity. In contrast, using primary digestive smooth muscle cultures we found that RBPMS2 over-expression induces a 2-fold increase of *KIT* mRNA level (Notarnicola and de Santa Barbara, unpublished data). All these data suggest that KIT and RBPMS2 could be expressed in the same mesenchymal cells during the early development and remodeling of mesenchymal-derived gastrointestinal cells, or that they are part of the same signaling pathway, or share a regulatory circuitry. More experiments are needed to confirm these hypotheses and to position RBPMS2 relative to the KIT signaling pathway.

Chromosomal alterations during GIST progression have been described and could be involved in GIST prognosis (Corless et al., 2011). Specifically, losses and gains on chromosome 15 between 15q22.1 and 15q25.3 have been clearly correlated with poor outcome (Ylipää et al., 2010). As the *RBPMS2* gene is localized on chromosome 15q22.31, we can hypothesize based on our results that elimination of a negative regulatory sequence necessary for correct RBPMS2 expression could alter the endogenous expression of RBPMS2, thus favoring dedifferentiation of mesenchymal cells that will give rise to GIST tumors. A through characterization of the correlation between alterations of this genome region and RBPMS2 expression is now required.

In conclusion, our study shows that most of the analyzed GISTs are characterized by abnormally elevated expression of RBPMS2, suggesting that RBPMS2 could be an indicator for tumor progression and a potential target for cancer therapy in GIST.

Conflict of interest statement

The authors declare that there are no conflicts of interest.

Contribution to authorship

Immunohistochemistry, and in situ hybridization were carried out by IH with the help of CR, FB and SF under the supervision of PdSB. GIST collection and analyses were carried out by JS, MJ, and IH. Quantitative PCR analysis was performed by IH with the help of CN, and MR under the supervision of PdSB and JV. GIST cell line analyses were carried out by AT under the supervision of JMV. PdSB wrote the paper.

Funding

The work was supported by ARC (Association pour la Recherche sur le Cancer), Région Languedoc-Roussillon (Chercheur d'Avenir), INCA GSO Emergence and Ligue contre le Cancer (Comité de l'Aude) to PdSB. IH was supported by a studentship of the French Ministry of Foreign Affairs and by an IGA studentship of Palacky University, Olomouc. AT is PhD student bursary on Télévie (Belgium) grant 7.4562.10. JMV is Research Director at FRS-FNRS (Belgium).

Acknowledgements

We thank members of INSERM U1046 for helpful discussions.

STUDY II

Function and mechanism of action of RBPMS2 in the development of GISTs

(Human Colon Smooth Muscle Cells Approach)

1 Introduction

The first reports of smooth muscle in culture were by Champy (1913), who described the cells as elongated elements with fibrillae that lost these characteristics with repeated mitoses, by Laqueur (1914), who noted spontaneous contractions in explants, and by Lewis and Lewis (1914), who described the intravital staining of cultured smooth muscle mitochondria. During the next 40 years many descriptive reports appeared in the literature on primary culture of smooth muscle from different tissues. A complete list of these up to 1950 can be found in the two-volume bibliography on tissue culture by Murray and Kopech (1953).

Since the late 1950's, most of the work on smooth muscle in culture has involved uptake, synthesis, and metabolism of lipids in cultured vascular muscle as an experimental model for atherosclerotic lesions (Chamley-Campbell et al. 1979). Other roles played by smooth muscle in the etiology of this disease have also been described, including proliferation and the synthesis of extracellular matrix components (Chamley-Campbell et al. 1979). Recent studies on cultured visceral smooth muscle have mainly concerned factors influencing its development differentiation, and innervations (Chamley-Campbell et al. 1979).

In the first part of my thesis, we showed that RBPMS2 is strongly expressed in GISTs, we were interested to analyze the function of RBPMS2 in the tumorigenesis process. In order to analyze its potential involvement in the development of GIST, we decided to characterize human adult Colonic Smooth Muscle Cells (hCSMC) line and developed stable hCSMC lines that expressed constitutively RBPMS2. In addition, to understand RBPMS2 function and mechanism of action we decided to identify RBPMS2 protein partners and analyzed a yeast two-hybrid screen of human RBPMS2 versus Human Placenta library and investigated the interaction of RBPMS2 with Eukaryotic translation Elongation Factor 2 (EEF2).

2 Materials and Methods

2.1 Cell cultures

Human Colon Smooth Muscle Cells (hCSMC) were isolated by ScienCell Research Laboratories from human adult colon musculature (Fig. 34). hCSMC are guaranteed to further expand for 15 population doublings at the condition provided by ScienCell Research Laboratories. The availability of human digestive SMC in culture will considerably enhance our ability to study the differentiation, contractile, and proliferative responses of this smooth muscle.

Smooth Muscle Cell Medium (SMCM) is a complete medium designed for optimal growth of normal human smooth muscle cells in vitro. It is a sterile, liquid medium which contains essential and non-essential amino acids, vitamins, organic and inorganic compounds, hormones, growth factors, trace minerals and a low concentration of fetal bovine serum. The medium was formulated (quantitatively and qualitatively) to provide a defined and optimally balanced nutritional environment that selectively promotes proliferation and growth of normal human smooth muscle cells in vitro. 500 ml of Basal Medium (SMCM) was completed with 10 ml of Fetal Bovine Serum (FBS), 5 ml of Smooth Muscle Cell Growth Supplement (SMCGS) and 5 ml of penicillin/streptomycin solution (P/S solution). We used also DMEM supplement with 20% FBS or DMEM in presence of 0,2% BSA and 5µg/ml insulin to stimulate differentiation of hCSMCs (Notarnicola et al., 2012).

In this study for Co-Immunoprecipitation we used the HEK293 cell line. Human Embryonic Kidney 293 cells, also often referred to as HEK293, 293 cells, or less precisely as HEK cells are a specific cell line originally derived from human embryonic kidney cells in the early 70s grown in tissue culture (Graham et al. 1977).

HEK293 cells were grown in Dulbecco´s modified Eagle medium (DMEM) supplement with 10% fetal bovine serum (FBS). 5µg of a human RBPMS2 and GFP or RBPMS2 and HA-tagged retroviral constructs were transfected with JetPEiTM (Polyplus) into HEK293 cells and analyzed after 24h.

2.2 Human Colon Smooth Muscle Cells and contractility

Adult hCSMC were cultured in DMEM or SMCM in presence of 0,2% BSA and 5µg/ml insulin in collagen coated plates for 7, 14, 17 and 22 days. Contractility and concentration exchange of calcium were observed on the same fields before and after 1mM respectively 100mM carbachol treatment, a muscarinergic agonist (Notarnicola et al. 2012). Contractility of HCSMCs was observed with Nikon inverted microscope on the same fields before and after treatment was imaged.

The introduction of the calcium-sensitive dye Fura-2 revolutionized the measurement of intracellular [Ca^{2+}] in population adherent cells and in subcellular region. Fura-2 is a ratiometric dye in that when Ca^{2+} binds, the excitation spectrum shifts rightward. In the presence of Ca^{2+}, maximum Fura-2 fluorescence (at 510 nm emission) is observed at a wavelength of 340 nm and in Ca^{2+} free conditions at 380 nm. Therefore, it follows that the concentration of free intracellular Ca^{2+} is proportional to the ration of fluorescence at 340/380 (F/Fo). The Grynkiewicz equation describes this relationship (Grynkiewicz et al. 1985):

$$[Ca^{2+}]_i \text{ (n}M\text{)} = K_d \times [(R - R_{min}) / R_{max} - R)] \times Sfb$$

where K_d (for Ca^{2+} binding to Fura-2 at 37°C) = 225 nM, R = 340/380 ratio, R_{max} = 340/380 ratio under Ca^{2+} saturating condition, R_{min} = 340/380 ratio under Ca^{2+} free conditions, and Sfb = ratio of baseline fluorescence (380 nm) under Ca^{2+} free and Ca^{2+} bound conditions. The K_d for Ca^{2+} binding to Fura-2 decreases with decreasing temperature (Grynkiewicz et al. 1985).

Cells were loaded by incubation with 1 µmol/L fura-2AM (Tef-labs) plus 0.02% pluronic acid F-127 (Molecular Probes Inc), during 30 min in culture medium at 37°C in a humidified air atmosphere. The loaded cells were then washed with PBS and replace in culture medium, mounted on the microscope stage at room temperature for 15 min to allow fura-2AM de-esterification. Measurements of the fura-2 fluorescence ratio were made from images captured digitally, every 2 seconds, by a cooled CCD camera (Photometrics) with a x20 objective lens mounted on an inverted microscope (Axiovert, Zeiss), and acquired after excitations at 340- and 380-nm using a lambda-DG4 excitation system (Sutter Instrument Company, USA). Ca^{2+} signals were then analyzed by using the Metafluor software (Universal Imaging Corporation, USA). The results are given as the variation

from basal values of the ratio of 340/380 nm recordings with fluorescence values corrected for background and dark currents.

2.3 Plasmids and lentivirus production

We used the bi-cistronic plasmid (pHRTK vector) that containing GFP alone and subcloned the full-length human *RBPMS2* cDNA to produce the pHRTK-GFP-RBPMS2 plasmid (Fig. 33).

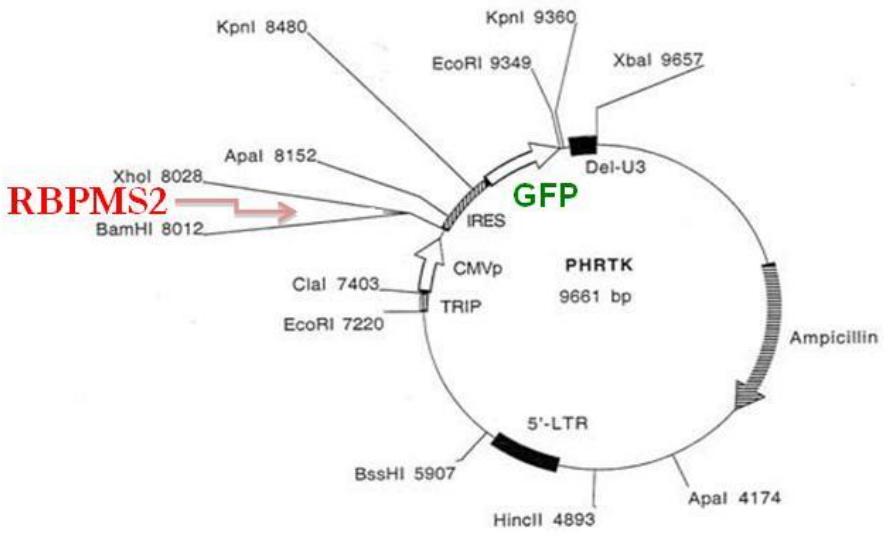

Figure 33. pHRTK vector contains GFP and the full-length human *RBPMS2* cDNA.

2.4 RNA Extraction and quantitative real-time PCR

Quantitative RT-PCR was performed to measure the mRNA expression levels of the studied genes with the LightCycler system (Roche Diagnostics, Mannheim, Germany). Total RNA was extracted from 10^6 cells using the High Pure RNA Isolation kit, and mRNA was reverse-transcribed using the Transcriptor First Strand cDNA Synthesis kit (both from Roche). PCR primers (Tab. 8) were designed using LightCycler probe design2 software. Ten microliters of a reaction mixture consisting of FastStart DNA MasterPLUS SYBR Green I (Roche), the forward and reverse primers, and an aliquot of the reverse-transcribed samples (1µl) were contained in a LightCycler glass capillary. Each sample

was analysed in triplicate. mRNA expression levels were determined by LightCycler analysis software (version 3.5), according to the standard curves. Data were represented as the mean level of gene expression relative to HPRT reference expression.

Table 8. Primers used for quantitative RT-PCR amplification of selected human genes.

Target transcript	Forward primer (5'-3')	Reverse primer (5'-3')	Amplicon size (bp)
Calponin	AGA AGT ATG ACC ACC AGC	CAG CCC AAT GAT GTT CCG	406
Desmin	AGG AGA TGA TGG AAT ACC GAC	TTT GCT CAG GGC TGG TTT	351
EEF2	GCA GTT TGC CGA GAT GTA TG	CTG GTG GCT GAC TTG CT	206
HPRT	TGT AAT GAC CAG TCA ACA GGG	TGA CCA AGG AAA GCA AAG TCT G	136
KIT	CCT TTG CTG ATT GGT TTC G	AGG AAG TTG TGT TGG GTC TA	162
PCNA	CTC CAT CCT CAA GAA GGT GTT	GGT GTC GAA GCC CTC AG	151
PDGFRA	ATG TGC CAG ACC CAG AT	CCC TCA CTG TTG TGT AAG GTT	139
RBPMS2	CTC CCA TGC TGC GTT CA	GGG TGG TGT CAG AGG AAG	92
SM22	GCA GTC CAA AAT CGA GAA GA	CTG TTG CTG CCC ATC TGA AG	503
TMEM16A	GCT TCC GCA GGG AGG AGT A	TCG TCG GCA TCT TCA GT	162
αSMA	TTC AAT GTC CCA GCC ATG TA	GAA GGA ATA GCC ACG CTC AG	222

2.5 Immunofluorescence

Cells were washed briefly with PBS, and fixed with 4% paraformaldehyde (PFA) for 15min at room temperature. After being washed with PBS, cells were incubated in 5% NDS serum (Donkey) and 0.1% Triton (Sigma-Aldrich) to inhibit nonspecific binding of antibodies. Primary antibodies with 1% NDS serum (Donkey) were applied, and cells were incubated for 90min at room temperature. After, cells were washed with PBS, Alexafluor 555 conjugated (anti-mouse or anti-rabbit) IgG and Alexafluor 488 conjugated (anti-mouse or anti-rabbit) IgG (1:2000) with 1% NDS serum (Donkey) were added and cells were incubated for 60min at room temperature. Cells nuclei were stained with Hoechst (Molecular Probes) for 5min.

2.6 Electrophoresis and Western Blotting

For protein immunoblotting experiments, protein extracts (20µg) were loaded on 10% polyacrylamide gels (Bio-Rad Laboratories) for electrophoresis, and blotted on nitrocellulose membranes. Membranes were exposed to primary antibodies overnight and further exposed to corresponding horseradish peroxidase-conjugated secondary antibodies. Detection was performed by chemiluminescence on Kodak films. GAPDH or/and Tubulin were used to confirm equal loading.

2.7 Co-Immunoprecipitation

Co-immunoprecipitation (Co-IP) is a popular technique to identify physiologically relevant protein-protein interactions by using target protein-specific antibodies to indirectly capture proteins that are bound to a specific target protein. These protein complexes can then be analyzed to identify new binding partners, binding affinities, the kinetics of binding and the function of the target protein.

HEK293 cells were lysed in Co-immunoprecipitation (CoIP) buffer (50mM Tris-HCl pH 8, 150 mM NaCl, 1mM EDTA, 1% NP40) for 2 h at 4°C. The samples were then centrifuged for 15 min at 20 000g in cold to get rid of debris. Supernatant was incubated with 5µg of antibody overnight with Protein A Sepharose (Invitrogen). Immunoprecipitates were washed with CoIP buffer three times before eluting the complexes were loaded on 10% polyacrylamide gels (Bio-Rad Laboratories) for electrophoresis, and blotted on nitrocellulose membranes. Membranes were exposed to primary antibodies overnight and further exposed to corresponding horseradish peroxydase-conjugated secondary antibodies. Detection was performed by chemiluminescence on Kodak films. GAPDH or/and Tubulin were used to confirm equal loading.

2.8 Microscopes and Statistical analysis

Contractility of HCSMCs was observed with Nikon inverted microscope on the same fields before and after treatment was imaged. Images of cells were acquired using a Nicon-AZ100 stereomicroscope and a Carl-Zeiss Axioimager microscope.

Statistical analysis was carried out using the Student´s t-test when two sets of data were compared. The ANOVA test was used when more than two sets were compared. A p value of less than 0.05 was considered significant.

3 Results

3.1 Characterization of human Colonic Smooth Muscle Cell model

In order to characterize the Human Colon Smooth Muscle Cells (hCSMCs), we cultured hCSMCs in collagen coated plates in different conditions in the presence of preconized media completed with 2% of Fetal Bovine Serum (FBS), Smooth Muscle Cell Growth Factor Supplement (containing 1%), that allow the growing of hCSMCs or media completed with 0,2% BSA and 5µg/ml insulin to stimulate their differentiation (Fig. 34B).

Cultured SMCs can display phenotypic modulation upon exogenous stimulation (Lagna et al. 2007; Notarnicola et al. 2012). Using H&E staining, we observed that cultured hCSMCs in BSA/insulin condition were spindle-shaped (Fig. 34B). In contrast, cultured hCSMCs in presence of growth factor present morphology close to mesenchymal and undifferentiated cells (Fig. 34A).

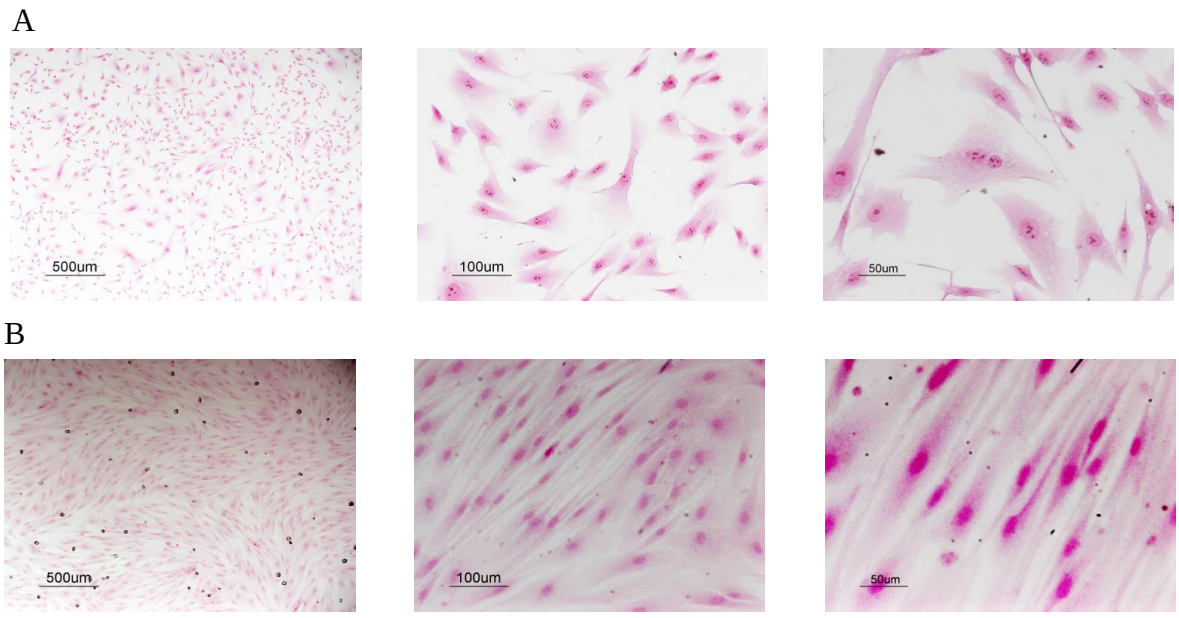

Figure 34. Analyse of the morphology of hCSMC cultured in different condition. After fixation with 4% PFA in PBS, Hematoxylin and Eosin staining were applied to the culture. (**A)** hCSMCs cultured in preconized commercial media harbor undifferentiated profiles. (**B**) hCSMCs cultured for 7 days in the presence of BSA/insulin media harbors differentiated morphologies.

We observed that hCSMCs in commercial media harbor a mixed phenotype presenting cell culture with high index of Ki67 positive cells and cell culture that present some positive cells for the expression of αSMA and SM22 specific smooth muscle markers and few or no cells presenting the expression of the differentiated marker CALPONIN. In contrast, we detected in media containing BSA and insulin without serum the presence of positive cells for CALPONIN and αSMA expression and lower expression Ki67 (Fig. 35). In addition, using our anti-RBPMS2 home-made antibodies, we did not detect by Western-blot analysis endogenous RBPMS2 protein in all hCSMC condition tested (data not shown). These immunofluorescence data showed that commercial media maintains the hCSMCs in proliferative/determinate stage, where BSA/insulin media is a pro-differentiating media conducting to the presence of well organize cluster of cells characteristics of differentiated SMCs.

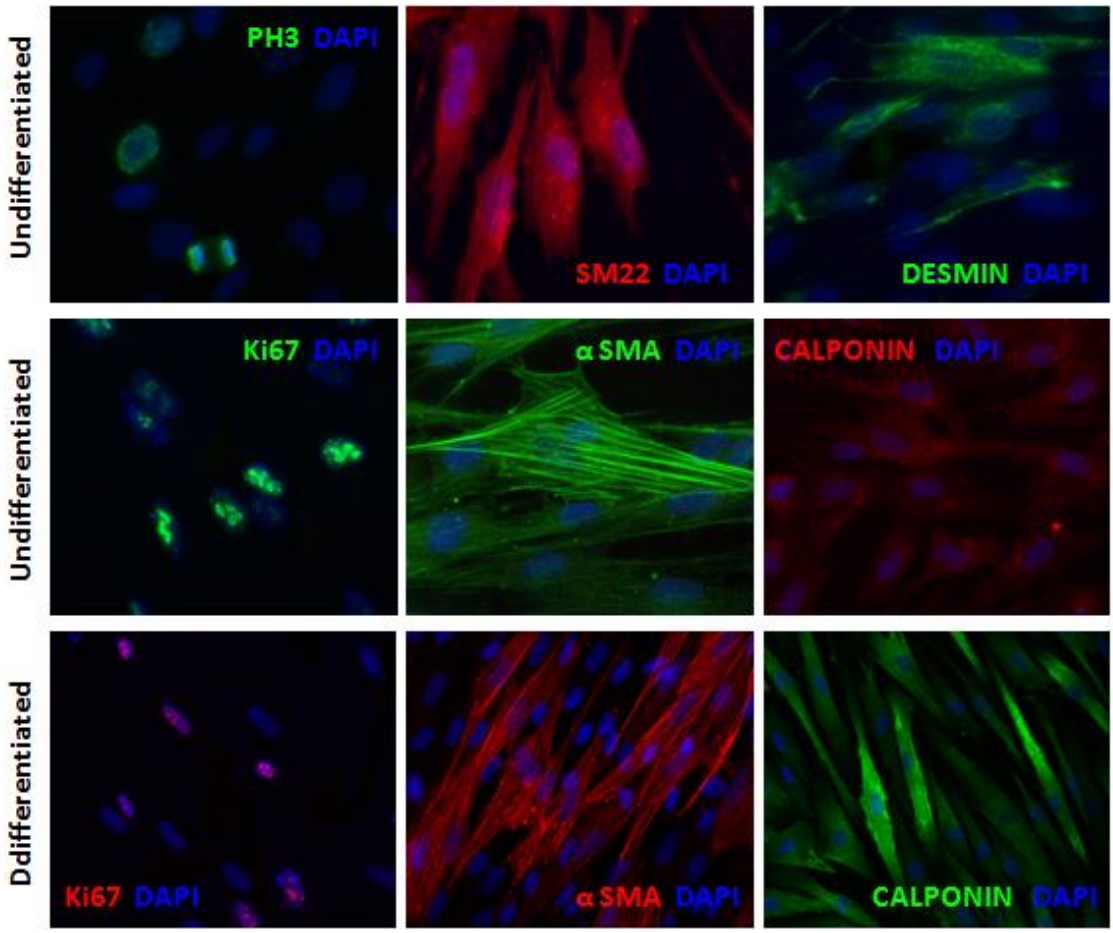

Figure 35. Characterization of differentiation and proliferation status of hCSMC cultured in commercial media. Immunofluorescence analysis of primary cultured SMC

undifferentiated: antibody against SMC alpha-Smooth Muscle Actin (αSMA) and Smooth Muscle Protein-22 (SM22), antibody against mesenchymal cell DESMIN and differentiated marker CALPONIN were used. Antibody against cellular marker for proliferation Ki67 and Phospho-Histone H3 (PH3) were used. hCSMCs differentiated for 7 days were analyzed with Ki67, αSMA and CALPONIN. Nuclei were visualized with Hoechst.

We also investigated the gene expression pattern of SMC markers of the adult hCSMC cultures in different media and conditions. Quantitative reverse-transcription polymerase chain reaction (qPCR) comparing RNAs from hCSMC undifferentiated and differentiated cultured for 7 days confirmed that BSA/Insulin treatment induces the expression of *αSMA* and *SM22* (marker of determination and differentiation of SMCs), *DESMIN* (marker of mesenchymal tissues) and *CALPONIN* (marker of differentiated SMCs) (Fig. 36). In addition, we observed higher expression of *Proliferating Cell Nuclear Antigen* (*PCNA*) in undifferentiated than in differentiated stages of hCSMCs, and observed low expression RBPMS2 in four conditions of hCSMC (data not showed). All these data demonstrated that Insulin/BSA treatment is able to induce the differentiation of hCSMCs in culture but also demonstrated differences in the media used.

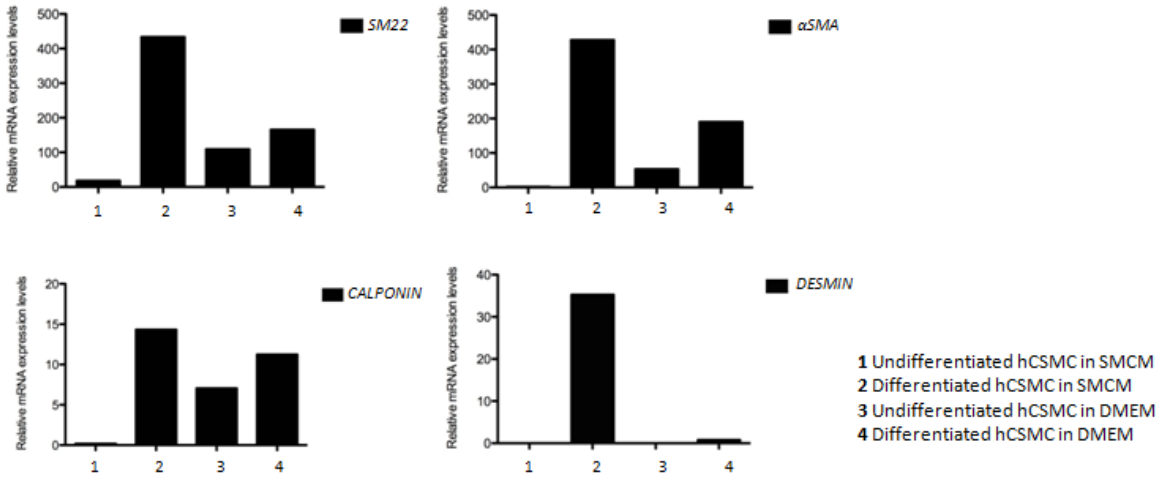

Figure 36. Characterization undifferentiated and differentiated (7 days) hCSMC in different medium (SMCM and DMEM). mRNA expression levels quantified by quantitative RT-PCR in hCSMC. Normalized relative mRNA expression levels were by HPRT.

Smooth muscle contraction is the fundamental event in gastrointestinal motion. Smooth muscle cells form electrical and mechanical junctions between cells that facilitate coordination of contractions. Excitation-contraction coupling occurs by Ca^{2+} entry via ion channels in the plasma membrane, leading to a rise in intracellular Ca^{2+}. Ca^{2+} binding to calmodulin activates myosin light chain kinase; subsequent phosphorylation of myosin initiates cross-bridge cycling. Myosin phosphatase dephosphorylates myosin to relax muscles, and a process known as Ca^{2+} sensitization regulates the activity of the phosphatase.

Gastrointestinal smooth muscles are 'autonomous' and generate spontaneous electrical activity (slow waves) that does not depend upon input from nerves. Here we analyze the exchange of calcium as an intracellular messenger requires quantitative measurement of cytosolic free Ca^{2+} concentrations, and comparison with stimuli and cell responses. Although exchange Ca^{2+} have revealed much important biological information such as potencional capacity of hCSMC to contract on culture. However, in our condition, we were not able under differentiation status and carbachol treatment to observe contractility of hCSMCs and detachment of cells from collagen plates.

In order to observe if hCSMC are still sensitive to carbachol treatment, we observe exchanged Ca^{2+} between intracellular and extracellular using Fura-2 analysis. For this, hCSMC in both type of medium (DMEM, SMCM) were treated with 1mM and 100mM carbachol and analyzed by using the Metafluor software (Fig. 37). The results are given as the variation from basal values of the ratio of 340/380 nm recordings with fluorescence values corrected for background and dark currents. These results indicate that spindle-shaped hCSMCs can be functional and they have potential of contractile activity.

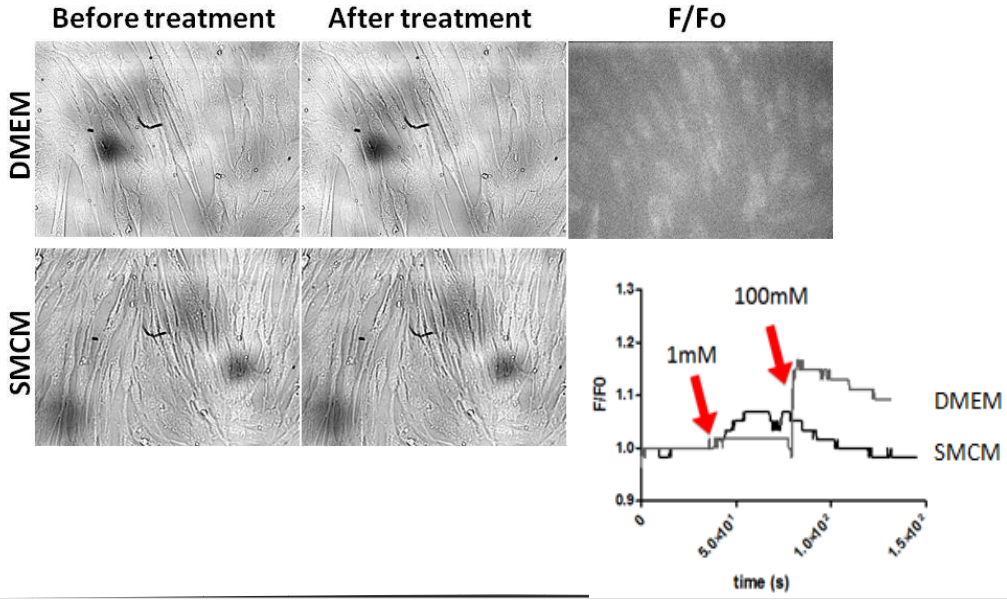

Figure 37. Contractile function of hCSMC. Measurement of contractile activity of differentiated hCSMC cultured in DMEM or SMCM in presence of 0,2% BSA and 5µg/ml insulin for 22 days (we tested also after 7, 14 and 17 days) and then stimulated with 1mM and 100mM carbachol (arrow). Images were acquired before and 5 min after carbachol addition. We did not observed contractility visual, but we indicated exchange calcium after treatment of carbachol.

3.2 Ectopic expression of RBPMS2 in hCSMCs

Using avian model and avian primary SMC culture, we showed that ectopic expression of RBPMS2 in differentiated embryonic digestive SMCs induces a dedifferentiation of these cells (Notarnicola et al. 2012). In the first part of my thesis project, we found that RBPMS2 expression was high in human GIST. Using the adult colon SMC cell line tat we characterize in the above section, we were interested to analyze the impact of RBPMS2 ectopic expression in these cells and their consequence on the differentiation and remodeling process.

As a first step, using a plasmid that allows us to produce integrative but replicative-deficient lentiviruses, we subcloned human RBPMS2 cDNA into the polylinker that allows the expression of RBPMS2 and GFP with the presence of the IRES sequence (pHRTK-GFP-RBPMS2). We analysed the efficiency of this plasmid by transient transfection on undifferentiated hCSMCs cultured in SMCM and observed coexpression of GFP and RBPMS2 in the same transfected hCSMC (Fig. 38). We also analyzed by Western blot the expression of RBPMS2 in transfected hCSMCs and observed a 27 kDa band corresponding to the predicted human RBPMS2 protein as previously published (Hapkova et al. 2013. In addition we observed that the expression of RBPMS2 is localized to the cytoplasmic compartment in hCSMCs (Fig. 38).

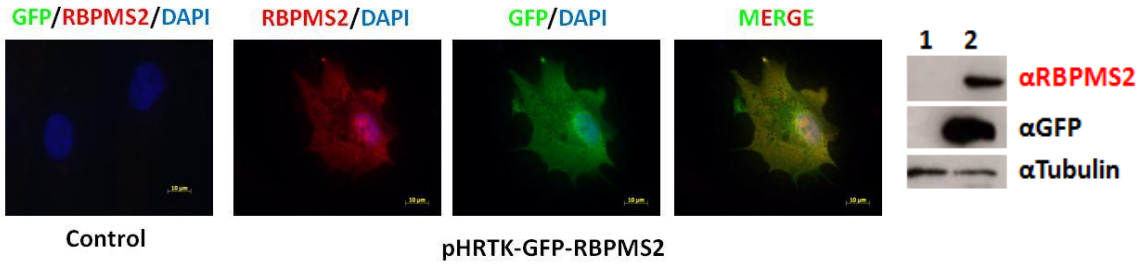

Figure 38. Ectopic expression of RBPMS2 in undifferentiated hCSMC. Immunofluorescence analysis of primary adult hCSMCs infected with pHRTK-GFP-RBPMS2 plasmid for 24h. Nuclei were visualized with Hoechts. Home-made antibodies against RBPMS2 and anti-GFP antibodies were used to identify cells transfected by pHRTK-GFP-RBPMS2 plasmid. Scale bar 50μm. Right panel shows Immunoblot analysis using αRBPMS2 (27 kilodaltons), αGFP (50 kilodaltons) antibodies and loading was verified by Tubulin expression (50 kilodaltons) in 1 correspond to hCSMC (control); 2 correspond to hCSMC transfected by pHRTK-GFP-RBPMS2 vector.

To determine how RBPMS2 regulates adult human SMC plasticity, we established primary culture hCSMC passage 5 in serum-free medium (DMEM) supplemented with insulin and BSA for 7 days. In this condition, hCSMC can display phenotypic modulation upon exogenous stimulation (Notarnicola et al. 2012). Control primary cultured hCSMC were spindle-shaped and homogenously expressed CALPONIN (SMC contractile marker) in highly organized filaments bundles. SMCs then were transfected with replication-defective lentiviruses plasmid (pHRTK-*GFP-RBPMS2* construct or pHRTK-*GFP* [control]) for 24h. Although in control cells the expression of CALPONIN remained unchanged (Fig. 38), in hCSMCs transfected with *RBPMS2* constructs, CALPONIN expression was lost in infected hCSMCs. In addition, we showed that hCSMC cultures transfected with RBPMS2 present an increase in the number of Ki67 positive cells compare to the GFP transfected control (Fig. 39).

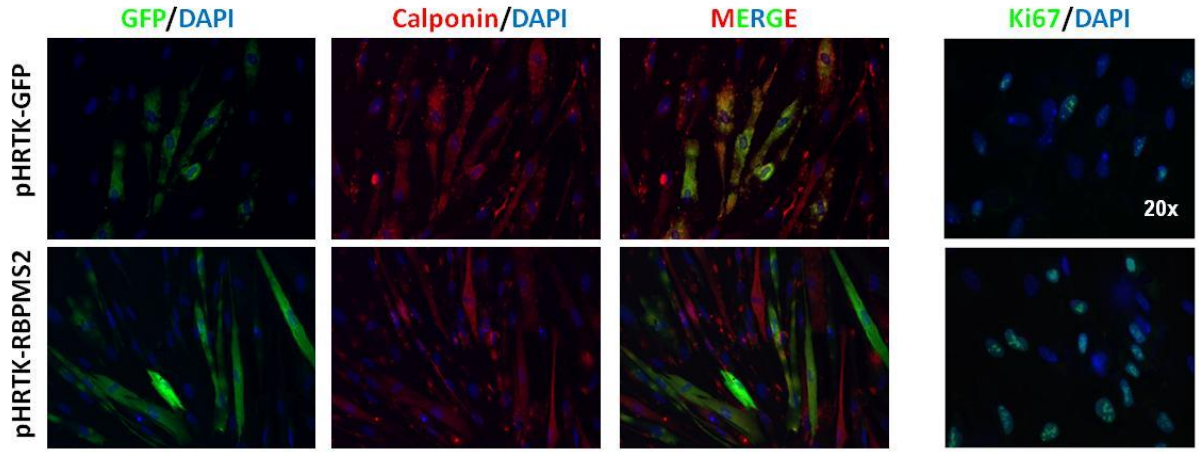

Figure 39. *RBPMS2* overexpression hinders hCSMC differentiation. Immunofluorescence analysis of primary cultured hCSMC passage 5 infected with pHRTK-*GFP* or pHRTK-

GFP-RBPMS2 retrovirus for 24h. Nuclei were visualized with Hoechst. Antibody against SMC (Calponin), cellular marker for proliferation (Ki67), and anti-GFP were used to identify cells transfected by pHRTK-*GFP-RBPMS2* retrovirus.

Altogether, these finding indicate that ectopic expression of *RBPMS2* reduces differentiation of hCSMC and increases cell proliferation rate.

3.3 Stable Cell Lines hCSMC-GFP and hCSMC-GFP-RBPMS2

As we previously demonstrated that transient ectopic expression of RBPMS2 hinders human adult colon SMC differentiation status, we decided to create stable hCSMC expressing RBPMS2 associated with GFP or GFP alone as control to give us the opportunity to study at long term the influence of RBPMS2 on digestive SMC.

Stable expression is achieved by integration of the lentivural particule containing *RBPMS2* cDNA (Tab. 9) into the target cell and finally the integration of RBPMS2 and GFP cDNA into host chromosome (Fig. 40). The exact mechanism by which plasmid DNA is integrated is not yet fully understood and remains a matter of research.

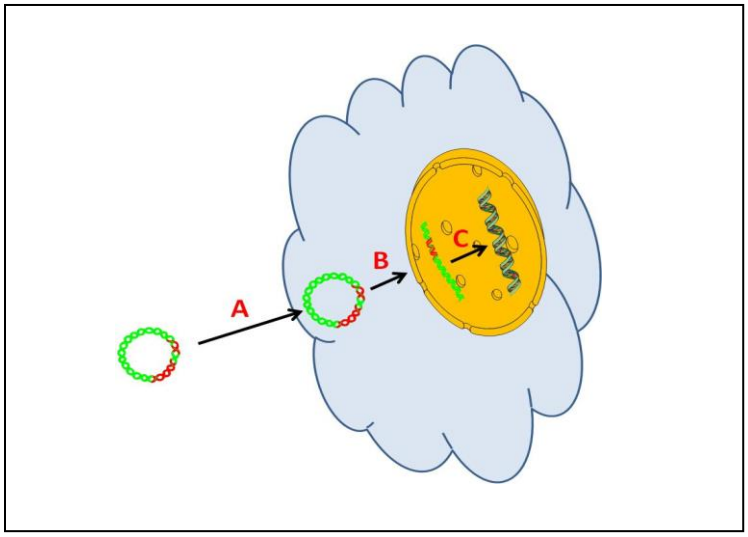

Figure 40. Integration of the lentiviral plasmid. (**A**) Initially *RBPMS2*-lentiviruses were added into the media of hCSMC at a concentration of 50viral unit/per cell; (**B**) line subsequently into the nucleus; (**C**) finally it was integrated into chromosomal DNA.

Table 9. Lentiviral particule production in Institute of Functional Genomics (IGF), Montpellier.

Vector	Dosage p24 (elisa)	Titre infectious (facs)
pHRTK-GFP	136 µg/ml	1.10^{e}9 TU/ml
pHRTK-GFP-RBPMS2	176 µg/ml	1,8.10^{e}9 TU/ml

The pHRTK-GFP-RBPMS2 plasmid allows the expression of both RBPMS2 and GFP cDNAs due to presence of IREs sequence. For the selection of stably infected cells we used the expression of GFP protein and positive GFP cells were twice sorted by FACS experiment. We used undifferentiated hCSMC as a control negative and hCSMC-GFP as a control positive (Fig. 41). We observed a homogenous population for the positive control hCSMC-GFP stable line with expression GFP in 99.62% of events. For RBPMS2 condition, two subpopulation of hCSMC-GFP-RBPMS2 stable line were observed and conduct to the cumulative expression in 96.58% of events.

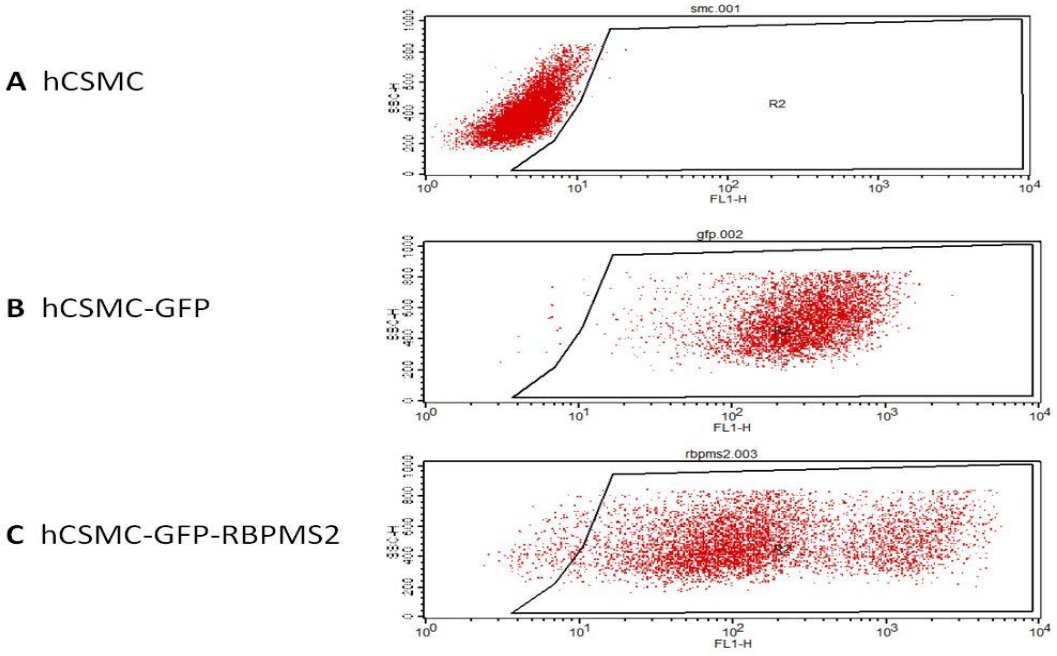

Figure 41. FACS of stable cell lines. FACS was evaluated 10000 events according to the size of the events (SSC-H) and level of expression GFP (FL1-H). (**A**) In negative control hCSMC we found a homogeneous population with contamination 0.28% of expression

GFP (error of measurement); (**B**) A homogenous population of positive control, hCSMC-GFP stable line with expression GFP in 99.62% of events; (**C**) Two subpopulation of hCSMC-GFP-RBPMS2 stable line with expression in 96.58% of events.

We investigated the expression of RBPMS2 protein expression in the GFP and RBPMS2 infected hCSMC and observed by immunofluorescence that hCSMCs-GFP-RBPMS2 expressed high positive cell for RBPMS2 whereas no positive cells where observed for RBPMS2 staining in hCSMCs-GFP (Fig.42).

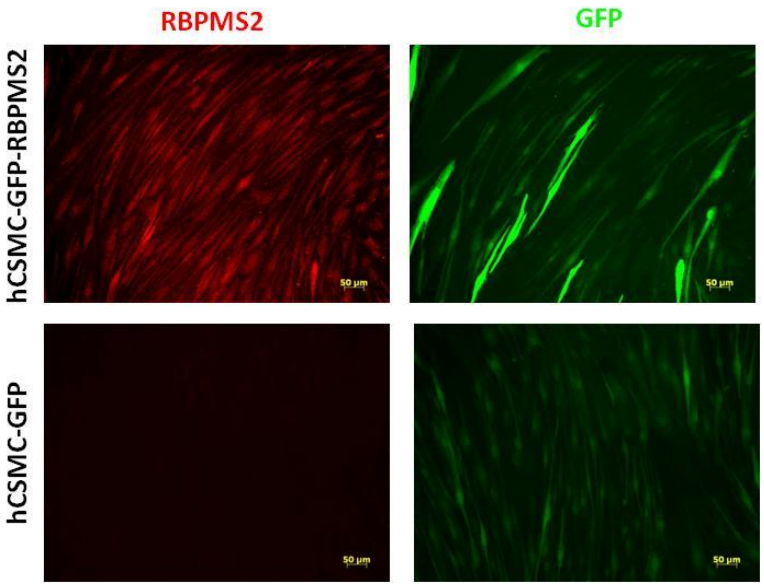

Figure 42. Immunofluorescence analysis of stable cell lines hCSMC-GFP and hCSMC-GFP-RBMS2 with αGFP antibodies and home-made αRBPMS2 antibodies. We observed two subpopulation of hCSMC-GFP-RBPMS2 (one with high level of GFP expression and one moderate expression of GFP) that expressed similar level of RBPMS2 protein. In contrast, we observed for hCSMC-GFP condition a homogenous population of cell that expressed GFP without expression RBPMS2. Scale bar 50µm.

We also investigated the gene expression pattern of hCSMC, hCSMC-*GFP-RBPMS2* and hCSMC-*GFP* cell lines in different differentiated and undifferentiated conditions. We observed that in differentiated condition, hCSMC-*GFP-RBPMS2* expressed of course high level of RBPMS2 expression associated with an increase of *C-KIT* expression and decreased of *PDGFRA* expression compared to the control GFP and

uninfected cell lines. Surprisingly, the induction of *CKIT* expression under RBPMS2 over-expression is not observed in undifferentiated condition (Fig. 43).

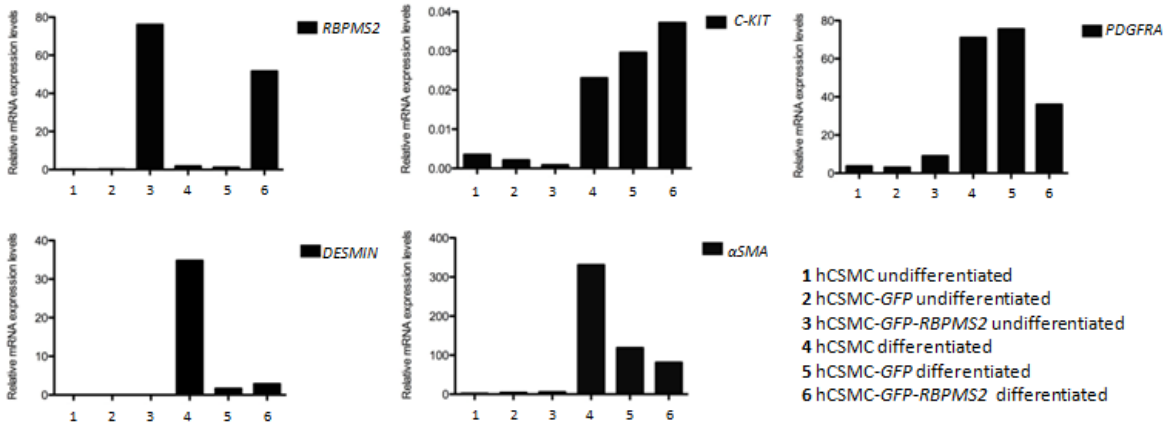

Figure 43. Characterization undifferentiated and differentiated for 7 days hCSMC, hCSMC-*GFP-RBPMS2* and hCSMC-*GFP* lines. Gene expression analysis by qPCR in primary cultured hCSMC. Normalized relative mRNA expression levels were by *HPRT*.

3.4 Identify protein partners of RBPMS2

Proteins are involved in many cellular processes such as signal transduction, enzyme catalysis and gene expression. Proteins often carry out their functions through interactions with other proteins to form multi-protein complexes. Learning more about protein interactors, substrates or inhibitors can provide insight into the protein function. The identification of interacting proteins in stable complexes in a cellular system is essentially achieved by different experimental procedures. Most biological processes involve the action and regulation of multiprotein complexes. A key goal in most areas of cell biology, therefore, is the characterization of the protein components of multiprotein complexes through the reliable identification of specific protein interaction partners.

Many proteins form strong, stable interactions, giving rise to permanent protein complexes. Because these complexes are much easier to study, most of the available experimental data (such as x-ray structures) have been obtained from stable complexes. However, transient protein–protein interactions are equally important: they play a major role in signal transduction, electron cascades and other essential physiological processes (Szilagyi et al. 2005).

Some approaches currently used to understand protein interactions are using the yeast two-hybrid system or tandem-affinity-purification mass spectroscopy, but these methods are limited in revealing how the proteins may interact.

To identify protein partners of RBPMS2 we analyzed yeast two hybrid screening of Human RBPMS2 versus Human Placenta library (Hybrigenics). From this analysis we obtained 69 positive clones from that 19 genes with high confidence include the Elongation factor 2 protein (EEF2). EEF2 is a protein that in humans is encoded by the *EEF2* gene. This gene encodes a member of the GTP-binding translation elongation factor family. It promotes the GTP-dependent translocation of the nascent protein chain from the A-site to the P-site of the ribosome. This protein is completely inactivated by EF-2 kinase phosporylation. Essential factor for protein synthesis in eukaryotic cell is localized on chromosome 19 (Fig. 44).

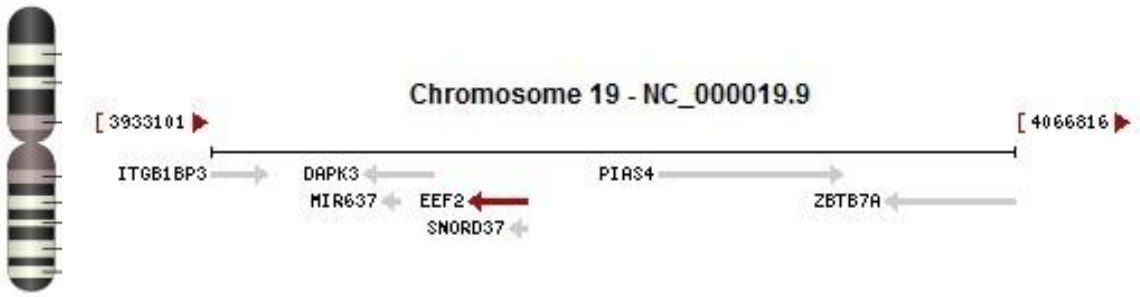

Figure 44. Localisation EEF2 on chromosome 19. Location: 19pter-q12 (19p13.3). From NCBI on 14.08.2012.

Eukaryotic protein synthesis is highly regulated by a variety of acute and chronic processes. Paramount among these processes is the reversible phosphorylation of protein synthetic components. Many of the factors involved in translation are phosphoproteins, and a certain amount is known about the kinases and phosphatases responsible for the phosphorylation and dephosphorylation of these factors. Considerably less is known about the overall physiological role of phosphorylation of translational components. In particular, two aspects remain to be fully understood, namely, the general involvement of Ca^{2+} in the regulation of protein synthesis and specifically, the role of Ca^{2+}-dependent phosphorylation of EEF2.

The increase in EEF-2 phosphorylation was a consequence of the activation of eEF-2 kinase (EEF-2K), which is a Ca^{2+}/calmodulin-dependent kinase (Diggle et al. 1998). The

activity of this kinase is increased in many cancers. Chen and colleagues showed stronger induction of EEF2 phosphorylation correlated with effect on cancer cell growth (Chen, Z. et al. 2011). Interestingly, EEF2 was highly expressed in lung adenocarcinoma, but not in the neighboring non-tumor lung tissue (Chen, C.Y. et al. 2011). Nakamura and colleagues reported overexpression of EEF2 in the majority of human gastric and colorectal cancers and that its overexpression promoted in vitro and in vivo the growth of these cancer cells through the promotion of progression of G2/M phase in the cell cycle (Nakamura et al. 2009).

In fast-twitch skeletal muscles, signaling downstream of Ca^{2+} and energy-turnover is involved in the suppression of protein synthesis during contractions. While AMPK signalling is not involved, the inhibition of EEF2 activity by phosphorylation downstream of Ca^{2+}–calmodulin–EEF-2K–EEF2 signalling cascade partially contributes to the suppression of protein synthesis during exercise/contractile activity (Rose et al. 2009). EEF2 phosphorylation play a key role for acutely inhibiting the consumption of energy by protein synthesis could be of particular importance in assuring continued supplies of metabolic energy for contraction and ion pumps in the heart during periods of relative energy insufficiency (McLeod & Proud, 2002).

After review of literature, we decided to investigate the candidate EEF2 protein as a potential protein partner of RBPMS2. To examine the potential RBPMS2/EEF2 interaction in vitro, we conducted coImmunoprecipitation assays (coIP) using HEK293 cell lysates expressing HA-tagged human RBPMS2 proteins and anti-MHAantibodies. We observed that HA-tagged RBPMS2 coprecipitates with endogenous human EEF2 protein (Fig. 45).

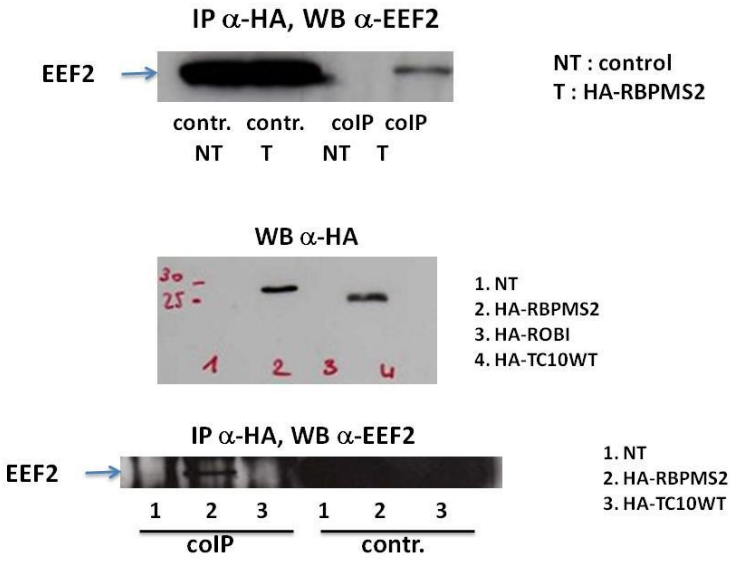

Figure 45. Co-Immunoprecipitation in HEK293. HEK293 were transfected with plasmids tagged HA, protein extracts were co-immunoprecipited with αHA and blotted with αEEF2.

3.4.1 EEF2 in hCSMC cell line and GIST

The identification of interaction partners in protein complexes is a major goal in cell biology. Identification of interaction between RBPMS2 and EEF2 led as to study expression of EEF2 in adult hCSMC (Fig. 46) and in GIST (Fig. 47). We decided analyze *EEF2* expression in our cell lines by qPCR. We observed lower lewel expression of *EEF2* in undifferentiated condition compared to differentiated cell lines, but we also observed that in differentiated hCSMC-*GFP-RBPMS2* line that the expression of *EEF2* was decreased compare to the GFP control cell line (Fig. 46).

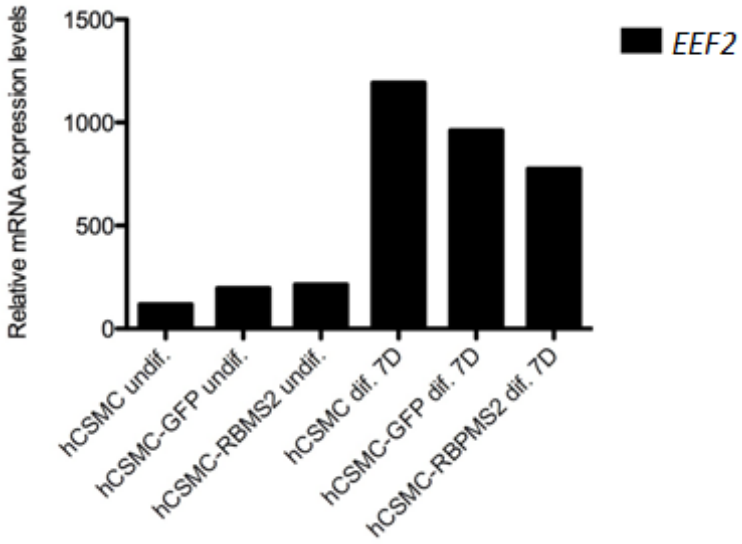

Figure 46. *EEF2* expression analysis by QPCR in adult hCSMC lines. *EEF2* expression in undifferentiated and differentiated hCSMC lines.

We also analyzed the expression of EEF2 protein in paraffin-embedded GIST section by immunohistochemistry analysis and we observed high expression of EEF2 in mesenchymal tumoral cells (Fig. 47).

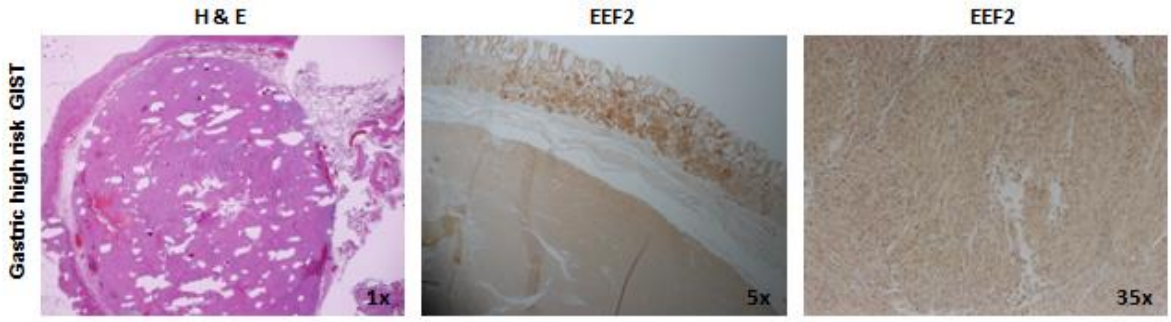

Figure 47. Expression EEF2 in GIST. Hematoxylin-eosin (H&E) staining and labeling with EEF2 antibodies in paraffin-embedded section of gastric high risk GIST.

3.5 Conclusion

In summary, we were interested to analyze the function of RBPMS2 in the tumorigenesis process. We first characterized one cellular model for our study and we showed that hCSMCs under BSA/insulin media conduct to the presence of well organize cluster of cells characteristics of differentiated SMCs. Under carbachol treatment, a muscarinergic agonist we observed exchange of intracellular Ca^{2+}, which have revealed potential capacity of hCSMC to contract on culture. In addition, we showed that ectopic expression of RBPMS2 in differentiated adult hCSMCs induces a dedifferentiation of these cells and increase their proliferative rate. Ours findings show that regulated expression of RBPMS2 is important for the correct development and differentiation of human adult visceral SMCs. We also identified EEF2 as a protein partner of RBPMS2. Previous studies showed that stronger induction of EEF2 phosphorylation correlated with effect on cancer cell growth. Our findings confirm this observation in human GISTs where we observed high expression of EEF2 in tumoral GIST tissues.

DISCUSSION

In our first study, we found that RBPMS2 mRNA and protein expression was significantly higher in GIST samples than in control gastrointestinal tissues, particularly in high risk tumors. The levels of *KIT* and *PDGFRA* did not significantly correlate with the amount of *RBPMS2* expression. However, *RBPMS2* mRNA levels were higher in GISTs harboring *KIT* mutations than in tumors with *PDGFRA* mutations or with wild type *KIT* and *PDGFRA*. This difference could be due to the different origins of *KIT* and *PDGFRA* expressing cells and would suggest that *RBPMS2* and *KIT* expression are linked. In the second part of my thesis we observed higher level of *KIT* expression in differentiated stable hCSMC line expressing RBPMS2 than in stable hCSMC line expressing only GFP or in control hCSMC line. These findings lead us to ask the question: What is the position in relation to RBPMS2 and C-KIT in GIST development and during tumorigenesis? However, in the GIST882 cell line that carries the KIT mutation K641E and shows high KIT activity we did not observe a correlation between *RBPMS2* expression and KIT activity. All these data suggest that KIT and RBPMS2 could be expressed in the same mesenchymal cells during the early development and remodeling of mesenchymal-derived gastrointestinal cells, or that they are part of the same signaling pathway, or share a regulatory circuitry as presented in the below model (Fig. 48). More experiments are needed to confirm these hypotheses and to position RBPMS2 relative to the KIT signaling pathway.

As previously showed in the laboratory sustained RBPMS2 expression hinders visceral SMC differentiation in vivo and in SMC primary cultures through up-regulation of Noggin expression that leads to inhibition of the BMP signaling pathway (Notarnicola et al. 2012). We also showed that in adult hCSMCs ectopic expression of RBPMS2 in differentiated adult SMCs triggers an increase of their proliferative rate and induces the alteration of their differentiation. Ours findings show that regulated expression of RBPMS2 is important for the correct development and differentiation of human visceral SMCs. In the second part of my thesis we created stable hCSMC expressing RBPMS2 associated with GFP or GFP alone as control to study at long term the influence of RBPMS2 on adult hCSMC. Future studies could involve implantation of hCSMC-GFP-RBPMS2 and hCSMC-GFP cells (as control) in NUDE mice and the observation of the development of these cells. These experiments will give us the opportunity to answer to some questions as: Is it possible to create a GIST tumor? Are SMCs expressing RBPMS2 independent to KIT activity and more aggressive? These models will also help us to obtain

an in vitro model to analyse the impact of the inhibition of RBPMS2 expression on the development of these implanted cells.

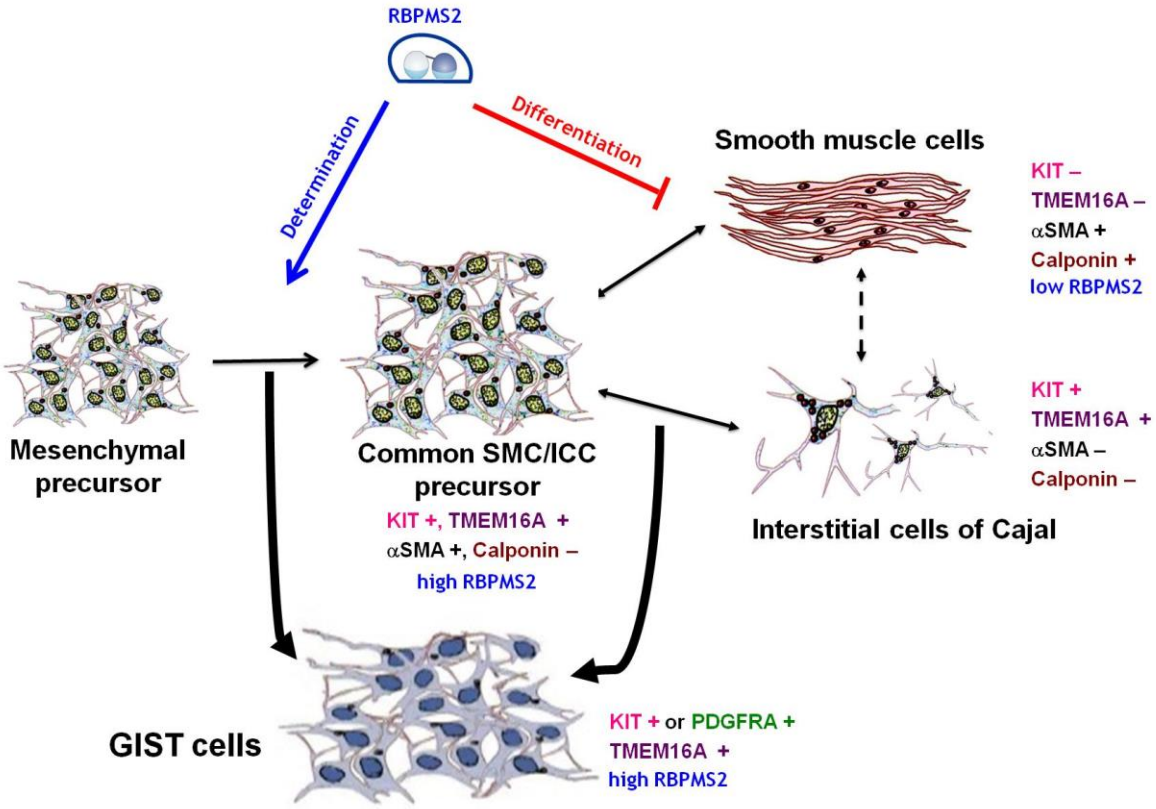

Figure 48. Model of the human gastrointestinal SMC development regulated by RBPMS2. RBPMS2 regulates the early stage of SMC differentiation and up-regulation of RBPMS2 induces a dedifferentiation of these cells and might potential function in GIST pathogenesis.

In addition, we identified EEF2 as a protein partner of RBPMS2. Previous studies showed that stronger induction of EEF2 phosphorylation correlated with effect on cancer cell growth. In the future we would analyze the functional role of this partner in the dedifferentiation process induces by RBPMS2 in SMCs (Fig. 47). We are also interested to analyze if the phosphorylation status of EEF2 could be important for its interaction with RBPMS2. These will conduct us to determine the potentional function of RBPMS2/EEF2 in signaling cascade during during hyperplastic and tumoral processes in digestive SMCs.

Perspectives

These results offer new issues and opportunities to advance in this research. For that we propose some ideas following these work. Future studies could involve implantation of hCSMC-GFP-RBPMS2 and hCSMC-GFP cells (as control) in an animal model and the observation of the development of these cells. According to the latest information, it is possible that the French laboratory INSERM U1046 will examine in vivo analysis of the impact of the expression and of developing our hCMLD cells (+/- RBPMS2) in the embryonic chicken model. These grafts may induce a specific form of neoplasms. Afterward it will be necessary to execute histomorphological analysis of these grafts, and also analysis of currently used treatments against GISTs on these grafts.

From the pathological point of view, we have to analyze expression RBPMS2 in a larger cohort of primary GISTs. Of course, it is necessary to analyze the expression of RBPMS2 in secondary or/and in peadiatric GISTs. This research may identify correlation between the expression level of RBPMS2 and life expectancy of patients with GISTs. And also, we can get answers or clarification in the following problems e.g.: RBPMS2 may be a new diagnostic tool for GISTs? RBPMS2 may be a new therapeutic target against GISTs? What results will have an anti-RBPMS2 marker on the various groups of GIST or ICC or SMC?

In addition, we identified EEF2 as a protein partner of RBPMS2. We should continue to research with other protein partners of RBPMS2, then analyze and determine their role in signaling cascade of dedifferentiation process induces by RBPMS2 in SMCs. From yeast two hybrid screening of Human RBPMS2 versus Human Placenta library (Hybrigenics) we obtained 19 genes with high confidence. Perhaps one of these genes (RBM35A or RBM35A) may be protein partners of RBPMS2, and be involved in the development of GIST.

SOUHRN

V první studii jsme analyzovali expresi RNA-binding proteinu RBPMS2 ve skupině vzorků GIST, které byly seřazeny podle jejich *KIT/PDGFRA* mutací, rizika agresivního chování a histologického typu (vřetenovitého, epiteloidního a smíšeného buněčného typu). Zjistili jsme, že exprese mRNA a proteinů RBPMS2 byla signifikantně vyšší u GIST vzorků, zejména u rizikových nádorů, než v kontrolních gastrointestinálních tkáních. Úrovně *KIT* a *PDGFRA* exprese nijak významně nekoreluje s velikostí exprese *RBPMS2*. Nicméně, hladina exprese mRNA *RBPMS2* byla vyšší v GIST s *KIT* mutacemi, než u nádorů s mutacemi *PDGFRA* nebo bez mutací *KIT/PDGFRA*. Tento rozdíl může být důsledkem různého původu buněk majících expresi *KIT* a *PDGFRA*. Což naznačuje, že RBPMS2 a KIT exprese jsou propojeny. Nicméně, v buněčné linii GIST882, která má *KIT* mutaci *K641E* a vykazuje vysokou aktivitu KIT, jsme nepozorovali korelaci mezi RBPMS2 expresí a KIT činností. Naše studie ukazuje, že většina analyzovaných GIST se vyznačuje abnormálně zvýšenou expresí RBPMS2, což naznačuje, že RBPMS2 může být stěžejní při progresi nádoru a může být potenciálním cílem protinádorové terapie.

Ve druhé části diplomové práce jsme chtěli analyzovat funkci RBPMS2 během nádorového procesu. Jako první jsme charakterizovali buněčný model a ukázali jsme, že viscerální buňky hladké svaloviny tlustého střeva v komerčních médiích se udržují v proliferačním stádiu a při přidání BSA a inzulínu do médií je navoděna diferenciace těchto buněk, která je charakteristická dobře organizovanými shluky buněk. Kontraktilitu buňek hladké svaloviny tlustého střeva jsme nepozorovali vizuálně, proto jsme analyzovali výměnu vápníku, který je intracelulární posel. Kvantitativní měření porovnává koncentraci volných cytoplasmických Ca^{2+}, ve srovnání s koncentrací po buněčné odpovědi na podnět. Při tomto experimentu jsme pozorovali výměnu Ca^{2+}, což potvrdilo potencionální schopnost kontrakce buňky hladké svaloviny tlustého střeva dospělého člověka v buněčné kultuře. Ukázali jsme, že transfektování RBPMS2 do diferencovaných buněk hladké svaloviny tlustého střeva dospělého člověka vyvolává dediferencování těchto buněk a zvyšuje jejich proliferační schopnost. Naše zjištění ukazují, že regulovaná exprese RBPMS2 je důležitá pro správný vývoj a diferenciaci buněk hladké svaloviny tlustého střeva dospělého člověka. Dále jsme zjistili, že EEF2 protein je partner RBPMS2. Předchozí studie ukázaly, že EEF2 ve fosforylovaném stavu má pozitivní vliv na růst nádorových buněk. Naše poznatky potvrzují vysokou expresi EEF2 v lidských GIST.

SUMMARY

In our first study we analyzed the expression of the RNA-binding protein RBPMS2 in a cohort of GIST samples that were classified according to their *KIT*/*PDGFRA* mutational status, risk of aggressive behavior and histological pattern (spindle, epithelioid and mixed cell phenotype). We found that RBPMS2 mRNA and protein expression was significantly higher in GIST samples than in control gastrointestinal tissues, particularly in high risk tumors. The levels of *KIT* and *PDGFRA* did not significantly correlate with the amount of *RBPMS2* expression. However, *RBPMS2* mRNA levels were higher in GISTs harboring *KIT* mutations than in tumors with *PDGFRA* mutations or with wild type *KIT* and *PDGFRA*. This difference could be due to the different origins of *KIT* and *PDGFRA* expressing cells and would suggest that *RBPMS2* and *KIT* expression are linked. However, in the GIST882 cell line that carries the KIT mutation K641E and shows high KIT activity we did not observe a correlation between *RBPMS2* expression and KIT activity. In conclusion, our study I shows that most of the analyzed GISTs are characterized by abnormally elevated expression of RBPMS2, suggesting that RBPMS2 could be an indicator for tumor progression and a potential target for cancer therapy in GIST.

In the second part of my thesis we were interested to analyze the function of RBPMS2 in the tumorigenesis process. We first characterized one cellular model for our study and we showed that hCSMCs under BSA/insulin media conduct to the presence of well organize cluster of cells characteristics of differentiated SMCs. Under carbachol treatment, a muscarinergic agonist we observed exchange of intracellular Ca^{2+}, which have revealed potential capacity of hCSMC to contract on culture. In addition, we showed that ectopic expression of RBPMS2 in differentiated adult hCSMCs induces a dedifferentiation of these cells and increase their proliferative rate. Ours findings show that regulated expression of RBPMS2 is important for the correct development and differentiation of human adult visceral SMCs. We also identified EEF2 as a protein partner of RBPMS2. Previous studies showed that stronger induction of EEF2 phosphorylation correlated with effect on cancer cell growth. Our findings confirm this observation in human GISTs where we observed high expression of EEF2 in tumoral GIST tissues.

CONCLUSION

Dans la première étude de ma thèse, nous avons analysé l'expression de la protéine de liaison à l'ARN RBPMS2 dans une cohorte de patients GIST qui ont été classés en fonction de leur statut mutationnel pour les gènes *KIT* et *PDGFRA*, du risque de comportement agressif et de la structure histologique (fusiforme, épithélioïde et mixte). Nous avons constaté que l'expression de RBPMS2 était significativement plus élevée dans les GIST que dans les tissus gastro-intestinaux de contrôle, en particulier dans les tumeurs à haut risque. Les niveaux d'expression *KIT* et *PDGFRA* ne sont pas significativement en corrélation avec l'expression de RBPMS2. Les niveaux d'ARNm *RBPMS2* étaient plus élevés dans les GIST avec mutations *KIT* que dans les tumeurs avec mutations *PDGFRA* ou en l'absence de ces mutations. Cette différence pourrait être due à des origines différentes des cellules qui expriment *KIT* et *PDGFRA* et suggère que les expressions de RBPMS2 et KIT pourraient être liées. Cependant, dans la lignée cellulaire GIST882 qui porte la mutation *KIT K641E* et présente une activité élevée *KIT*, nous n'avons pas observé de corrélation entre l'expression de *RBPMS2* et l'activité *KIT*. En conclusion, notre étude montre que la plupart des GIST analysés sont caractérisées par l'expression anormalement élevée de RBPMS2, ce qui suggère que RBPMS2 pourrait être un indicateur de la progression tumorale et une cible potentielle pour le traitement du GIST.

Dans la deuxième partie de ma thèse nous avions pour objectif d'analyser la fonction de RBPMS2 dans le tumorigenese. Nous avons dans un premier temps caractérisé un modèle cellulaire de cellules musculaires lisses de colon adulte (hCSMCs) et nous avons montré qu'en condition insuline/BSA, les hCSMCs présentaient un statut de cellules différenciées. De plus, dans ces conditions, nous avons observé que sous stimulation carbachol, ces cellules présentaient un échange calcique intracellulaire démontrant leur capacité potentielle à se contracter. Nous avons montré que l'expression ectopique de RBPMS2 dans hCSMCs adultes différenciées induisait une dédifférenciation de ces cellules et une augmentation de leur prolifération. Nos résultats suggèrent que l'expression régulée de RBPMS2 est importante pour le développement et la différenciation des SMC humaines adultes viscérales. Nous aussi avons identifié la protéine EEF2 comme étant une protéine partenaire de RBPMS2. Des études antérieures ont montré que le renforcement de l'induction de la phosphorylation EEF2 était corrélé avec un effet sur la croissance des cellules cancéreuses. Nos résultats confirment cette observation dans les GIST où nous avons observé une forte expression EEF2.

PUBLICATIONS AND PRESENTATIONS DURING THIS THESIS

In international journals

Hapkova, I., Bernex, F., de Santa Barbara P. and Vesely J. (2014) Gastrointestinal Stromal Tumour: From the clinic to the molecules. *J Cancer Res Ther.* 2(3): 54-67. doi: 10.14312/2052-4994.2014-8

Hapkova, I., Skarda, J., Rouleau, C., Thys, A., Notarnicola, C., Janikova, M., Bernex, F., Rypka, M., Vanderwinden, J.M., Faure, S., Vesely, J. and de Santa Barbara, P. (2013). High expression of the RNA-Binding Protein RBPMS2 in gastrointestinal stromal tumors. *Exp Mol Pathol*. 94(2):314-21. doi: 10.1016/j.yexmp.2012.12.004

Rouleau, C., Rico, C., **Hapkova, I**. and de Santa Barbara, P. (2012). Immunohistochemal analysis of Bone Morphological Protein signaling pathway in human myometrium. *Exp Mol Pathol* 93(1):56-60. doi: 10.1016/j.yexmp.2012.04.007

Oral presentations at congresses

Hapkova, I., Skarda, J., Notarnicola, C., Bernex, F., Rypka, M., Faure, S., Vesely, J. and de Santa Barbara, P. (2012). RNA-Binding Protein with Multiple Splicing 2 (RBPMS2) is highly expressed in Gastrointestinal Stromal Tumours (GIST). 4th International Student Medical Congress Kosice, 26-29 June 2012: Kosice, Slovak Republic.

Hapkova, I., Skarda, J., Notarnicola, C., Bernex, F., Rypka, M., Faure, S. and De Santa Barbara, P. (2011). New approach to the study of Gastrointestinal Stromal Tumors (GIST). 7èmes Journées du Cancéropole Grand Sud Ouest, 18-20 October 2011: Bordeaux, France.

Written presentations at congresses (poster)

Notarnicola, C., Sagnol, S., **Hapkova, I.,** Bernex, F., Rouleau, C., Faure, S. & de Santa Barbara, P. (2011). Development of visceral smooth muscle and associated pathologies. Grand Colloque Biologie & Santé 5-7 Julliet 2011: Lyon, France

Hapkova, I., Skarda, J., Notarnicola, C., Bernex, F., Rypka, M., Faure, S. and De Santa Barbara, P. (2011). New approach to the study of Gastrointestinal Stromal Tumors (GIST). 4th European Course of in vivo Preclinical Assays in Cancer Therapy, 18-20 May 2011 Paris, France

Hapkova, I., Skarda, J., Notarnicola, C., Bernex, F., Rypka, M., Faure, S. and De Santa Barbara, P. (2011). New approach to the study of Gastrointestinal Stromal Tumors (GIST). 7èmes Journées du Cancéropole Grand Sud Ouest, 18-20 October 2011: Bordeaux, France.

REFERENCES

Agaimy, A., Märkl, B., Arnholdt ,H., Wünsch, P.H., Terracciano, L.M., Dirnhofer, S., Hartmann, A., Tornillo, L. and Bihl, M.P. (2009). Multiple sporadic gastrointestinal stromal tumours arising at different gastrointestinal sites: pattern of involvement of the muscularis propria as a clue to independent primary GISTs. *Virchows Arch* 455(2): 101-108.

Agaimy, A., Terracciano, L.M., Dirnhofer, S., Tornillo, L., Foerster, A., Hartmann, A. and Bihl, M.P. (2009). V600E BRAF mutations are alternative early molecular events in a subset of KIT/PDGFRA wild-type gastrointestinal stromal tumours. *J Clin Pathol* 62(7): 613-6.

Agaram, N.P., Laquaglia, M.P., Ustun, B., Guo, T., Wong, G.C., Socci, N.D., Maki, R.G., DeMatteo, R.P., Besmer, P. and Antonescu, C.R. (2008). Molecular characterization of pediatric gastrointestinal stromal tumors. *Clin Cancer Res* 14(10): 3204-15.

Agaram, N.P., Wong, G.C., Guo, T., Maki, R.G., Singer, S., Dematteo, R.P., Besmer, P. and Antonescu, C.R. (2008). Novel V600E BRAF mutations in imatinib-naive and imatinib-resistant gastrointestinal stromal tumors. *Genes Chromosomes Cancer* 47(10): 853-9.

Anantharaman, V., Koonin, E.V. and Aravind, L. (2002). Comparative genomics and evolution of proteins involved in RNA metybolism. *Nucleic Acids Res* 30: 1427-1464.

Andersson, J., Sihto, H., Meis-Kindblom, J.M., Joensuu, H., Nupponen, N. and Kindblom, L.G. (2005). NF1-associated gastrointestinal stromal tumors have unique clinical, phenotypic, and genotypic characteristics. *Am J Surg Pathol* 29(9): 1170-6.

Antonescu, C.R. (2011). The GIST paradogm: lessons for other kinase-driven cancers. *J Pathol* 223: 251-261.

Antonescu, C.R., Viale, A., Sarran, L., Tschernyavsky, S.J., Gonen, M., Segal, N.H., Maki, R.G., Socci, N.D., DeMatteo, R.P. and Besmer, P. (2004). Gene expression in gastrointestinal stromal tumors is distinguished by KIT genotype and anatomic site. *Clin Cancer Res* 10(10): 3282-90.

Appelman, H.D. (1996). Smooth muscle tumors of the gastrointestinal tract. What we know now that Stout didn´t know. *Am J Surg Pathol* 10: 83-99.

Bandziulis, R.J., Swanson, M.S. and Dreyfuss, G. (1989). RNA-binding proteins as developmental regulators. *Genes Dev* 3(4): 431-7.

Bardsley, M.R., Horváth, V.J., Asuzu, D.T., Lorincz, A., Redelman, D., Hayashi, Y., Popko, L.N., Young, D.L., Lomberk, G.A., Urrutia, R.A., Farrugia, G., Rubin, B.P. and Ordog, T. (2010). Kitlow stem cells cause resistance to Kit/platelet-derived growth factor alpha inhibitors in murine gastrointestinal stromal tumors. *Gastroenterology* 139(3): 942-52.

Bateman, A., Birney, E., Cerruti, L., Durbin, R., Etwiller, L., Eddy, S.R., Griffiths-Jones, S., Howe, K.L., Marshall, M. and Sonnhammer, E.L. (2002). The Pfam protein families database. *Nucleic Acids Res* 30(1): 276-80.

Bauer, S., Duensing, A., Demetri, G.D. and Fletcher, J.A. (2007). KIT oncogenic signaling mechanisms in imatinib-resistant gastrointestinal stromal tumor: PI3-kinase/AKT is a crucial survival pathway. *Oncogene* 26(54): 7560-8.

Bauer, S., Yu, L.K., Demetri, G.D. and Fletcher, J.A. (2006). Heat shock protein 90 inhibition in imatinib-resistant gastrointestinal stromal tumor. *Cancer Res* 66(18): 9153-61.

Benjamin, R.S, Rankin, C., Fletcher, C., Blanke, C., Von Mehren, M., Maki, R., Bramwell, V., Baker, L., Borden, E. and Demetri, G.D. (2003). Phase III dose-randomized study of imatinib mesylate (STI571) for GIST: Intergroup S0033 early results. *Proc Am Soc Clin Oncol* 22: 814.

Bergmann, F., Gunawan, B., Hermanns, B., Höer, J., Schumpelick, V. and Füzesi, L. (1998). Cytogenetic and morphologic characteristics of gastrointestinal stromal tumors. Recurrent rearrangement of chromosome 1 and losses of chromosomes 14 and 22 as common anomalies. *Verh Dtsch Ges Pathol* 82: 275-8.

Bernex, F., De Sepulveda, P., Kress, C., Elbaz, C., Delouis, C. and Panthier, J.J. (1996). Spatial and temporal patterns of c-kit-expressing cells in WlacZ/+ and WlacZ/WlacZ mouse embryos. *Development* 122(10): 3023-33.

Besmer, P., Murphy, J.E., George, P.C., Qiu, F.H., Bergold, P.J., Lederman, L., Snyder, H.W.Jr., Brodeur, D., Zuckerman, E.E. and Hardy, W.D. (1986). A new acute transforming feline retrovirus and relationship of its oncogene v-kit with the protein kinase gene family. *Nature* 320(6061): 415-21.

Bielefeldt-Ohmann, H., Barouch, D.H., Bakke, A.M., Bruce, A.G., Durning, M., Grant, R., Letvin, N.L., Ryan, J.T., Schmidt, A., Thouless, M.E. and Rose, T.M. (2005). Intestinal stromal tumors in a Simian Immunodeficiency Virus-infected, Simian Retrovirus-2 negative rhesus macaque (Macaca mulatta). *Vet Pathol* 42: 391-396.

Birney, E., Kumar, S. and Krainer, A.R. (1993). Analysis of the RNA-recognition motif and RS and RGG domains: conservation in metazoan pre-mRNA splicing factors. *Nucleic Acids Res* 21(25): 5803-16.

Biron, P., Cassier, P.A., Fumagalli, E., Blesius, A., Debiec-Rychter, M., Adenis, A., Verweij, J., Hohenberger, P., Blay, J. and Casali, P.G. (2010). Outcome of patients (pts) with PDGFRAD842V mutant gastrointestinal stromal tumor (GIST) treated with imatinib (IM) for advanced disease. *J Clin Oncol* 28: 15s.

Blay, J. Y., Le Cesne, A., Cassier, P. A. and Ray-Coquard, I. L. (2012). Gastrointestinal stromal tumors (GIST): a rare entity, a tumor model for personalized therapy, and yet ten different molecular subtypes. *Discov Med* 13(72):357-67.

Blume-Jensen, P. and Hunter, T. (2001). Oncogenic kinase signalling. *Nature* 411: 355-365.

Blume-Jensen, P., Claesson-Welsh, L., Siegbahn, A., Zsebo, K.M., Westermark, B. and Heldin, C.H. (1991). Activation of the human c-kit product by ligand-induced dimerization mediates circular actin reorganization and chemotaxis. *EMBO J* 10(13): 4121-8.

Brabec, P., Sufliarsky, J., Linke, Z., Plank, L., Mrhalova, M., Pavlik, T., Klimes, D. and Gregor, J. (2009). A whole population study of gastrointestinal stromal tumors in the Czech Republic and Slovakia. *Neoplasma* 56(5): 459-464.

Burd, C.G. and Dreyfuss, G. (1994). Conserved structures and diversity of functions of RNA-binding proteins. *Sience* 265: 615-621.

Cajal, S.R. (1911). Histologie du sytéme nerveux de l´homme et des vertébrés. *2nd ed. Paris: Maloine* 891-942.

Carney, J.A. and Stratakis, C.A. (2002). Familial paraganglioma and gastric stromal sarcoma: a new syndrome distinct from the Sarney triad. *Am J med Genet* 108(2): 132-139.

Cassier, P.A, Ducimetiere, F., Lurkin, A., Ranchere-Vince, D., Scoazec, J-Y., Bringuier, P-P., Decouvelaere, A-V., Meeus, P., Cellier, D., Blay, J-Y. and Ray-Coquard, I. (2010). A prospective epidemiological study of new incident GISTs during two consecutive years in Rhône Alpes region: incidence and molecular distribution of GIST in a European region. *British Journal of Cancer* 103: 165-170.

Caterino, S., Lorenzon, L., Petrucciani, N., Iannicelli, E., Pilozzi, E., Romiti, A., Cavallini, M. and Ziparo, V. (2011). Gastrointestinal stromal tumors: correlation between

symptoms at presentation, tumor location and prognostic factors in 47 consecutive patients. *World J Surg Oncol* 9: 13.

Chamley-Campbell, J., Campbell, G.R. and Ross, R. (1979). The smooth muscle cell in culture. *Physiol Rev* 59(1): 1-61.

Champy, C. (1913). Quelques résultats de la méthode de culture de tissus. I. Généralitiés. II. Le muscle lisse (note préliminaire). *Arch. Zool Exp. Gen.* 53: 42-51.

Chen, C.Y., Fang, H.Y., Chiou, S.H., Yi, S.E., Huang, C.Y., Chiang, S.F., Chang, H.W., Lin, T.Y., Chiang, I.P. and Chow, K.C. (2011). Sumoylation of eukaryotic elongation factor 2 is vital for protein stability and anti-apoptotic activity in lung adenocarcinoma cells. Cancer Sci. 102(8):1582-9.

Chen, L.L., Trent, J.C., Wu, E.F., Fuller, G.N., Ramdas, L., Zhang, W., Raymond, A.K., Prieto, V.G., Oyedeji, C.O., Hunt, K.K., Pollock, R.E., Feig, B.W., Hayes, K.J., Choi, H., Macapinlac, H.A., Hittelman, W., Velasco, M.A., Patel, S., Burgess, M.A., Benjamin, R.S. and Frazier, M.L. (2004). A missense mutation in KIT kinase domain 1 correlates with imatinib resistance in gastrointestinal stromal tumors. *Cancer Res* 64(17): 5913-9.

Chen, Z., Gopalakrishnan, S.M., Bui, M.H., Soni, N.B., Warrior, U., Johnson, E.F., Donnelly, J.B. and Glaser, K.B. (2011). 1-Benzyl-3-cetyl-2-methylimidazolium iodide (NH125) induces phosphorylation of eukaryotic elongation factor-2 (eEF2): a cautionary note on the anticancer mechanism of an eEF2 kinase inhibitor. J Biol Chem 286(51):43951-8.

Chi, P., Chen, Y., Zhang, L., Guo, X., Wongvipat, J., Shamu, T., Fletcher, J.A., Dewell, S., Maki, R.G., Zheng, D., Antonescu, C.R., Allis, C.D. and Sawyers, C.L. (2010). ETV1 is a lineage survival factor that cooperates with KIT in gastrointestinal stromal tumours. *Nature* 467(7317): 849-53.

Cléry, A., Blatter, M. and Allain, F.H. (2008). RNA recognition motifs: boring? Not quite. *Curr Opin Struct Biol* 18(3): 290-8.

Coindre, J.M., Emile, J.F., Monges, G., Ranchere-Vince, D. and Scoazec, J.Y. (2005). Tumeurs stromales gastro-intestinales: definition, caracteristiques histologiques, immunohistochimiques et genetiques, strategie diagnostic. *Ann Pathol* 25: 358-85.

Come, C., Magnino, F., Bibeau, F., et al., (2006). Snail and slug play distinct roles during breast carcinoma progression. *Clin. Cancer Res* 12: 5395-5402.

Cooper, T.A., Wan, L. and Dreyfuss, D. (2009). RNA and disease. *Cell* 136: 777-793.

Corless, C.L. (2004). Assessing the prognosis of gastrointestinal stromal tumors: a growing role for molecular testing. *Am. J. Clin. Pathol*. 122: 11-13.

Corless, C.L., Barnett, C.M. and Heinrich, M.C. (2011). Gastrointestinal stromal tumours: origin and molecular oncology. *Nat Rev Cancer* 11(12): 865-78.

Corless, C.L., Beadling, C., Justusson, E. and Heinrich, M.C. (2009). Evaluation of the presence of IGF1R overexpression in wild-type and kinase mutant GI stromal tumors. *J Clin Oncol* 27 (15S): 10506.

Corless, C.L., Fletcher, J.A. and Heinrich M.C. (2004). Biology of Gastrointestinal Stromal Tumours. *J Clin Oncol* 22: 3813-3825.

Corless, C.L., Schroeder, A., Griffith, D., Town, A., McGreevey, L., Harrell, P., Shiraga, S., Bainbridge, T., Morich, J. and Heinrich, M.C. (2005). PDGFRA mutations in gastrointestinal stromal tumors: frequency, spectrum and in vitro sensitivity to imatinib. *J Clin Oncol* 23: 5357-64.

Curtis, D., Lehmann, R. and Zamore, P.D. (1995). Translational regulation in development. *Cell* 81: 171-178.

de Santa Barbara, P., van den Brink, G.R. and Roberts, D.J. (2002). Molecular etiology of gut malformations and diseases. *Am J Med Genet* 115(4): 221-30.

Debiec-Rychter, M., Wasag, B., Stul, M., De Wever, I., Van Oosterom, A., Hagemeijer, A. and Sciot, R. (2004). Gastrointestinal stromal tumours (GISTs) negative for KIT (CD117 antigen) immunoreactivity. *J Pathol* 202(4): 430-8.

Delahaye, N.F., Rusakiewicz, S., Martins, I., et al., (2011). Alternatively spliced NKp30 isoforms affect the prognosis of gastrointestinal stromal tumors. *Nat Med* 17: 700-707.

Dematteo, R.P., Heinrich, M.C., El-Rifai, W.M. and Demetri, G. (2002). Clinical management of gastrointestinal stromal tumors: before and after STI-571. *Hum Pathol* 33(5): 466-77.

Demetri, G.D. (2002). Targeting the molecular pathophysiology of gastrointestinal stromal tumors with imatinib. *Hematol Oncol Clin North Am* 16(5): 1115-24.

Demetri, G.D. (2011). Differential properties of current tyrosine kinase inhibitors in gastrointestinal stromal tumors. *Semin Oncol* 1: S10-9.

Demetri, G.D., Benjamin, R.S., Blanke, C.D., Blay, J.Y., Casali, P., Choi, H., Corless, C.L., Debiec-Rychter, M., DeMatteo, R.P., Ettinger, D.S., Fisher, G.A., Fletcher, C.D., Gronchi, A., Hohenberger, P., Hughes, M., Joensuu, H., Judson, I., Le Cesne,

A., Maki, R.G., Morse, M., Pappo, A.S., Pisters, P.W., Raut, C.P., Reichardt, P., Tyler, D.S., Van den Abbeele, A.D., von Mehren, M., Wayne, J.D. and Zalcberg, J. (2007). NCCN task force report: management of patients with gastrointestinal stromal tumor (GIST)-update of the NCCN clinical practice guidelines. *J Natl Compr Canc Netw* 5 (Suppl 2): S1-S29.

Demetri, G.D., van Oosterom, A.T., Garrett, C.R., Blackstein, M.E., Shah, M.H., Verweij, J., McArthur, G., Judson, I.R., Heinrich, M.C., Morgan, J.A., Desai, J., Fletcher, C.D., George, S., Bello, C.L., Huang, X., Baum, C.M. and Casali, P.G. (2006). Efficacy and safety of sunitinib in patients with advanced gastrointestinal stromal tumour after failure of imatinib: a randomised controlled trial. *Lancet* 368(9544): 1329-38.

Demetri, G.D., von Mehren, M., Antonescu, C.R., DeMatteo, R.P., Ganjoo, K.N., Maki, R.G., Pisters, P.W.T., Raut, C.P., Riedel, R.F., Schuetze, S., Sundar, H.M., Trent, J.C. and Wayne, J.D. (2010). NCCN Task Force Report: Update on the Management of Patients with Gastrointestinal Stromal Tumours. *J Natl Compr Canc Netw* 8 (Suppl 2): S1-S41.

Demetri, G.D., von Mehren, M., Blanke, C.D., Van den Abbeele, A.D., Eisenberg, B., Roberts, P.J., Heinrich, M.C., Tuveson, D.A., Singer, S., Janicek, M., Fletcher, J.A., Silverman, S.G., Silberman, S.L., Capdeville, R., Kiese, B., Peng, B., Dimitrijevic, S., Druker, B.J., Corless, C., Fletcher, C.D. and Joensuu, H. (2002). Efficacy and safety of imatinib mesylate in advanced gastrointestinal stromal tumors. *N Engl J Med* 347(7): 472-80.

Deneubourg, L., Ralea, S., Gromova, P., Parsons, R., Vanderwinden, J.M. and Erneux C. (2011). Abnormal elevated PTEN expression in the mouse antrum of a model of GIST Kit(K641E/K641E). *Cell Signal* 23(11): 1857-68.

Diggle, T.A., Redpath, N.T., Heesom, K.J. and Denton, R.M. (1998). Regulation of protein-synthesis elongation-factor-2 kinase by cAMP in adipocytes. Biochem J 336: 525–529.

Dissanayake, K., Toth, R., Blakey, J., Olsson, O., Campbell, D.G., Prescott, A.R. and MacKintosh, C. (2011). ERK/p90(RSK)/14-3-3 signalling has an impact on expression of PEA3 Ets transcription factors via the transcriptional repressor capicúa. *Biochem J* 433(3): 515-25.

Dreyfuss, G., Kim, V.N. and Kataoka, N. (2002). Messenger-RNA-binding proteins and the messages they carry. *Nat Rev Mol Cell Biol* 3(3): 195-205.

Dreyfuss, G., Swanson, M.S. and Piñol-Roma, S. (1998). Heterogeneous nuclear ribonucleoprotein particles and the pathway of mRNA formation. *Trends Biochem Sci* 13(3): 86-91.

Duensing, A., Joseph, N.E., Medeiros, F., Smith, F., Hornick, J.L., Heinrich, M.C., Corless, C.L., Demetri, G.D., Fletcher, C.D. and Fletcher, J.A. (2004). Protein Kinase C theta (PKCtheta) expression and constitutive activation in gastrointestinal stromal tumors (GISTs). *Cancer Res* 64(15): 5127-31.

Eide, C.A., Adrian, L.T., Tyner, J.W., Mac Partlin, M., Anderson, D.J., Wise, S.C., Smith, B.D., Petillo, P.A., Flynn, D.L., Deininger, M.W., O'Hare, T. and Druker, B.J. (2011). The ABL switch control inhibitor DCC-2036 is active against the chronic myeloid leukemia mutant BCR-ABLT315I and exhibits a narrow resistance profile. *Cancer Res* 71(9): 3189-95.

Espinosa, I., Lee, C.H., Kim, M.K., Rouse, B.T., Subramanian, S., Montgomery, K., Varma, S., Corless, C.L., Heinrich, M.C., Smith, K.S., Wang, Z., Rubin, B., Nielsen, T.O., Seitz, R.S., Ross, D.T., West, R.B., Cleary, M.L. and van de Rijn, M. (2008). A novel monoclonal antibody against DOG1 is a sensitive and specific marker for gastrointestinal stromal tumors. *Am J Surg Pathol* 32(2): 210-8.

Faure S. and de Santa Barbara, P. (2011). Molecular embryology of the foregut. *J. Pediatr. Gastroenterol.* Nutr. 52, S2-3.

Ferrero, D., Pogliani, E.M., Rege-Cambrin, G., Fava, C., Mattioli, G., Dellacasa, C., Campa, E., Perfetti, P., Fumagalli, M. and Boccadoro, M. (2006). Corticosteroids can reverse severe imatinib-induced hepatotoxicity. *Haematologica* 91(6 Suppl): ECR27.

Fletcher, C.D., Berman, J.J., Corless, C.L., Gorstein, F., Lasota, J., Longley, B.J., Miettinen, M., O'Leary, T.J., Remotti, H., Rubin, B.P., Shmookler, B., Sobin, L.H., Weiss, S.W. (2002). Diagnosis of gastrointestinal stromal tumors: A consensus approach. *Hum Pathol* 33: 459-65.

Fletcher, J.A, Corless, C.L., Dimitrijevic, S., Von Mehren, M., Eisenberg, B., Joensuu, H., Fletcher, C.D.M., Blanke, C., Demetri, G.D. and Heinrich M.C. (2003). Mechanisms of resistance to imatinib mesylate (IM) in advanced gastrointestinal stromal tumor (GIST). *Proc Am Soc Clin Oncol* 22.

Franquemont, D.W. (1995). Differentiation and risk assessment of gastrointestinal stromal tumors. *Am J Clin Pathol* 103: 41-47.

Frantisek, J., Hron, P. and Hozmanova, F. (2008). Gastrointestinal stromal tumour in a guinea pig. In: Proceedings of the 26th ESVP Meeting. Dubrovnik, 17-21 Septembre 2008. *E.S.V.P*. 120.

Frost, D., Lasota, J. and Miettinen, M. (2003). Gastrointestinal Stromal Tumors and Leiomyomas in the Dog: A Histopathologic, Immunohistochemical, and Molecular Genetic Study of 50 Cases. *Vet Pathol* 40: 42–54.

Fujimoto, H., Shibutani, M., Kuroiwa, K., Inoue, K., Woo, G.H. and Hirose, M. (2006). A case report of a spontaneous gastrointestinal stromal tumor (GIST) occurring in a F344 rat. *Toxicol Pathol* 34: 164-167.

Fukasawa, T., Chong, J.M., Sakurai, S., Koshiishi, N., Ikeno, R., Tanaka, A., Matsumoto, Y., Hayashi, Y., Koike, M. and Fukayama, M. (2000). Allelic loss of 14q and 22q, NF2 mutation, and genetic instability occur independently of c-kit mutation in gastrointestinal stromal tumor. *Jpn J Cancer Res* 91(12): 1241-9.

Gajiwala, K.S., Wu, J.C., Christensen, J., Deshmukh, G.D., Diehl, W., DiNitto, J.P., English, J.M., Greig, M.J., He, Y.A., Jacques, S.L., Lunney, E.A., McTigue, M., Molina, D., Quenzer, T., Wells, P.A., Yu, X., Zhang, Y., Zou, A., Emmett, M.R., Marshall, A.G., Zhang, H.M. and Demetri, G.D. (2009). KIT kinase mutants show unique mechanisms of drug resistance to imatinib and sunitinib in gastrointestinal stromal tumor patients. *Proc Natl Acad Sci U S A* 106(5): 1542-7.

Gastrointestinal Stromal Tumor Meta-Analysis Group (MetaGIST). (2010). Comparison of two doses of imatinib for the treatment of unresectable or metastatic gastrointestinal stromal tumors: a meta-analysis of 1,640 patients. *J Clin Oncol* 28(7): 1247-53.

George, S., von Mehren, M., Heinrich, M.C., Wang, Q., Corless, C.L., Butrynski, J.E., Morgan, J.A., Wagner, A.J., Choy, E., Tap, W.D., Manola, J., Yap, J.T, Van Den Abbeele, A.D., Solomon, S., Fletcher, J.A. and Demetri, G.D. (2011). A multicenter phase II study of regorafenib in patients (pts) with advanced gastrointestinal stromal tumor (GIST), after therapy with imatinib (IM) and sunitinib (SU). *J Clin Oncol* 29: 2011.

Gerber, W.V., Yatskievych, T.A., Antin, P.B., Correia, K.M., Conlon, R.A. and Krieg, P.A. (1999). The RNA-binding protein gene, hermes, is expressed at high levels in the developing heart. *Mech Dev* 80(1): 77-86.

Glisovic, T., Jennifer, L., Yong, J. and Dreyfuss, G. (2008). RNA-binding proteins and post-transcriptional gene regulation. *FEBS Letters* 582: 1977-1986.

Goettsch, W.G., Bos, S.D., Breekveldt-Postma, N., Casparie, M., Herings, R.M. and Hogendoorn, P.C. (2005). Incidence of gastrointestinal stromal tumours is underestimated: Results of a nation-wide study. *Eur J Cancer* 41: 2868-2872.

Golden, T. and Stout A.P. (1941). Smooth muscle tumours of the gastrointestinal tract and retroperitineal tissues. *Surg. Gynecol. Obstet*. 73:784-790.

Gordon, P.M. and Fisher, D.E. (2010). Role for the proapoptotic factor BIM in mediating imatinib-induced apoptosis in a c-KIT-dependent gastrointestinal stromal tumor cell line. *J Biol Chem* 285(19):14109-14.

Graham, F.L., Smiley, J., Russell, W.C. and Nairn, R. (1977). Characteristics of a human cell line transformed by DNA from human adenovirus type 5. *J Gen Virol* 36(1): 59-74.

Gramza, A.W., Corless, C.L. and Heinrich, M.C. (2009). Resistance to Tyrosine Kinase Inhibitors in Gastrointestinal Stromal Tumors. *Clin Cancer Res* 15(24): 7510-7518.

Gromova, P., Rubin, B.P., Thys. A., Erneux, C. and Vanderwinden, J.M. (2011). Neurotensin receptor 1 is expressed in gastrointestinal stromal tumors but not in interstitial cells of Cajal. *PlosOne.* 6, e14710.

Grynkiewicz, G., Poenie, M. and Tsien, R.Y. (1985). A New Generation of Ca^{2+} Indicators with Greatly Improved Fluorescence Properties. *J Biol Chem* 260(6): 3440-3450.

Guilhot, F. (2004). Indications for imatinib mesylate therapy and clinical management. *Oncologist* 9(3): 271-81.

Gunawan, B., von Heydebreck, A., Sander, B., Schulten, H.J., Haller, F., Langer, C., Armbrust, T., Bollmann, M., Gasparov, S., Kovac, D. and Füzesi, L. (2007). An oncogenetic tree model in gastrointestinal stromal tumours (GISTs) identifies different pathways of cytogenetic evolution with prognostic implications. *J Pathol* 211(4): 463-70.

Gupta, A., Roy, S., Lazar, A.J., Wang, W.L., McAuliffe, J.C., Reynoso, D., McMahon, J., Taguchi, T., Floris, G., Debiec-Rychter, M., Schoffski, P., Trent, J.A., Debnath, J. and Rubin, B.P. (2010). Autophagy inhibition and antimalarials promote cell death in gastrointestinal stromal tumor (GIST). *Proc Natl Acad Sci U S A* 107(32): 14333-8.

Hafner, S., Harmon, B.G. and King, T. (2001). Gastrointestinal stromal tumors of the equine cecum. *Vet Pathol* 38: 242-246.

Haga, H.A., Ytrehus, B., Rudshaug, I.J. and Ottesen, N. (2008). Gastrointestinal stromal tumor and hypoglycemia in a Fjord pony: case report. *Acta Vet Scand* 50: 9.

Hagger, R., Gharaie, S., Finlayson, C. and Kumar, D. (1998). Regional and transmural density of interstitial cells of Cajal in human colon and rectum. *Am J Physiol*. 275: G1309-16.

Hanks, SK., Quinn, A.M. and Hunter, T. (1988). The protein kinase family: Conserved features and deduced phylogeny of the catylytic domains. *Science* 241(4861): 42-52.

Heinrich, M.C., Corless, C.L., Demetri, G.D., Blanke, C.D., von Mehren, M., Joensuu, H., McGreevey, L.S., Chen, C-J., Van den Abbeele, A.D., Druker, B. J., Kiese, B., Eisenberg, B., Roberts, P.J., Singer, S., Fletchher, C.D.M., Silberman, S., Dimitrijevic, S. and Fletcher J.A. (2003). Kinase mutations and imatinib response in patients with metastatic gastrointestinal stromal tumor. *J. Clin. Oncol*. 21: 4342-4349.

Heinrich, M.C., Corless, C.L., Duensing, A., McGreevey, L., Chen, C.J., Joseph, N., Singer, S., Griffith, D.J., Haley, A., Town, A., Demetri, G.D., Fletcher, C.D. and Fletcher, J.A. (2003). PDGFRA activating mutations in gastrointestinal stromal tumors. *Science* 299: 708-710.

Heinrich, M.C, Wise, S., Hood, M., Smith, B., Kaufman, M., Lu, W., Wang, Y., Griffith, D., Flynn, D. and Fletcher, J.A. (2010). In vitro activity of novel KIT/PDGFRA switch pocket kinase inhibitors against mutations associated with drug-resistant GI stromal tumors. *Clin Oncol* 28: 15s.

Heinrich, M.C., Griffith, D., McKinley, A., Patterson, J., Presnell, A., Ramachandran, A. and Debiec-Rychter, M. (2012). Crenolanib Inhibits the Drug-Resistant PDGFRA D842V Mutation Associated with Imatinib-Resistant Gastrointestinal Stromal Tumors. *Clin Cancer Res* Epub ahead of print.

Heinrich, M.C., Griffith, D.J., Druker, B.J., Wait, C.L., Ott, K.A. and Zigler, A.J. (2000). Inhibition of c-kit receptor tyrosine kinase activity by STI 571, a selective tyrosine kinase inhibitor. *Blood* 96(3): 925-32.

Heinrich, M.C., Maki, R.G., Corless, C.L., Antonescu, C.R., Harlow, A., Griffith, D., Town, A., McKinley, A., Ou, W.B., Fletcher, J.A., Fletcher, C.D., Huang, X., Cohen, D.P., Baum, C.M. and Demetri, G.D. (2008). Primary and secondary kinase genotypes correlate with the biological and clinical activity of sunitinib in imatinib-resistant gastrointestinal stromal tumor. *J Clin Oncol* 26(33): 5352-9.

Heinrich, M.C., Owzar, K., Corless, C.L., Hollis, D., Borden, E.C., Fletcher, C.D., Ryan, C.W., von Mehren, M., Blanke, C.D., Rankin, C., Benjamin, R.S., Bramwell, V.H., Demetri, G.D., Bertagnolli, M.M. and Fletcher, J.A. (2008). Correlation of kinase genotype and clinical outcome in the North American Intergroup Phase III Trial of imatinib mesylate for treatment of advanced gastrointestinal stromal tumor: CALGB 150105 Study by Cancer and Leukemia Group B and Southwest Oncology Group. *J Clin Oncol* 26(33): 5360-7.

Heldin, C.H. (1992). Structural and functional studies on platelet-derived growth factor. *EMBO J* 11: 4251-4259.

Herrera, G.A., Cerezo, L., Jones, J.E., Sack, J., Grizzle, W. E., Pollack, W. J. and Lott, R. L. (1989). Gastrointestinall autonomic nerve tumors. "Plexosarcomas". *Arch Pathol Lab Med* 113: 846-853.

Herrera, G.A., Pinto de Morales, H., Grizzle, W.E. and Hang, S.G. (1984). Malignant small bowel neoplasm of enteric plexus derivation (plexosarcoma). Light and electron microscopic study confirming the origin of the neoplasm. *Dig. Dis. Sci*. 29(3): 275-284.

Hirota, S., Isozaki, K., Moriyama, Y., Hashimoto, K., Nishida, T., Ishiguro, S., Kawano, K., Hanada, M., Kurata, A., Takeda, M., Tunio, G.M., Matsuzawa, Y., Kanakura, Y., Shinomura, Y. and Kitamura, Y. (1998). Gain-of function mutations of c-kit in human gastrointestinal stromal tumors. *Science* 279(5350): 577-580.

Hirota, S., Ohashi, A., Nishida, T., Isozaki, K., Kinoshita, K., Shinomura, Y. and Kitamura, Y. (2003). Gain-of-function mutations of platelet-derived growth factor receptor alpha gene in gastrointestinal stromal tumors. *Gastroenterology* 125(3): 660-7.

Hostein, I., Faur, N., Primois, C., Boury, F., Denard, J., Emile, J.F., Bringuier, P.P., Scoazec, J.Y. and Coindre, J.M. (2010). BRAF mutation status in gastrointestinal stromal tumors. *Am J Clin Pathol* 133(1): 141-8.

Hudson, B.P., Martinez-Yamout, M.A., Dyson, H.J. and Wright, P.E. (2004). Recognition of the mRNA AU-rich element by the zinc finger domain of TIS11d. *Nat Struct Mol Biol* 11(3): 257-64.

Iino, S., Horiguchi, K., Horiguchi, S. and Nojyo, Y. (2009). c-Kit-negative fibroblast-like cells express platelet-derived growth factor receptor alpha in the murine gastrointestinal musculature. *Histochem Cell Biol* 131(6): 691-702.

Isozaki, K., Terris, B., Belghiti, J., Schiffmann, S., Hirota, S. and Vanderwinden, J.M. (2000). Germline-activating mutation in the kinase domain of KIT gene in familial gastrointestinal stromal tumors. *Am J Pathol* 157(5): 1581-5.

Janeway, K.A., Albritton, K.H., Van Den Abbeele, A.D., D'Amato, G.Z., Pedrazzoli, P., Siena, S., Picus, J., Butrynski, J.E., Schlemmer, M., Heinrich, M.C. and Demetri, G.D. (2009). Sunitinib treatment in pediatric patients with advanced GIST following failure of imatinib. *Pediatr Blood Cancer* 52(7): 767-71.

Janeway, K.A., Kim, S.Y., Lodish, M., Nosé, V., Rustin, P., Gaal, J., Dahia, P.L., Liegl, B., Ball, E.R., Raygada, M., Lai, A.H., Kelly, L., Hornick, J.L.; NIH Pediatric and Wild-Type GIST Clinic, O'Sullivan, M., de Krijger, R.R., Dinjens, W.N., Demetri, G.D., Antonescu, C.R., Fletcher, J.A., Helman, L. and Stratakis, C.A. (2011). Defects in succinate dehydrogenase in gastrointestinal stromal tumors lacking KIT and PDGFRA mutations. *Proc Natl Acad Sci U S A* 108(1): 314-8.

Janeway, K.A., Liegl, B., Harlow, A., Le, C., Perez-Atayde, A., Kozakewich, H., Corless, C.L., Heinrich, M.C. and Fletcher, J.A. (2007). Pediatric KIT wild-type and platelet-derived growth factor receptor alpha-wild-type gastrointestinal stromal tumors share KIT activation but not mechanisms of genetic progression with adult gastrointestinal stromal tumors. *Cancer Res* 67(19): 9084-8.

Jin, T., Nakatani, H., Taguchi, T., Nakano, T., Okabayashi, T., Sugimoto, T., Kobayashi, M. and Araki, K. (2006). STI571 (Glivec) suppresses the expression of vascular endothelial growth factor in the gastrointestinal stromal tumor cell line, GIST-T1. *World J Gastroenterol* 12(5): 703-8.

Joensuu, H., Fletcher, C., Dimitrijevic, S., Silberman, S., Roberts, P. and Demetri, G. (2002). Management of malignant gastrointestinal stromal tumours. *Lancet Oncol* 3(11): 655-64.

Joensuu, H., Roberts, P.J., Sarlomo-Rikala, M., Andersson, L.C., Tervahartiala, P., Tuveson, D., Silberman, S., Capdeville, R., Dimitrijevic, S., Druker, B. and Demetri, G.D. (2001). Effect of the tyrosine kinase inhibitor STI571 in a patient with a metastatic gastrointestinal stromal tumor. *N Engl J Med*. 344(14): 1052-6.

Kang, D.Y., Park, C.K., Choi, J.S., Jin, S.Y., Kim, H.J., Joo, M., Kang, M.S., Moon, W.S., Yun, K.J., Yu, E.S., Kang, H. and Kim, K.M. (2007). Multiple gastrointestinal stromal tumors: Clinicopathologic and genetic analysis of 12 patients. *Am J Surg Pathol* 31(2): 224-32.

Kawagishi, J., Kumabe, T., Yoshimoto, T. and Yamamoto, T. (1995). Structure, organization, and transcription units of the human alpha-platelet-derived growth factor receptor gene, PDGFRA. *Genomics* 30(2): 224-32.

Kielkopf, C.L., Lücke, S. and Green, M.R. (2004). U2AF homology motifs: protein recognition in the RRM world. *Genes Dev* 18(13): 1513-26.

Kim, K.M., Kang, D.W., Moon, W.S., Park, J.B., Park, C.K., Sohn, J.H., Jeong, J.S., Cho, M.Y., Jin, S.Y., Choi, J.S. and Kang, D.Y. (2006). PKCtheta expression in gastrointestinal stromal tumor. *Mod Pathol* 19(11): 1480-6.

Kim, K.M., Kang, D.W., Moon, W.S., Park, J.B., Park, C.K., Sohn, J.H., Jeong, J.S., Cho, M.Y., Jin, S.Y., Choi, J.S., Kang, D.Y.; Gastrointestinal Stromal Tumor Committee and The Korean Gastrointestinal Pathology Study Group. (2005) Gastrointestinal Stromal Tumors in Koreans: It's Incidence and the Clinical, Pathologic and Immunohistochemical Findings. *J Korean Med Sci* 20: 977-984.

Kim, M.Y., Hur, J. and Jeong, S. (2009). Emerging roles of RNA and RNA-binding protein network in cancer cells. *BMB reports* 125-130.

Kindblom, L. G., Remotti, H. E., Aldenborg, F., and Meis-Kindblom, J. M. (1998). Gastrointestinal pacemaker cell tumor (GIPACT): gastrointestinal stromal tumors show phenotypic characteristics of the interstitial cells of Cajal. *Am. J. Pathol*. 152: 1259-1269.

Komuro, T. (2006). Structure and organization of interstitial cells of Cajal in the gastrointestinal tract. *J Physiol* 576(Pt 3): 653-8.

Kurahashi, M., Zheng, H., Dwyer, L., Ward, S.M., Don Koh, S. and Sanders, K.M. (2011). A functional role for the 'fibroblast-like cells' in gastrointestinal smooth muscles. *J Physiol* 589(Pt 3): 697-710.

Lagna, G., Ku, M.M., Nguyen, P.H., Neuman, N.A., Davis, B.N. and Hata, A. (2007). Control of phenotypic plasticity of smooth muscle cells by bone morphogenetic protein signaling through the myocardin-related transcription factors. *J Biol Chem* 282(51): 37244-55.

Laqueur, E. (1914). Uberlebensdauer von Säugetierorganen mit Automatie. *Zentralbl. Physiol.* 28: 728.

Lasota, J., Corless, C.L., Heinrich, M.C., Debiec-Rychter, M., Sciot, R., Wardelmann, E., Merkelbach-Bruse, S., Schildhaus, H.U., Steigen, S.E., Stachura, J., Wozniak, A., Antonescu, C., Daum, O., Martin, J., Del Muro, J.G. and Miettinen, M. (2008).

Clinicopathologic profile of gastrointestinal stromal tumors (GISTs) with primary KIT exon 13 or exon 17 mutations: a multicenter study on 54 cases. *Mod Pathol* 21(4): 476-84.

Lauwers, G. Y., Erlandson, R. A., Casper, E. S., Brennan, M. F. and Woodruff, J. M. (1993). Gastrointestinal autonomic nerve tumors. A clinicopathological, immunohistochemical, and ultrastructural study of 12 cases. *Am. J. Surg. Pathol.* 17: 887-897.

Le Guen, L., Notarnicola, C., de Santa Barbara, P. (2009). Intermuscular tendons are essential for the development of vertebrate stomach. *Development*. 136, 791-801.

Lee, J.R., Joshi, V., Griffin, J.W., Jr., Lasota, J. and Miettinen, M. (2001). Gastrointestinal autonomic nerve tumor: immunohistochemical and molecular identity with gastrointestinal stromal tumor. *Am. J. Surg. Pathol.* 25(8): 979-987.

Lee,M.H. and Schedl, T. (2006). RNA-binding proteins. *WormBook* 1.79.1.

Lemmon, M.A. and Schlessinger, J. (2010). Cell signaling by receptor-tyrosine kinases. *Cell* 141(7): 1117-1134.

Lewis, M.R. and Lewis, W.H. (1914). Mitochondria in tissue culture. Science 39: 330-333

Liegl, B., Kepten, I., Le, C., Zhu, M., Demetri, G.D., Heinrich, M.C., Fletcher, C.D., Corless, C.L., Fletcher, J.A. (2008). Heterogeneity of kinase inhibitor resistance mechanisms in GIST. *J Pathol* 216(1): 64-74.

Liegl-Atzwanger, B., Fletcher J. A. and Fletcher, C.D.M. (2010). Gastrointestinal stromal tumours. *Virchows Arch* 456: 111-127.

Liu, Y., Tseng, M., Perdreau, S.A., Rossi, F., Antonescu, C., Besmer, P., Fletcher, J.A., Duensing, S. and Duensing, A. (2007). Histone H2AX is a mediator of gastrointestinal stromal tumor cell apoptosis following treatment with imatinib mesylate. *Cancer Res* 67(6): 2685-92.

Lukong, K.E., Chang, K.W., Khandjian, E.W. and Richard, S. (2008). RNA-binding proteins in human genetic disease. *Cell* 24: 416-425.

Lunde, B.M., Moore, C. and Varani, G. (2007). RNA-binding proteins: modular design for efficient function. *Nat.Rev.Mol.Cell Biol.* 8: 479-490.

Maas, C., ter Haar, G., van der Gaag, I. and Kirpensteijn, J. (2007). Reclassification of small intestinal and cecal smooth muscle tumors in 72 dogs: clinical, histologic, and immunohistochemical evaluation. *Vet Surg* 36: 302-313.

Maeda, H., Yamagata, A., Nishikawa, S., Yoshinaga, K., Kobayashi, S., Nishi, K. and Nishikawa, S. (1992). Requirement of c-kit for development of intestinal pacemaker system. *Development* 116(2): 369-75.

Mahadevan, D., Cooke, L., Riley, C., Swart, R., Simons, B., Della Croce, K., Wisner, L., Iorio, M., Shakalya, K., Garewal, H., Nagle, R. and Bearss, D. (2007). A novel tyrosine kinase switch is a mechanism of imatinib resistance in gastrointestinal stromal tumors. *Oncogene* 26(27): 3909-19.

Maris, C., Dominguez, C. and Allain, F.H. (2005). The RNA recognition motif, a plastic RNA-binding platform to regulate post-transcriptional gene expression. *FEBS J* 272(9): 2118-31.

Mauro, M.J., O'Dwyer, M., Heinrich, M.C. and Druker, B.J. (2002). STI571: a paradigm of new agents for cancer therapeutics. *J Clin Oncol* 20(1): 325-34.

Mazurt, M. T. and Clark H. B. (1983). Gastric stromal tumors. Reappraisal of histogenesis. *Am. J. Surg. Pathol.* 7: 507-519.

McLeod, L.E. and Proud, C.G. (2002). ATP depletion increases phosphorylation of elongation factor eEF2 in adult cardiomyocytes independently of inhibition of mTOR signalling. FEBS Lett 531(3):448-52.

McLin, V.A., Henning, S.J. and Jamrich, M. (2009). The role of the visceral mesoderm in the development of the gastrointestinal tract. *Gastroenterology* 136(7): 2074-91.

Medeiros, F., Corless, C.L., Duensing, A., Hornick, J.L., Oliveira, A.M., Heinrich, M.C., Fletcher, J.A. and Fletcher, C.D. (2004). KIT-negative gastrointestinal stromal tumors: proof of concept and therapeutic implications. *Am. J. Surg. Pathol.* 28(7): 889-94.

Miettinen M., Lasota J. 2006. Gastrointestinal stromal tumors: review on morphology, molecular pathology, prognosis, and differential diagnosis. *Arch Pathol Lab Med*. 130, 1466-78.

Miettinen, M. and Lasota, J. (2001). Gastrointestinal stromal tumors-definition, clinical, histological, immunohistochemical, and molecular genetic features and differential diagnosis. *Virchows Arch.* 438(1): 1-12.

Miettinen, M. and Lasota, J. (2006). Gastrointestinal stromal tumors: pathology and prognosis at different sites. *Semin Diagn Pathol* 23: 70-83.

Miettinen, M. and Lasota, J. (2006). Gastrointestinal stromal tumors: review on morphology, molecular pathology, prognosis, and differential diagnosis. *Arch Pathol Lab Med* 130: 1466-1478.

Miettinen, M., Fetsch, J.F., Sobin, L.H. and Lasota, J. (2006). Gastrointestinal stromal tumors in patients with neurofibromatosis 1: a clinicopathologic and molecular genetic study of 45 cases. *Am. J. Surg. Pathol.* 30(1): 90-6.

Miettinen, M., Furlong, M., Sarlomo-Rikala, M., Burke, A., Sobin, L.H. and Lasota, J. (2001). Gastrointestinal stromal tumors, intramural leiomyomas, and leiomyosarcomas in the rectum and anus: a clinicopathologic, immunohistochemical, and molecular genetic study of 144 cases. *Am. J. Surg. Pathol*. 25(9): 1121-33.

Miettinen, M., Lasota, J. and Sobin, L.H. (2005). Gastrointestinal stromal tumors of the stomach in children and young adults: a clinicopathologic, immunohistochemical, and molecular genetic study of 44 cases with long-term follow-up and review of the literature. *Am. J. Surg. Pathol*. 29(10): 1373-81.

Miettinen, M., Makhlouf, H., Sobin, L.H. and Lasota, J. (2006). Gastrointestinal stromal tumors of the jejunum and ileum: a clinicopathologic, immunohistochemical, and molecular genetic study of 906 cases before imatinib with long-term follow-up. *Am. J. Surg. Pathol.* 30(4): 477-89.

Miettinen, M., Makhlouf, H., Sobin, L.H. and Lasota, J. (2006). Gastrointestinal stromal tumors of the jejunum and ileum: a clinicopathologic, immunohistochemical, and molecular genetic study of 906 cases before imatinib with long-term follow-up. *Am. J. Surg. Pathol.* 30(4): 477-89.

Miettinen, M., Moniha, J.M., Sarlomo-Rikala, M., Kovatich, A.J., Carr, N.J., Emorty, T.S. and Sabin, L.H. (1999). Gastrointestinal stromal tumors/smooth muscle tumors/GISTs on the omentum and mesentery - clinicopathologic and immunohistochemical study of 26 cases. *Am. J. Sur. Pathol*. 22: 1109-1118.

Miettinen, M., Sarlomo-Rikala, J. and Lasota, J. (1999). Gastrointestinal stromal tumors - new findings on their biology. *Hum Pathol* 23: 1209-1220.

Miettinen, M., Sarlomo-Rikala, M., Sobin, L.H. and Lasota, J. (2000). Esophageal stromal tumors: a clinicopathologic, immunohistochemical, and molecular genetic study of 17 cases and comparison with esophageal leiomyomas and leiomyosarcomas. *Am. J. Surg. Pathol.* 24(2): 211-22.

Miettinen, M., Sobin, L.H. and Lasota, J. (2005). Gastrointestinal stromal tumors of the stomach: a clinicopathologic, immunohistochemical, and molecular genetic study of 1,765 cases with long-term follow-up. *Am. J. Surg. Pathol*. 29(1): 52-68.

Miettinen, M., Sobin, L.H. and Sarlomo-Rikala, M. (2000). Immunohistochemical spectrum of GISTs at different sites and their differential diagnosis with a reference to CD117 (KIT). *Mod Pathol* 13(10): 1134-42.

Miettinen, M., Virolainen, M. and Maarit, S.R. (1995). Gastrointestinal stromal tumors-Value of CD34 antigen in their identification and separation from true leioyomas and schwannomas. *Am. J. Surg. Patrol.* 19: 207-216.

Miettinen, M., Wang, Z.F. and Lasota, J. (2009). DOG1 antibody in the differential diagnosis of gastrointestinal stromal tumors: a study of 1840 cases. *Am. J. Surg. Pathol.* 33(9): 1401-8.

Mol, C.D., Dougan, D.R., Schneider, T.R., Skene, R.J., Kraus, M.L., Scheibe, D.N., Snell, G.P., Zou, H., Sang, B.C. and Wilson, K.P. (2004). Structural basis for the autoinhibition and STI-571 inhibition of c-Kit tyrosine kinase. *J Biol Chem* 279(30): 31655-63.

Mostafa, R.M., Moustafa, Y.M. and Hamdy, H. (2010). Interstitial cells of Cajal, the Maestro in health and disease. *World J Gastroenterol* 16(26): 3239-48.

Mukaisho, K., Miwa, K., Totsuka, Y., Shimomura, A., Sugihara, H., Wakabayashi, K. and Hattori, T. (2006). Induction of gastric GIST in rat and establishment of GIST cell line. *Cancer Lett* 231(2): 295-303.

Murray, M. R. and Kopech, G. (1953). A Bobliography of the Research in Tissue Culture 1894/1950. *New York: Academic* 2 vol.

Nakamura, J., Aoyagi, S., Nanchi, I., Nakatsuka, S., Hirata, E., Shibata, S., Fukuda, M., Yamamoto, Y., Fukuda, I., Tatsumi, N., Ueda, T., Fujiki, F., Nomura, M., Nishida, S., Shirakata, T., Hosen, N., Tsuboi, A., Oka, Y., Nezu, R., Mori, M., Doki, Y., Aozasa, K., Sugiyama, H. and Oji, Y. (2009). Overexpression of eukaryotic elongation factor eEF2 in gastrointestinal cancers and its involvement in G2/M progression in the cell cycle. Int J Oncol 34(5):1181-9.

Ng, E.H., Pollock, R.E., Munsell, M.F., Atkinson, E.N. and Romsdahl, M.M. (1992). Prognostic factors influencing survival in gastrointestinal leiomyosarcomas. Implications for surgical management and staging. *Ann Surg* 215(1): 68-77.

Nguyen, S.Q., Divino, C.M., Wang, J.L. and Dikman, S.H. (2006). Laparoscopic management of gastrointestinal stromal tumors. *Surg Endosc* 20(5): 713-6.

Nilsson, B., Nilsson, O. and Ahlman, H. (2009). Treatment of gastrointestinal stromal tumours: imatinib, sunitinib -- and then? *Expert Opin Investig Drugs* 18(4): 457-68.

Nilsson, B.P, Bumming, P., Meis-Kindblom, J.M., Oden, A., Dortok, A., Gustavsson, B., Sablinska, K. and Kindblom, L.B. (2005). Gastrointestinal stromal tumors: The incidence, prevalence, clinical course, and prognostication in the preimatinib mesylate era. *Cancer* 103: 821-829.

Nishida, T., Hirota, S., Taniguchi, M., Hashimoto, K., Isozaki, K., Nakamura, H., Kanakura, Y., Tanaka, T., Takabayashi, A., Matsuda, H., Kitamura, Y. (1998). Familial gastrointestinal stromal tumours with germline mutation of the KIT gene. *Nat Genet* 19(4): 323-4.

Notarnicola, C., Rouleau, C., Le Guen, L., Virsolvy, A., Richard, S., Faure, S. and De Santa Barbara, P. (2012). The RNA-Binding Protein RBPMS2 Regulates Development of Gastrointestinal Smooth Muscle. *Gastroenterology* 143: 687-697.

Olson, L.E. and Soriano, P. (2009). Increased PDGFRalpha activation disrupts connective tissue development and drives systemic fibrosis. *Dev Cell* 16(2): 303-13.

Ördög, T., Redelman, D., Horváth, V.J., Miller, L.J., Horowitz, B., Sanders, K.M. (2004). Quantitative analysis by flow cytometry of interstitial cells of Cajal, pacemakers, and mediators of neurotransmission in the gastrointestinal tract. *Cytometry A* 62(2): 139-49.

Pasini, B., McWhinney, S.R., Bei, T., Matyakhina, L., Stergiopoulos, S., Muchow, M., Boikos, S.A., Ferrando, B., Pacak, K., Assie, G., Baudin, E., Chompret, A., Ellison, J.W., Briere, J.J., Rustin, P., Gimenez-Roqueplo, A.P., Eng, C., Carney, J.A. and Stratakis, C.A. (2008). Clinical and molecular genetics of patients with the Carney-Stratakis syndrome and germline mutations of the genes coding for the succinate dehydrogenase subunits SDHB, SDHC, and SDHD. *Eur J Hum Genet* 16(1): 79-88.

Pauls, K., Merkelbach-Bruse, S., Thal, D., Büttner, R. and Wardelmann, E. (2005). PDGFRalpha- and c-kit-mutated gastrointestinal stromal tumours (GISTs) are characterized by distinctive histological and immunohistochemical features. *Histopathology* 46(2): 166-75.

Peterson, M.R., Piao, Z., Weidner, N. and Yi, E.S. (2006). Strong PDGFRA positivity is seen in GISTs but not in other intra-abdominal mesenchymal tumors:

Immunohistochemical and mutational analyses. *Appl Immunohistochem Mol Morphol* 14(4): 390-6.

Philippar, U., Schratt, G., Dieterich, C., Müller, J.M., Galgóczy, P., Engel, F.B., Keating, M.T., Gertler, F., Schüle, R., Vingron, M. and Nordheim, A. (2004). The SRF target gene Fhl2 antagonizes RhoA/MAL-dependent activation of SRF. *Mol Cell* 16(6): 867-80.

Prakash, S., Sarran, L., Socci, N., DeMatteo, R.P., Eisenstat, J., Greco, A.M., Maki, R.G., Wexler, L.H., LaQuaglia, M.P., Besmer, P., Antonescu, C.R. (2005). Gastrointestinal stromal tumors in children and young adults: a clinicopathologic, molecular, and genomic study of 15 cases and review of the literature. *J Pediatr Hematol Oncol* 27(4): 179-87.

Query, C.C., Bentley, R.C. and Keene, J.D. (1989). A common RNA recognition motif identified within a defined U1 RNA binding domain of the 70K U1 snRNP protein. *Cell* 57(1): 89-101.

Rahbari, R., Sheahan, T., Modes, V., Collier, P., Macfarlane, C. and Badge, R.M. (2009). A novel L1 retrotransposon marker for HeLa cell line identification. *Biotechniques* 46(4): 277-84.

Rankin, C., Von Mehren, M., Blanke, C., Benjamin, R., Fletcher, C.D.M., Bramwell, V., Crowley, J., Borden, E. and Demetri, G.D. (2004). Dose effect of imatinib (IM) in patients (pts) with metastatic GIST - Phase III Sarcoma Group Study S0033. Proc *Am Soc Clin Oncol* 23: 815.

Reed, J., Ouban, A., Schickor, F.K., Muraca, P., Yeatman, T. and Coppola, D. (2002). Immunohistochemical staining for c-Kit (CD117) is a rare event in human colorectal carcinoma. *Clin Colorectal Cancer* 2(2): 119-22.

Reichardt, P., Pink, D., Lindner, T., Heinrich, M.C., Cohen, P.S., Wang, Y., Yu, R., Tsyrlova, A., Dimitrijevic, S. and Blanke, C. (2005). A phase I/II trial of the oral PKC-inhibitor PKC412 (PKC) in combination with imatinib mesylate (IM) in patients (pts) with gastrointestinal stromal tumor (GIST) refractory to IM. *J Clin Oncol* 23: 16S.

Renouf, D.J., Wilson, L. nad Blanke, C.D. (2009). Successes and challenges in translational research: the development of targeted therapy for gastrointestinal stromal tumours. *Clin. Cancer Res*. 15, 3908-3911.

Reynoso, D., Nolden, L.K., Yang, D., Dumont, S.N., Conley, A.P., Dumont, A.G., Zhou, K., Duensing, A. and Trent, J.C. (2011). Synergistic induction of apoptosis by the Bcl-2 inhibitor ABT-737 and imatinib mesylate in gastrointestinal stromal tumor cells. *Mol Oncol* 5(1): 93-104.

Ricci, A. J-R., Ciccarellio, O., Cartun, R.W. and Newcomb, P. (1987). A clinicopathologic and immunohistochemical study of 16 patiens with small intestinal leiomyosarcoma. Liminet utulity of immunophenotyping. *Cancer* 60(8): 1790-1799.

Rose, A.J., Alsted, T.J., Jensen, T.E., Kobberø, J.B., Maarbjerg, S.J., Jensen, J. and Richter, E.A. (2009). A Ca(2+)-calmodulin-eEF2K-eEF2 signalling cascade, but not AMPK, contributes to the suppression of skeletal muscle protein synthesis during contractions. J Physiol 587(7):1547-63.

Rossi, G., Valli, R., Bertolini, F., Marchioni, A., Cavazza, A., Mucciarini, C., Migaldi, M., Federico, M., Trentini, G.P. and Sgambato, A. (2005). PDGFR expression in differential diagnosis between KIT-negative gastrointestinal stromal tumours and other primary soft-tissue tumours of the gastrointestinal tract. *Histopathology* 46(5): 522-31.

Rouleau, C., Matécki, S., Kalfa, N., Costes, V. and de Santa Barbara, P. (2009). Activation of MAP kinase (ERK1/2) in human neonatal colonic enteric nervous system. *Neurogastroenterol Motil* 21(2): 207-14.

Rouleau, C., Matecki, S., Kalfa, N., et al., (2009). Activation of MAP kinase (ERK1/2) in human neonatal colonic enteric nervous system. *Neurogastroenterol. Motil*. 21, 207-214.

Rouleau, C., Rico, C., Hapkova, I. And de Santa Barbara, P. (2012). Immunohistochemical analysis of bone morphological protein signaling pathway in human myometrium. *Exp Mol Pathol* 93(1): 56-60.

Rubin, B. P., Fletcher, J. A. and Fletcher, C. D. (2000). Molecular Insights into the Histogenesis and Pathogenesis of Gastrointestinal Stromal Tumors. *Int. J. Surg. Pathol.* 8: 5-10.

Rubin, B.P, Heinrich, M.C. and Corless, C.L. (2007). Gastrointestinal stromal tumor. *Lancet* 369: 1731-41.

Rubin, B.P., Antonescu, C.R., Scott-Browne, J.P., Comstock, M.L., Gu, Y., Tanas, M.R., Ware, C.B. and Woodell, J. (2005). A knock-in mouse model of gastrointestinal stromal tumor harboring kit K641E. *Cancer Res* 65(15): 6631-9.

Sakurama, K., Noma, K., Takaoka, M., Tomono, Y., Watanabe, N., Hatakeyama, S., Ohmori, O., Hirota, S., Motoki, T., Shirakawa, Y., Yamatsuji, T., Haisa, M., Matsuoka, J., Tanaka, N. and Naomoto, Y. (2009). Inhibition of focal adhesion kinase as a potential therapeutic strategy for imatinib-resistant gastrointestinal stromal tumor. *Mol Cancer Ther* 8(1): 127-34.

Sanders, K.M., Koh, S.D. and.Ward, S.M. (2006). Interstitial cells of cajal as pacemakers in the gastrointestinal tract. *Annu. Rev. Physiol*. 68, 307-343.

Sarlomo-Rikala, M., Kovatich, A.J., Barusevicius, A. and Miettinen, M. (1998). CD117: a sensitive marker for gastrointestinal stromal tumors that is more specific than CD34. *Mod pathol* 11: 728-34.

Saturday, G.A., Lasota, J., Frost, D., Brasky, K.B., Hubbard, G. and Miettinen, M. (2005). KIT-positive gastrointestinal stromal tumor in a 22-year-old male chimpanzee (Pan troglodytes). *Vet Pathol* 42: 362-365.

Scherer, W.F., Syverton, J.T. and Gey, G.O. (1953). Studies on the propagation in vitro of poliomyelitis viruses. IV. Viral multiplication in a stable strain of human malignant epithelial cells (strain HeLa) derived from an epidermoid carcinoma of the cervix. *J Exp Med* 97(5): 695-710.

Schöffski, P., Reichardt, P., Blay, J.Y., Dumez, H., Morgan, J.A., Ray-Coquard, I., Hollaender, N., Jappe, A. and Demetri, G.D. (2010). A phase I-II study of everolimus (RAD001) in combination with imatinib in patients with imatinib-resistant gastrointestinal stromal tumors. *Ann Oncol* 21(10): 1990-8.

Seremetis, M.G., Lyons, W.S., deGuzman, V.C. and Peabody, J.W. Jr. (1976). Leiomyomata of the esophagus. An analysis of 838 cases. *Cancer* 38(5): 2166-77.

Shek, T.W., Luk, I.S., Loong, F., Ip, P. and Ma, L. (1996). Inflammatory cell-rich gastrointestinal autonomic nerve tumor. An expansion of its histologic spectrum. *Am J Surg Pathol* 20(3): 325-31.

Shiu, M.H., Farr, G.H., Papachristou, D.N. and Hajdu, S.I. (1982). Myosarcomas of the stomach: natural history, prognostic factors and management. *Cancer* 49(1): 177-87.

Singer, S., Rubin, B.P., Lux, M.L., Chen, C.J., Demetri, G.D., Fletcher, C.D. and Fletcher, J.A. (2002). Prognostic value of KIT mutation type, mitotic activity, and histologic subtype in gastrointestinal stromal tumors. *J Clin Oncol* 20(18): 3898-905.

Sommer, G., Agosti, V., Ehlers, I., Rossi, F., Corbacioglu, S., Farkas, J., Moore, M., Manova, K., Antonescu, C.R. and Besmer, P. (2003). Gastrointestinal stromal tumors

in a mouse model by targeted mutation of the Kit receptor tyrosine kinase. *Proc Natl Acad Sci U S A* 100(11): 6706-11.

St Johnston, D. (2005). Moving messages: the intracellular localization of mRNAs. *Nat. Rev. Mol. Cell. Biol.* 6: 363-375.

Stout, A.P. (1962). Bizarre smooth muscle tumors of the stomach. *Cancer* 15: 400-409.

Stramatakos, M., Douzinas, E., Stefanaki, C., Safioleas, P., Polyzou, E., Levidou, G. and Safioleas, M. (2009). Gastrointestinal stromal tumor. *World Journal of Srgical Oncology* 7: 61-69.

Suster, S. and Fletcher, C.D. (1996). Gastrointestinal stromal tumors with prominent signet-ring cell features. *Mod Pathol* 9: 609-613.

Szilágyi, A., Grimm, V., Arakaki, A.K. and Skolnick, J. (2005). Prediction of physical protein-protein interactions. *Phys Biol* 2 :S1-16.

Taguchi, T., Sonobe, H., Toyonaga, S., Yamasaki, I., Shuin, T., Takano, A., Araki, K., Akimaru, K. and Yuri, K. (2002). Conventional and molecular cytogenetic characterization of a new human cell line, GIST-T1, established from gastrointestinal stromal tumor. *Lab Invest* 82(5): 663-5.

Tamborini, E., Bonadiman, L., Greco, A., Albertini, V., Negri, T., Gronchi, A., Bertulli, R., Colecchia, M., Casali, P.G., Pierotti, M.A., Pilotti, S. (2004). A new mutation in the KIT ATP pocket causes acquired resistance to imatinib in a gastrointestinal stromal tumor patient. *Gastroenterology* 127(1): 294-9.

Tarn, C., Merkel, E., Canutescu, A.A., Shen, W., Skorobogatko, Y., Heslin, M.J., Eisenberg, B., Birbe, R., Patchefsky, A., Dunbrack, R., Arnoletti, J.P., von Mehren, M. and Godwin, A.K. (2005). Analysis of KIT mutations in sporadic and familial gastrointestinal stromal tumors: therapeutic implications through protein modeling. *Clin Cancer Res* 11(10): 3668-77.

Tarn, C., Rink, L., Merkel, E., Flieder, D., Pathak, H., Koumbi, D., Testa, J.R., Eisenberg, B., von Mehren, M. and Godwin, A.K. (2008). Insulin-like growth factor 1 receptor is a potential therapeutic target for gastrointestinal stromal tumors. *Proc Natl Acad Sci U S A* 105(24): 8387-92.

Thion, L. and Erard, M. (2002). Structure/function relationships within the RNA recognition motif family applied to the hermes gene product. *Protein Pept Lett* 9(2): 127-32.

Torihashi, S., Nishi, K., Tokutomi, Y., Nishi, T., Ward, S. and Sanders, K.M. (1999). Blockade of kit signaling induces transdifferentiation of interstitial cells of cajal to a smooth muscle phenotype. *Gastroenterology* 117(1): 140-8.

Torihashi, S., Ward, S.M., Sanders, K.M. (1997). Development of c-Kit-positive cells and the onset of electrical rhythmicity in murine small intestine. *Gastroenterology*. 112(1): 144-55.

Tryggvason, G., Gislason, H.G., Magnusson, M.K. and Jonasson, J.G. (2005). Gastrointestinal stromal tumors in Iceland, 1990-2003: The Icelandic GIST study, a population-based incidence and pathologic risk stratification study. *Int J Cancer* 117: 289-293.

Tuveson, D.A., Willis, N.A., Jacks, T., Griffin, J.D., Singer, S., Fletcher, C.D., Fletcher, J.A. and Demetri, G.D. (2001). STI571 inactivation of the gastrointestinal stromal tumor c-KIT oncoprotein: biological and clinical implications. *Oncogene* 20(36): 5054-8.

Ueyama, T., Gui, K-J., Hashimoto, H., Daimaru, Y. and Enjoji, M. (1992). Aclinicopathologic and immunohistological study of gastrointestinal stromal tumors. *Cancer* 69: 947-955.

Ullrich, A. and Schlessinger, J. (1990) Signal transduction by receptors with tyrosine kinase activity. *Cell* 61: 203-212.

Van Glabbeke, M., Verweij, J., Casali, P.G., Simes, J., Le Cesne, A., Reichardt, P., Issels, R., Judson, I.R., van Oosterom, A.T. and Blay, J.Y. (2006). Predicting toxicities for patients with advanced gastrointestinal stromal tumours treated with imatinib: a study of the European Organisation for Research and Treatment of Cancer, the Italian Sarcoma Group, and the Australasian Gastro-Intestinal Trials Group (EORTC-ISG-AGITG). *Eur J Cancer* 42(14): 2277-85.

van Kouwenhove, M., Kedde, M. and Agami, R. (2011). MicroRNA regulation by RNA-binding proteins and its implications for cancer. *Nature* 11: 644-656.

van Oosterom, A.T., Judson, I., Verweij, J., Stroobants, S., Donato di Paola, E., Dimitrijevic, S., Martens, M., Webb, A., Sciot, R., Van Glabbeke, M., Silberman, S. and Nielsen, O.S. (2001). Safety and efficacy of imatinib (STI571) in metastatic gastrointestinal stromal tumours: a phase I study. *Lancet* 358(9291): 1421-3.

Vanderwinden, J.M. and Rumessen, J.J. (1999). Interstitial cells of Cajal in human gut and gastrointestinal disease. *Microsc Res Tech* 47(5): 344-60.

Velarde, R., Mentaberre, G., Sánchez, J., Marco, I. and Lavín, S. (2008). KIT-positive gastrointestinal stromal tumors in two spanish ibex (Capra pyrenaica hispanica). *Vet J* 177: 445-447.

Verweij, J., Casali, P.G., Zalcberg, J., LeCesne, A., Reichardt, P., Blay, J.Y., Issels, R., van Oosterom, A., Hogendoorn, P.C., Van Glabbeke, M., Bertulli, R., Judson, I. (2004). Progression-free survival in gastrointestinal stromal tumours with high-dose imatinib: randomised trial. *Lancet* 364(9440): 1127-34.

Verweij, J., van Oosterom, A., Blay, J.Y., Judson, I., Rodenhuis, S., van der Graaf, W., Radford, J., Le Cesne, A., Hogendoorn, P.C., di Paola, E.D., Brown, M. and Nielsen, O.S. (2003). Imatinib mesylate (STI-571 Glivec, Gleevec) is an active agent for gastrointestinal stromal tumours, but does not yield responses in other soft-tissue sarcomas that are unselected for a molecular target. Results from an EORTC Soft Tissue and Bone Sarcoma Group phase II study. *Eur J Cancer* 39(14): 2006-11.

von Mehren, M., Blanke, C., Joensuu, H., Heinrich, M.C., Roberts, P., Eisenberg, B., Silberman, S., Dimitrijevic, S., Kiese, B., Fletcher, J., Fletcher, C. and Demetri., G.D. (2002). High incidence of durable responses induced by imatinib mesylate (Gleevec) in patients with unresectable and metastatic gastrointestinal stromal tumors (GISTs). *Proc Am Soc Clin Oncol* 21: 403a.

Walker, P. and Dvorak, A.M. (1986). Gastrointestinal autonomic nerve (GAN) tumor. Ultrastructural evidence for a newly recognized entity. *Arch Pathol Lab Med* 110(4): 309-316.

Wardelmann, E., Losen, I., Hans, V., Neidt, I., Speidel, N., Bierhoff, E., Heinicke, T., Pietsch, T., Büttner, R. and Merkelbach-Bruse, S. (2003). Deletion of Trp-557 and Lys-558 in the juxtamembrane domain of the c-kit protooncogene is associated with metastatic behavior of gastrointestinal stromal tumors. *Int J Cancer* 106(6): 887-95.

Weinstein, I.B. (2002). Cancer. Addiction to oncogenes--the Achilles heal of cancer. *Science* 297(5578): 63-4.

Welsh, R.A. and Meyer, A.T. (1969). Ultrastructure of gastric leiomyoma. *Arch. Pathol*. 87(1): 71-81.

West, R.B., Corless, C.L., Chen, X., Rubin, B.P., Subramanian, S., Montgomery, K., Zhu, S., Ball, C.A., Nielsen, T.O., Patel, R., Goldblum, J.R., Brown, P.O., Heinrich, M.C. and van de Rijn, M. (2004). The novel marker, DOG1, is expressed ubiquitously in

gastrointestinal stromal tumors irrespective of KIT or PDGFRA mutation status. *Am J Pathol* 165(1): 107-13.

Williams, L.T. (1989). Signal transduction by the platelet-derived growth factor receptor. *Sience* 243: 1564-1570.

Willmore-Payne, C., Layfield L.J. and Holden, J.A. (2005). C-KIT mutation analysis for diagnostic of gastrointestinal stromal tumors in fine needle aspiration specimens. *Cancer* 105: 165-170.

Wilmore, H.P., McClive, P.J., Smith, C.A. and Sinclair, A.H. (2005). Expression profile of the RNA-binding protein gene hermes during chicken embryonic development. *Dev Dyn* 233(3): 1045-51.

Wozniak, A., Sciot, R., Guillou, L., Pauwels, P., Wasag, B., Stul, M., Vermeesch, J.R., Vandenberghe, P., Limon, J. and Debiec-Rychter, M. (2007). Array CGH analysis in primary gastrointestinal stromal tumors: cytogenetic profile correlates with anatomic site and tumor aggressiveness, irrespective of mutational status. *Genes Chromosomes Cancer* 46(3): 261-76.

Xiang, Z., Kreisel, F., Cain, J., Colson, A. and Tomasson, M.H. (2007). Neoplasia driven by mutant c-KIT is mediated by intracellular, not plasma membrane, receptor signaling. *Mol Cell Biol* 27(1): 267-82.

Xin, M., Small, E.M., Sutherland, L.B., et al., (2009). MicroRNAs miR-143 and miR-145 modulate cytoskeletal dynamics and responsiveness of smooth muscle cells to injury. *Genes Dev* 23: 2166-2178.

Yan, B.M., Kaplan, G.G., Urbanski, S., Nash, C.L. and Beck, P.L. (2008). Epidemiology of gastrointestinal stromal tumors in a defined Canadian Health Region: a population-based study. *Int J Surg Pathol* 16: 241-250.

Yarden, Y., Escobedo, J.A., Kuang, W.J., Yang-Feng, T.L., Daniel, T.O., Tremble, P.M., Chen, E.Y., Ando, M.E., Harkins, R.N., Francke, U., Fried, V.A., Ullrich, A. and Williams, L.T. (1986). Structure of the receptor for platelet-derived growth factor helps define a family of closely related growth factor receptors. *Nature* 323(6085): 226-32.

Yin, H., Jiang, Y., Li, H., Li, J., Gui, Y. and Zheng, X.L. (2011). Proteasomal degradation of myocardin is required for its transcriptional activity in vascular smooth muscle cells. *J Cell Physiol* 226(7): 1897-906.

Ylipää, A., Hunt, K.K., Yang, J., Lazar, A.J., Torres, K.E., Lev, D.C., Nykter, M., Pollock, R.E., Trent, J. and Zhang, W. (2011). Integrative genomic characterization and a genomic staging system for gastrointestinal stromal tumors. *Cancer* 15: 117(2): 380-9.

Yun, H.Y., Sung, R., Kim, Y.C., Choi, W., Kim, H.S., Kim, H., Lee, G.J., You, R.Y., Park, S.M., Yun, S.J., Kim, M.J., Kim, W.S., Song, Y.J., Xu, W.X. and Lee, S.J. (2010). Regional Distribution of Interstitial Cells of Cajal (ICC) in Human Stomach. *Korean J Physiol Pharmacol* 14(5): 317-24.

Yuzawa, S., Opatowsky, Y., Zhang, Z., Mandiyan, V., Lax, I. and Schlessinger, J. (2007). Structural basis for activation of the receptor tyrosine kinase KIT by stem cell factor. *Cell* 130(2): 323-34.

Zeng, L., Carter, A. D. and Childs, S. J. (2009). miR-145 directs intestinal maturation in zebrafish. *Proc Natl Acad Sci U S A* 106(42):17793-8.

Zhang, L., Smyrk, T.C., Young, W.F. Jr., Stratakis, C.A. and Carney, J.A. (2010). Gastric stromal tumors in Carney triad are different clinically, pathologically, and behaviorally from sporadic gastric gastrointestinal stromal tumors: findings in 104 cases. *Am J Surg Patho* l34(1): 53-64.

ANNEXE

Experimental and Molecular Pathology 93 (2012) 56–60

Contents lists available at SciVerse ScienceDirect

Experimental and Molecular Pathology

journal homepage: www.elsevier.com/locate/yexmp

Immunohistochemical analysis of bone morphological protein signaling pathway in human myometrium

Caroline Rouleau [a,b,*], Caroline Rico [a], Ilona Hapkova [a], Pascal de Santa Barbara [a]

[a] INSERM 1046 Unit, "Médecine expérimentale Coeur et muscle", Montpellier University Hospital, 371 avenue du Doyen gaston Giraud, 34295 Montpellier, France
[b] Institute of Pathology, Lausanne University Hospital, rue du Bugnon 25, 1011 Lausanne, Switzerland

ARTICLE INFO

Article history:
Received 5 March 2012
Available online 17 April 2012

Keywords:
BMP
Human myometrium
Uterine smooth muscle cells
Noggin
P-SMAD1/5

ABSTRACT

We assessed by immunohistochemistry the expression of the phosphorylated (activated) form of Smad1 and 5 (P-SMAD1/5), of Noggin and of two smooth muscle cell markers (α-SMA and SM22) in a series of human myometrium samples and in a smooth muscle cell line derived from human myometrium (HUt-SMC, PromoCell, USA). Myometrium samples were removed from two cadavers (a fetus at 26 weeks of gestation and a neonate) and from ten non-menopausal women who underwent hysterectomy for adenomyosis and leiomyoma. P-SMAD1/5 expression was never detected in myometrium (both normal and pathological specimens), but only as a nuclear positive staining in glandular and luminal epithelial cells in sections in which also the endometrial mucosa was present. Noggin was strongly expressed especially in myometrium and adenomyosis samples from non-menopausal patients in comparison to the neonatal and fetal myometrium specimens in which muscle cells were less positive. In more than 95% of HUt-SMCs, α-SMA and Desmin were co-expressed, indicating a pure smooth muscle phenotype. When progesterone was added to the culture medium, no P-SMAD1/5 expression was detected, whereas the expression Noggin and SM22, a marker of differentiated smooth muscle cells, increased by 3 fold ($p = 0.002$) and 4.3 fold ($p = 0.001$), respectively ($p = 0.002$).
Our results suggest that, in non-menopausal normal human myometrium, the BMP pathway might be inhibited and that this inhibition might be enhanced by progesterone, which increases the differentiation of smooth muscle cells (SM22 levels). These findings could help in the identification of new mechanisms that regulate uterine motility.

Introduction

The myometrium is the thick muscle layer of the uterine wall. It is located between the inner layer of the uterine mucosa (the endometrium) and the perimetrium and is characterized by two–three badly defined layers of smooth muscle fibers organized in crisscrossing bundles (Robboy et al., 2009). The myometrium derives embryologically from the part of the splanchnic mesoderm that will give rise to a transient common chamber between the urinary and digestive systems (De Santa Barbara et al., 2002). The growth of the myometrium starts during fetal life and gradually continues after birth and during the cyclic changes at puberty. Like the endometrium, the myometrium is very sensitive to sexual hormones (estrogen, progesterone) to which it responds with morphological and functional changes (Robboy et al., 2009). During pregnancy, the myometrium becomes considerably thicker due to the presence of high concentrations of estrogens and progesterone. During delivery, the contractile functions of the myometrium allow the expulsion of the fetus and ensure the vasoconstriction of the placental vessels (Teixeira et al., 2008). Uterine leiomyoma, the most common benign gynecologic tumor in women, results from hindered differentiation and deregulated proliferation of smooth muscle cells. Estrogens and progesterone may play an important role in its growth. Uterine adenomyosis, also called endometriosis of the uterus, is a benign condition in which endometrial cells penetrate deep into the uterine myometrium. It commonly affects the posterior wall (posterior side) of the uterus and does not cause cancer.

Bone morphogenetic proteins (BMP) are secreted signaling molecules that belong to the Transforming Growth Factor β (TGFβ) superfamily. BMP ligands were initially identified as regulators of bone formation, but subsequent studies have demonstrated that they regulate different developmental processes throughout embryogenesis and organogenesis (De Santa Barbara et al., 2003). BMP signaling activity is controlled at many levels, including ligand transcription, ligand–receptor interactions and signal transduction (Faure et al., 2002). This complexity makes more difficult the molecular dissection

* Corresponding author at: Institute of pathology, Lausanne University Hospital, rue du Bugnon 25, 1011 Lausanne, Switzerland. Fax: +41 21 314 71 51.
E-mail addresses: r-caroline@hotmail.fr (C. Rouleau), rico.caroline@yahoo.fr (C. Rico), ilona.hapkova@inserm.fr (I. Hapkova), pascal.de-santa-barbara@inserm.fr (P. de Santa Barbara).

0014-4800/$ – see front matter © 2012 Elsevier Inc. All rights reserved.
doi:10.1016/j.yexmp.2012.04.007

of the pathways and the specific tissue patterning functions that are regulated by these molecules. The intracellular mediators Smad1, 5 and 8 transduce the signals of the BMP2, 4 and 7 ligands and are specifically phosphorylated by the same BMP-type I receptors at the last two serine residues in the carboxy-terminal SSVS motif (Kretzschmar et al., 1997). Anti-phosphorylated Smad1/5/8 (anti-P-SMAD1/5/8) antibodies that specifically detect the phosphorylated (and thus activated) form of Smad1, 5 and 8 have been developed and constitute an important tool to map BMP activation in vertebrates (Faure et al., 2000, 2002; Kretzschmar et al., 1997). Indeed, BMP activation often cannot be predicted based only on the mRNA or protein expression patterns of BMP ligands and/or receptors (Faure et al., 2002; Moniot et al., 2004). For instance, using this antibody we previously described how BMP signaling activity is regulated during visceral smooth muscle cell differentiation. Furthermore, using in vivo approaches, we also showed that aberrant modulation of BMP activity during visceral smooth muscle development hinders the differentiation of these cells and increases their proliferation leading to dedifferentiation (De Santa Barbara et al., 2005). These data highlight that tightly regulated BMP activity is needed to ensure visceral smooth muscle cell differentiation.

In the uterus, studies carried out in animal models indicate that, in the endometrium and myometrium, BMP ligands have a cyclic expression, suggesting that this signaling pathway could be implicated also in the uterine physiology (Erickson et al., 2004). Moreover, during development, the BMP signaling pathway plays a crucial role in the regression of the Müllerian ducts in males by transducing the signals of the anti-Müllerian hormone (Orvis et al., 2008). Finally, during uterine decidualization, the BMP2 and 7 ligands modulate the differentiation of endometrial stromal cells by mediating the intracellular effects of progesterone (PG) (Kodama et al., 2010; Li et al., 2007; Stoikos et al., 2008).

We thus hypothesized that components of the BMP signaling pathway could be involved in myometrium physiology by regulating the effects of steroid hormones (such as PG) as already described for the endometrium. We thus investigated by immunohistochemistry the expression of components of the BMP signaling pathway in human uterine myometrium tissue sections and in a smooth muscle cell line derived from human myometrium.

Material and methods

Human samples

Two myometrium samples were removed post-mortem: one from a spontaneously aborted female fetus at 26 weeks of gestation and the other one from a full term female neonate who died shortly after birth. The other samples (n = 16) were from ten non-menopausal women operated at the Arnaud de Villeneuve Hospital University Center of Montpellier (France) and included six healthy myometrium and ten pathological (leiomyoma and adenomyosis) specimens. The samples mirrored the paraffin-embedded specimens used for diagnosis. This research project was approved by the Centre de Protection des Personnes Méditerranée IV.

HUt-SMC lines

The smooth muscle cell line HUt-SMC (PromoCell, USA), which was derived from human myometrium, was grown at 37 °C, 5% CO_2 in 100 mm dishes (BD Biosciences) in the medium suggested by the vendor (Promocell, USA) with 5% fetal bovine serum, 0.5% epidermal growth factor (EGF), basic fibroblast growth factor (BFGF) and Insulin (maintenance medium). To test the effect of sexual hormones on cell differentiation, cells were incubated in Dulbecco's modified Eagle medium (DMEM) in the presence of 10% fetal bovine serum (proliferation medium), supplemented or not with 10 nM β-estradiol (E2) (Sigma) or 10 nM PG (Sigma) for 48 h. Cell cultures were examined by phase-contrast microscopy (Olympus, Japan).

Immunohistochemistry

Paraffin-embedded sections (3 μm thick) were immunostained by using standardized automated procedures and a Dako autostainer (Universal Staining System, Dakocytomation, Trappes, France), as previously described (Rouleau et al., 2009). Antigen retrieval was achieved by heating sections at 98 °C in 1 mM EDTA (pH 9.0) for 1 h. The BMP pathway was investigated with the rabbit monoclonal anti-P-SMAD1/5 (1:100; clone 41D10, Cell Signaling) antibody that detects phosphorylated SMAD1/5 (Duband et al., 1993) and the goat polyclonal anti-Noggin (1:50; Santa Cruz) antibody that detects the protein that binds to BMP ligands, thus inhibiting their interaction with BMP receptors. Other primary antibodies were a mouse antibody against α-SMA (1:400; clone 1A4, Sigma), which is an early marker of smooth muscle cells; a mouse antibody specific for SM22 (1:400; clone 1B8, Abcam), a marker of differentiated smooth muscle cells (Duband et al., 1993), and the mouse monoclonal anti-Desmin (clone cDE-U-10, Sigma) antibody. Immunohistochemistry control experiments were performed by excluding the primary antibody (data not shown).

For immunofluorescence, HUt-SMCs were fixed in 4% paraformaldehyde and incubated at room temperature with the relevant primary antibodies for 1 h. After washing, cells were incubated with Alexa 488 anti-mouse (Invitrogen, France, 1:2000 dilution) or Alexa 555 anti-rabbit (Invitrogen, France, 1:2000 dilution) secondary antibodies for 30 min. Cells were rinsed again, mounted in FluorSave reagent (Calbiochem, Germany) and analyzed with a fluorescence microscope (Leica DMLB2, Leica Microsystem, CH) coupled to a camera (Leica DFC 300FX, Leica Microsystem, CH). Levels of Noggin and P-SMAD1/5/8 fluorescence in 5–10 fields, each containing at least 25 cells, were measured and the TRITC fluorescence/Hoechst fluorescence ratio calculated with the *Cells and Maps* program (http://www.bram.org/serf/). This program counts the total fluorescence intensity (pixels per cell) in both the TRITC and Hoechst channels and computes the TRITC fluorescence/Hoechst fluorescence ratio to evaluate the relative Noggin and P-SMAD1/5 content per cell.

Statistics

Statistical analysis was carried out using the Student's *t*-test when two sets of data were compared. The ANOVA test was used when more than two sets were compared. A p value of less than 0.05 was considered significant.

Results

Immunodetection of BMP members and smooth muscle markers in normal developing and adult human myometrium

Histological analysis of paraffin-embedded uterine sections revealed from the inside to the outside, respectively, the mucosa and the myometrium. In non-menopausal women, the myometrium was composed of haphazardly organized thick bundles of smooth muscle cells (Fig. 1A). In the neonate sample (Fig. 1B), the myometrium was slightly thicker than in the fetal uterine sample (Fig. 1C).

Immunohistochemical analysis showed a strong and diffuse expression of α-SMA, an early marker of smooth muscle cells, in all myometrium samples (Figs. 1D–F). On the other hand, SM22, which is a marker of differentiated smooth muscle cells, was very weakly expressed in fetal myometrium (Fig. 1I) and its expression gradually increased in neonatal myometrium (Fig. 1H) to become very strong in the myometrium of non-menopausal women (Fig. 1G). No activity of the BMP signaling pathway was detected in the myometrium by

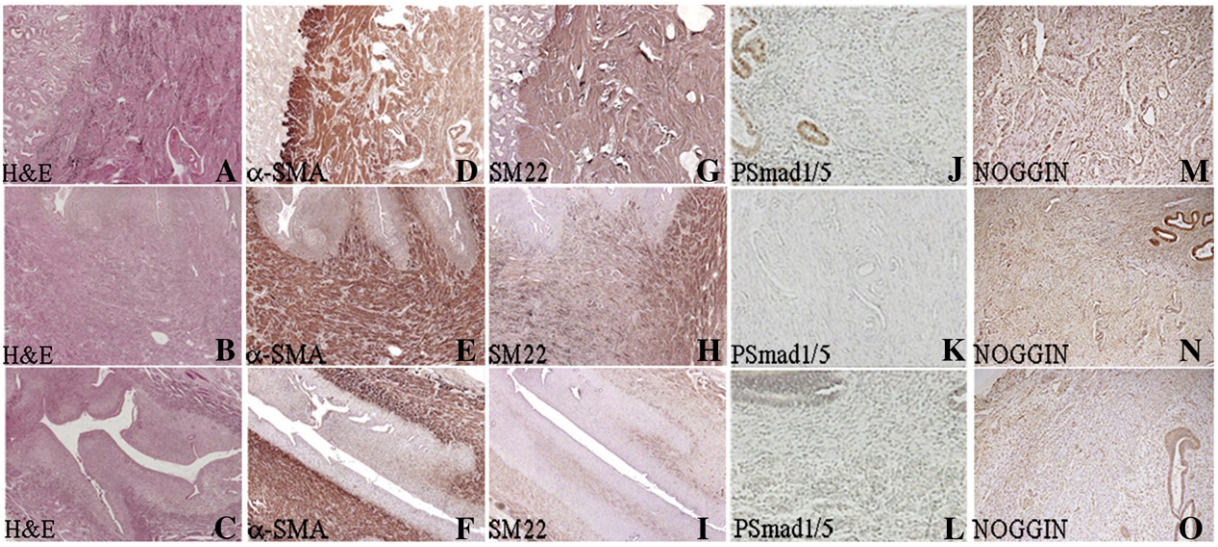

Fig. 1. Detection of smooth muscle cell markers, P-SMAD1/5 and Noggin in normal human myometrium. Hematoxylin–eosin-stained sections (A, B, C), and immunodetection of α-SMA (D, E, F), SM22 (G, H, I), P-SMAD1/5 (J, K, L) and Noggin (M, N, O). Normal myometrium tissue sections from a non-menopausal woman (A, D, G, J, M), a female neonate (B, E, H, K, N) and a female fetus (C, F, I, L, O). Original magnification ×100.

using the anti-P-SMAD1/5 antibody (Figs. 1J, K, L). Conversely, in samples in which the mucosa was present, a nuclear positive staining was observed in glandular and luminal epithelial cells at the luminal surface (Fig. 1J). Finally, Noggin, which inhibits BMP signaling, was strongly expressed particularly in myometrium specimens from non-menopausal patients (Fig. 1M) and slightly more weakly in neonate and fetal myometrium (Figs. 1N, O) in which muscle cells were less differentiated.

Immunodetection of BMP members and smooth muscle markers in human pathological myometrium

In contrast to normal myometrium (Fig. 2A), adenomyosis is characterized by the presence of islets of mucosa (endometrial glands and stroma) within the myometrium (Fig. 2B) and leiomyoma corresponds to a benign proliferation of usually well differentiated smooth muscle cells (Fig. 2C).

In specimens with adenomyosis, α-SMA (Fig. 2E) and SM22 (Fig. 2H) were both strongly expressed in smooth muscle fibers, but not in the islets of endometrial mucosa, thus facilitating their identification. On the other hand, in leiomyoma tissue sections, smooth muscle cells were less positive for both markers (Figs. 2F and I). No positive immunostaining could be observed for P-SMAD1/5 in any of the tissue samples (Figs. 2J, K, L). In specimens with adenomyosis, Noggin was expressed in smooth muscle cells surrounding the islets of endometrial mucosa (Fig. 2N) and the expression level was comparable to that of normal non-menopausal myometrium (Fig. 2M). Noggin was also expressed in leiomyomas (Fig. 2O), but much less strongly than in the normal myometrium (Fig. 2M).

Effects of estradiol and progesterone on uterine smooth muscle cells

HUt-SMC cultures were analyzed using both morphological and immunohistochemical approaches. HUt-SMC cultures were characterized

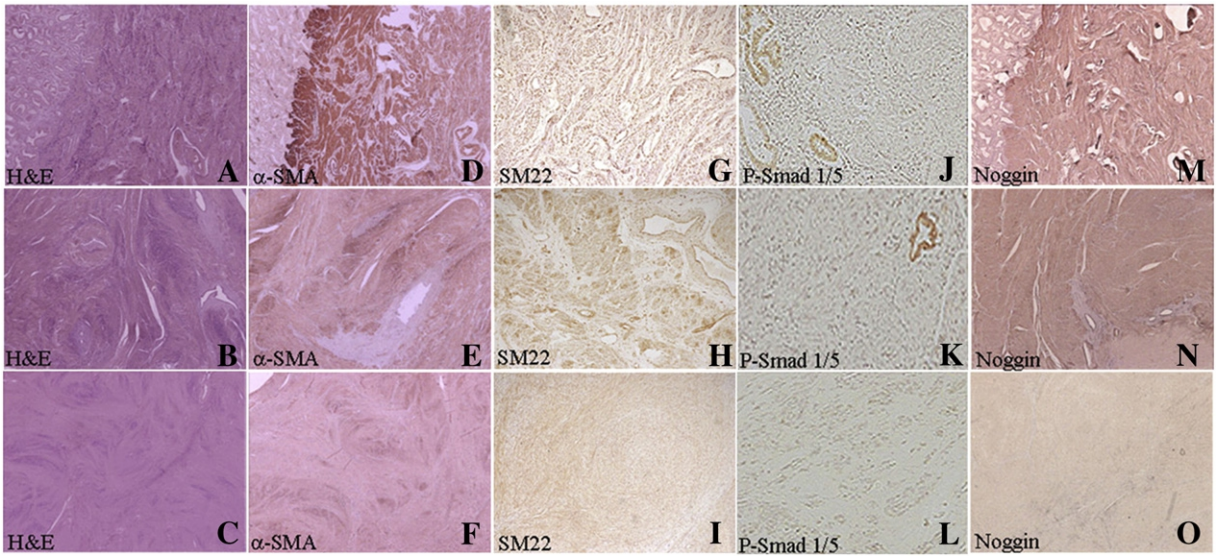

Fig. 2. Detection of smooth muscle cell markers, P-SMAD1/5 and Noggin in myometrium pathological samples. Hematoxylin–eosin-stained sections (A, B, C) and immunodetection of α-SMA (D, E, F), SM22 (G, H, I), P-SMAD1/5 (J, K, L) and Noggin (M, N, O). Tissue sections from normal myometrium (A, D, G, J, M), adenomyosis (B, E, H, K, N) and leiomyoma (C, F, I, L, O). Original magnification ×100.

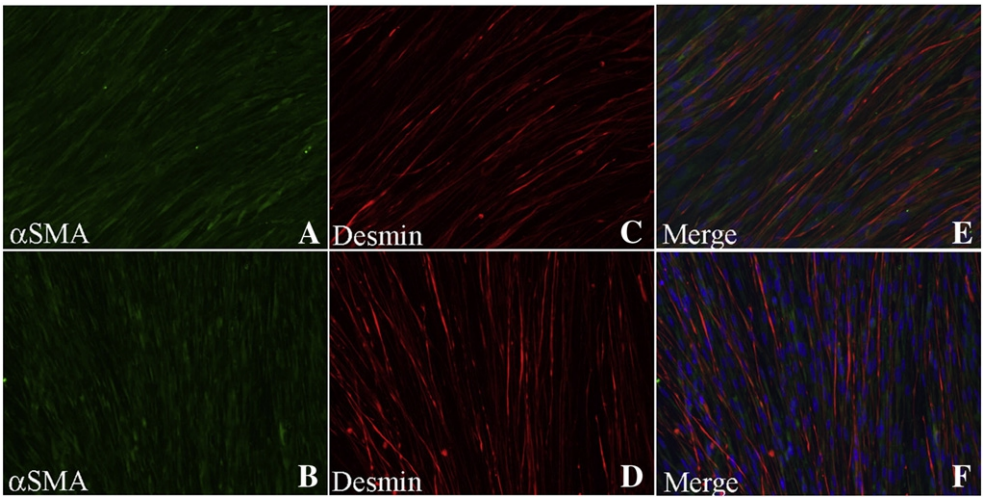

Fig. 3. Immunophenotype of HUt-SMCs. Co-expression of α-SMA (A, B) and Desmin (C, D), merged images in (E, F), in HUt-SMCs grown in maintenance medium (5% fetal bovine serum) (control) (A, C, E) or in proliferation medium (10% fetal bovine serum) in the presence of 10 nM PG for 48 h (B, D, F). Original magnification ×200.

by the presence of uniform fusiform spindle-shaped cells, with scant cytoplasm and ovoid nuclei (Fig. 3). More than 95% of cells expressed both α-SMA and Desmin (a mesenchymal marker), indicating a homogenous smooth muscle phenotype (Figs. 3A, C, E). When cells were grown in proliferation medium in the presence or not of E2 or PG for 48 h, a weak P-SMAD1/5 nuclear expression was detected only in control cultures (Fig. 4A) but not in those with E2 or PG (Figs. 4B and C), whereas Noggin (Fig. 4D) increased ($p = 0.002$) by 2.3 fold (E2) and 3 fold (PG) (Figs. 4E and F), as indicated by the quantification of the fluorescence per cell. The levels of α-SMA and Desmin were not affected by PG (Figs. 3B, D, F) and E2 (data not shown), whereas SM22 (Fig. 4J) expression increased ($p = 0.001$) by 2.7 fold (E2) and 4.3 (PG) (Figs. 4K and L). These findings suggest that the inhibition of BMP activity might be enhanced in the presence of progesterone which also increased SM22 expression.

Discussion

The aim of this study was to assess the expression and localization of proteins of the BMP signaling pathway in human myometrium. In the absence of data in humans, we decided to use normal uterine specimens at different stages of development (fetus, neonate and non-menopausal adult women) and also samples of very frequent benign myometrial pathologies (adenomyosis and leiomyoma). Expression of P-SMAD1/5 was not detected in any all tested samples, suggesting that SMAD1 and 5 are not phosphorylated in human myometrium. This result needs to be confirmed in a larger sample. Conversely, Noggin, the inhibitor of BMP signaling, was expressed in normal myometrium and it expression showed variations (stronger in non-menopausal than in neonate and fetal myometrium) that were comparable to those observed for SM22. Despite the limited number of studied samples, this result suggests that Noggin expression could be influenced by growth and/or differentiation of smooth muscle fibers in the myometrium. The distribution of smooth muscle markers in the different samples suggests that from the fetal stage, the myometrium contains cells that are determined to become smooth muscle (α-SMA+++, SM22+) and that will progressively differentiate during myometrium growth. Like the endometrium, the myometrium is very sensitive to ovarian steroids (E2, PG) and responds with morphological and functional changes (Teixeira et al.,

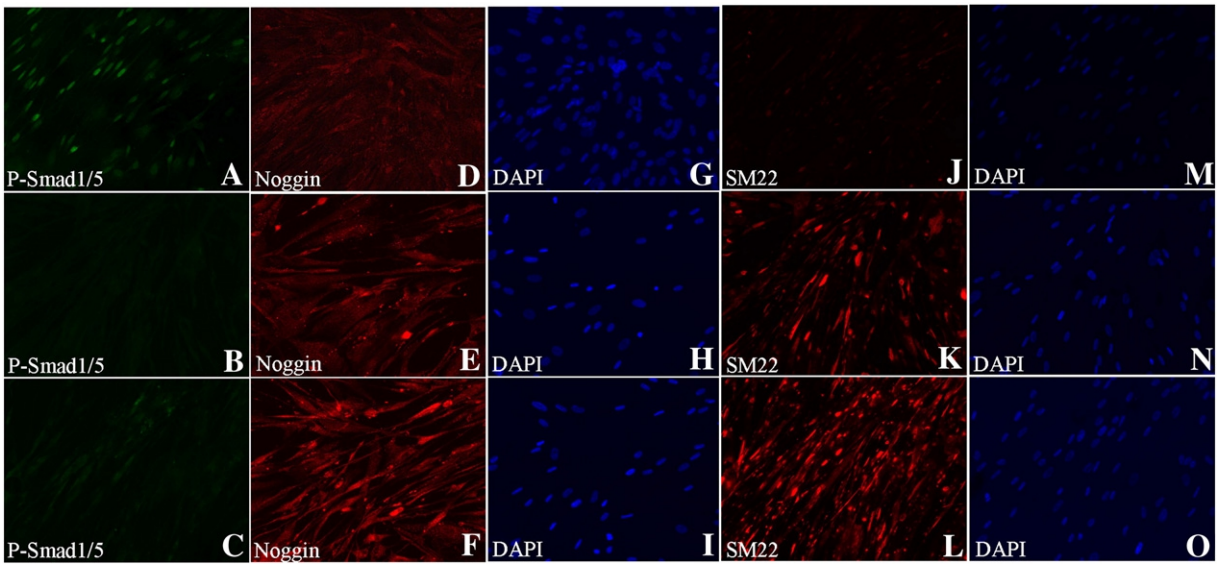

Fig. 4. Detection of P-SMAD1/5, Noggin and smooth muscle cell markers in HUt-SMCs. Immunodetection of P-SMAD1/5 (A, B, C), Noggin (D, E, F) and SM22 (J, K, L). Cells were grown in proliferation medium (10% fetal bovine serum) without (control cultures) (A, D, G, J, M), or with 10 nM E2 (B, E, H, K, N) or PG (C, F, I, L, O) for 48 h. Dapi (G, H, I, M, N, O). Original magnification ×200.

2008). As the hormonal status of the non-menopausal patients was not known in all cases and our population was very small, we decided to use HUt-SMCs, which are smooth muscle cells of myometrial origin, to determine whether the expression of proteins of the BMP signaling pathway was influenced by steroid hormones (E2 and PG). HUt-SMCs were characterized by the presence of homogenous smooth muscle cells as indicated by the co-expression of α-SMA and Desmin. Following the addition of E2 or PG in the culture medium, only the expression of SM22, a marker of late differentiation (Duband et al., 1993), was increased, whereas the expression of α-SMA (early marker) remained unchanged. No significant P-SMAD1/5 expression was detected in cultures. Conversely, Noggin expression was strongly increased following incubation with E2 or PG. These in vitro results are in agreement with the expression data in myometrium tissue sections and suggest that, in normal adult myometrium, [i] the BMP signaling pathway is inhibited and [ii] this inhibition is increased in the presence of PG or E2 that also stimulates the differentiation of smooth muscle cells (as indicated by the increased expression of SM22).

In conclusion, the results of this study are compatible with our hypothesis that BMP signaling molecules might play a role in the physiology of myometrium. Our results should be strengthened by contractility tests of myometrial cells in the presence of steroid hormones and agents that modulate the BMP signaling pathway. As the contractile characteristics of the myometrium are difficult to test outside pregnancy, animal models (pregnant mice) should be set up to better understand the physiology of uterine motricity and possibly to identify new regulatory mechanisms.

Conflict of interest statement

The authors declare that there are no conflicts of interest.

Contribution to authorship

Immunohistochemistry assays on tissue samples and cell lines were carried out by CRi and IH, under the supervision of CRo and P de SB. CRo wrote the paper and is the corresponding author. The manuscript was revised by P de SB.

Funding

The work was supported by the Région Languedoc-Roussillon (Chercheur d'Avenir), INCA GSO (Projet Emergent), Ligue Contre le Cancer (Comité de l'Aude) and Association Française contre les Myopathies (AFM) to PDSB. I.H. was supported by a Ministère des Affaires Etrangères fellowship.

Acknowledgments

We are indebted to Elisabetha Andermacher for editing the manuscript. We thank Anna Thalamo for her help in fluorescence counting and members of INSERM U1046 for helpful discussions.

References

De Santa Barbara, P., van den Brink, G.R., Roberts, D.J., 2002. Molecular etiology of gut malformations and diseases. Am. J. Med. Genet. 115, 221–230.
De Santa Barbara, P., van den Brink, G.R., Roberts, D.J., 2003. Development and differentiation of the intestinal epithelium. Cell. Mol. Life Sci. 60, 1322–1332.
De Santa Barbara, P., Williams, J., Goldstein, A.M., et al., 2005. Bone morphogenetic protein signaling pathway plays multiple roles during gastrointestinal tract development. Dev. Dyn. 234, 312–322.
Duband, J.L., Gimona, M., Scatena, M., et al., 1993. Calponin and SM22 as differentiation markers of smooth muscle spatiotemporal distribution during avian embryonic development. Differentiation 55, 1–11.
Erickson, G.F., Fuqua, L., Shimasaki, S., 2004. Analysis of spatial and temporal expression patterns of bone morphogenetic protein family members in the rat uterus over the estrous cycle. J. Endocrinol. 182, 203–217.
Faure, S., Lee, M.A., Keller, T., et al., 2000. Endogenous pattern of TGFbeta superfamily signaling during early *Xenopus* development. Development 127, 2917–2931.
Faure, S., Santa, De, Barbara, P., Roberts, D.J., Whitman, M., 2002. Endogenous patterns of BMP signaling during early chick development. Dev. Biol. 244, 44–65.
Kodama, A., Yoshino, O., Osuga, Y., et al., 2010. Progesterone decreases bone morphogenetic protein BMP7 expression and BMP7 inhibits decidualization and proliferation in endometrial stromal cells. Hum. Reprod. 25, 751–756.
Kretzschmar, M., Doody, J., Massaqué, J., 1997. Opposing BMP and EGF signaling pathways converge on the TGF-beta family mediator Smad1. Nature 389, 618–622.
Li, Q., Kannan, A., Wang, W., et al., 2007. Bone morphogenetic protein 2 functions via a conserved signaling pathway involving Wnt4 to regulate uterine decidualization in the mouse and the human. J. Biol. Chem. 282, 31725–31732.
Moniot, B., Biau, S., Faure, S., et al., 2004. SOX9 specifies the pyloric sphincter epithelium through mesenchymal–epithelial signals. Development 131, 3795–3804.
Orvis, G.D., Jamin, S.P., Kwan, K.M., et al., 2008. Functional redundancy of TGF-beta family type I receptors and receptor-Smads in mediating anti-Mullerian hormone-induced Mullerian duct regression in the mouse. Biol. Reprod. 78, 994–1001.
Robboy, S.J., Mutter, G.S., Prat, J., et al., 2009. Pathology of the Female Genital Tract. Elsevier (Churchill Livingstone), London.
Rouleau, C., Matecki, S., Kalfa, N., et al., 2009. Activation of MAP Kinase (ERK1/2) in human neonatal colonic enteric nervous system. Neurogastroenterol. Motil. 21, 207–214.
Stoikos, C.J., Harrison, C.A., Salamonsen, L.A., Dimitriadis, E., 2008. A distinct cohort of the TGFbeta superfamily members expressed in human endometrium regulate decidualization. Hum. Reprod. 23, 1447–1456.
Teixeira, J., Rueda, B.R., Pru, J.K., 2008. Uterine stem cells. StemBook [Internet]. Harvard Stem Cell Institute, Cambridge (MA).